RUTHENIUM BASED HOMOGENEOUS OLEFIN METATHESIS

By

MEGAN MICHELLE KIRK

DISSERTATION

Submitted in fulfilment of the requirements for the degree

MAGISTER SCIENTIAE

In

CHEMISTRY

FACULTY OF NATURAL AND AGRICULTURAL SCIENCES

UNIVERSITY OF THE FREE STATE

SUPERVISOR: PROF. ANDREAS ROODT (UFS)

CO-SUPERVISOR: DR. WOLFGANG MEYER (Sasol Technology)

NOVEMBER 2005

Acknowledgements

Thanks be to God for the grace and blessings to carry out this work.

I would like to dedicate this thesis to my wonderful husband Richard and my children, Kenneth and Kathy, who have sacrificed a great deal to enable me to continue with my studies. Your encouragement, support and love are much appreciated.

In addition I would like to extend my sincere gratitude to:

Cathy Dwyer, for introducing me to homogeneous catalysis and drawing me into the homogeneous metathesis group at Sasol,

the Sasol Homogeneous metathesis team, Cathy Dwyer, Wolfgang Meyer, Ann McConnell, Grant Forman, Werner Janse van Rensburg, Wynand Serfontein and Mike Green, for working with me on many aspects of this work,

Wolfgang Meyer, Werner Janse van Rensburg and Gideon Steyl for the modelling calculations,

Infrachem laboratories, for many gas chromatograms,

Andre Roodt, my supervisor, for much guidance and support throughout the study,

Sasol Technology and Johan Coetzee, for giving me the opportunity to complete this work.

Megan Kirk

Part of this study resulted in the following publication

'DFT Prediction and Experimental Observation of Substrate Induced Catalyst Decomposition in Ruthenium Catalysed Olefin Metathesis'

Janse van Rensburg, W., Steynberg, P.J., Meyer, W.H., Kirk, M.M., Forman, G.S.;
J. Amer. Chem. Soc., **2004**, *126(44)*, 14332-14333.

Abbreviations

ADMET	Acyclic diene metathesis
CCl_3Br	Bromotrichloromethane
CCl_4	Carbon tetrachloride
$CDCl_3$	Deuterated chloroform
C_6D_6	Deuterated benzene
CM	Cross metathesis
CTL	Coal to liquids
DFT	Density functional theory
gCOSY	gradient Correlated Spectroscopy
GC/MS	Gas chromatograph/mass spectrometer
HMBC	Heteronuclear multiple bond correlation
HP IR	High pressure infra red
HP NMR	High pressure NMR
HSQC	Heteronuclear single quantum coherence
HTFT	High temperature Fischer Tropsch
L	Ligand
LTFT	Low temperature Fischer Tropsch
Mes	2,4,6-trimethylphenyl
NAr	N-2,6-isopropylbenzeneimido ligand
NHC	1,3-dimesityl-4,5-dihydroimidazole-2-ylidene
OCT®	Olefin conversion technology®
P	Phosphine ligand
PCy_3	Tricyclohexylphosphine
pfg	pulsed field gradient
$O{=}PCy_3$	Tricyclohexylphosphine oxide
Phoban	Phosphabicyclononane
PLOT	Porous layer open tubular
RCM	Ring-closing metathesis
ROMP	Ring-opening metathesis polymerisation
ROIMP	Ring-opening insertion metathesis polymerisation
SHOP	Shell Higher Olefins Process

SSPD	Sasol slurry phase distillate
TIC	Total ion chromatogram
1D NMR	1 dimensional NMR
2D NMR	2 dimensional NMR

Table of Contents

List of Tables

List of Schemes

List of figures

Abstract

The aim of this study was to investigate the decomposition of the methylidenes **4a** $[Ru(Cl)_2(PCy_3)_2CH_2]$ and **6** $[Ru(Cl)_2(PCy_3)(NHC)CH_2]$ and alkylidene **5** $[Ru(Cl)_2(PCy_3)_2CHR]$, formed in the homogeneous olefin metathesis reaction using either the first generation Grubbs catalyst **2a** $[Ru(Cl)_2(PCy_3)_2CHPh]$ or the second generation Grubbs catalyst **3** $[Ru(Cl)_2(NHC)(PCy_3)CHPh]$. (NHC = 1,3-dimesityl-4,5-dihydroimidazole-2-ylidene).

Grubbs catalyst di-bromide **2b** $[Ru(Br)_2(PCy_3)_2CHPh]$ was found to react with chlorinated solvents with the formation of $CDCl_2Br$ and CCl_3Br, indicating that there is a direct reaction with the solvent itself ($CDCl_3$) and not HCl in the solvent. A mechanism is proposed for this reaction.

The intermolecular halide exchange reaction was observed during this study and used to gain insight into the bimolecular decomposition pathway. A mechanism where Grubbs catalyst **2a** acts as a ligand in a reaction with the 14 electron intermediate **7b** $[Ru(Br)_2(PCy_3)CHPh]$ is proposed for intermolecular halide exchange (see scheme below). It is proposed that the intermolecular halide exchange reaction occurs continuously in all solutions of Grubbs catalyst, with the formation of the dimeric intermediate **45** (see below).

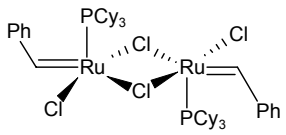

45

The decomposition of Grubbs catalyst **2a** in $CDCl_3$ results in the formation of paramagnetic species and consequently in the loss of the ^{31}P NMR signal. It has recently been reported that phenol and $SnCl_2$ dramatically increase the life time of Grubbs catalyst **2a**. An understanding of the formation and behaviour of dimeric intermediate **45** lead to the proposal of a mechanism for

the inhibition of bimolecular decomposition in the presence of phenol and $SnCl_2$ in $CDCl_3$.

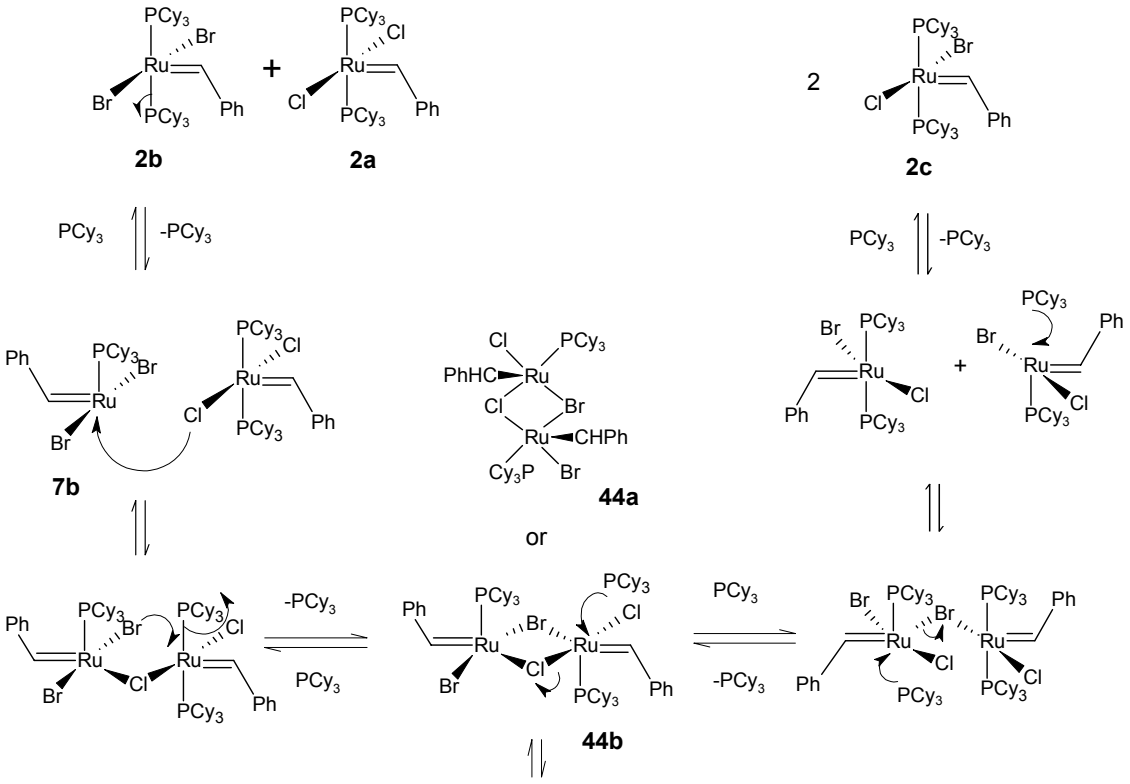

*Proposed mechanism for the intermolecular halide exchange between Grubbs catalyst **2a** and Grubbs catalyst di-bromide **2b***

To inhibit the formation of the dimeric intermediate **45** above, the use of solid and dissolved salts as additives was studied. ^{31}P and ^{1}H NMR studies showed that the presence of Bu_4NBr dissolved in $CDCl_3$ results in halide substitution at Grubbs catalyst **2a** $[Ru(Cl)_2(PCy_3)_2CHPh]$ to form a mixed halide catalyst **2c** $[RuBrCl(PCy_3)_2CHPh]$ and finally Grubbs catalyst di-bromide **2b** $[Ru(Br)_2(PCy_3)_2CHPh]$. Improved conversion and selectivity were obtained when solid and dissolved salts were added to the reaction mixture in the self metathesis of 1-octene.

Molecular modelling has indicated that there is a possibility of ethylene induced decomposition of the Grubbs catalyst methylidene **4a** $[Ru(Cl)_2(PCy_3)_2CH_2]$ with the formation of propene as shown below.

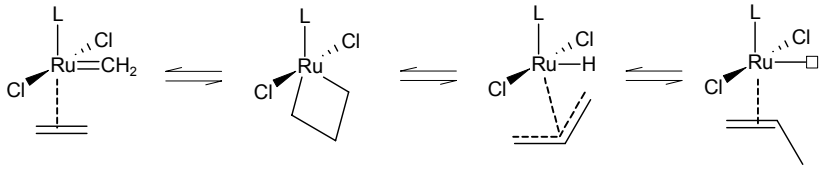

The ethylene induced β-hydride decomposition pathway

^1H NMR experiments monitoring the ethylene induced decomposition of methylidenes **4a** and **6** in C_6D_6 overnight clearly showed the formation of α-olefins, supporting the proposed β-hydride decomposition pathway. This pathway includes the formation of a hydride species that is highly likely to be isomerisation active and may lead to the decreased selectivity found experimentally.

This study was taken further by carrying out ethylene induced decomposition in $CDCl_3$, where it was found that there is no propene formation but rather addition of $CDCl_3$ across the double bond *via* the Kharasch reaction. This indicates that the β-hydride pathway is inhibited in chlorinated solvents, which may be part of the reason why better selectivities are obtained in the presence of chlorinated solvents.

Opsomming

Die doel van hierdie studie was om die ontbinding van die metilideenspesies, **4a** $[Ru(Cl)_2(PCy_3)_2CH_2]$, **6** $[Ru(Cl)_2(PCy_3)(NHC)CH_2]$ en die alkielideen **5** $[Ru(Cl)_2(PCy_3)_2CHR]$, wat gedurende enige homogene olefienmetatese waarin die Grubbs-katalisator **2a** $[Ru(Cl)_2(PCy_3)_2CHPh]$, of die tweede generasie Grubbs-katalisator **2a** $[Ru(Cl)_2(NHC)(PCy_3)CHPh]$ (NHC = N heterosikliese karbeen) gebruik word, te bestudeer.

Die studie het getoon dat die dibroomkompleks, Grubbs katalisator **2b** $[Ru(Br)_2(PCy_3)_2CHPh]$, direk met gechlorineerde oplosmiddels (soos $CDCl_3$, en nie met die HCl daarin) reageer om $CDCl_2Br$ en CCl_3Br as newe-produkte te lewer. ‘n Meganisme is vir hierdie reaksie voorgestel.

Die intermolekulêre halieduitruiling wat tydens hierdie studie waargeneem is, het addisionele inligting ten opsigte van die bimolekulêre ontbindingsroete gelewer.

'n Meganisme waarin Grubbs-katalisator **2a** as 'n ligand in die reaksie met die 14-elektron tussenproduk **7b** $[Ru(Br)_2(PCy_3)CHPh]$ optree, is gevolglik vir die intermolekulêre halieduitruiling voorgestel (sien skema hieronder). Dit is verder voorgestel dat hierdie halieduitruiling in alle Grubbs-katalisatoroplossings plaasvind via die dimeriese intermediêre spesie, **45**.

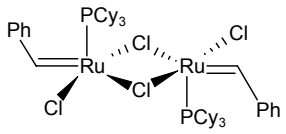

45

Die ontbinding van Gubbs-katalisator **2a** in $CDCl_3$ vorm 'n paramagnetiese spesie en gevolglike verlies van die ^{31}P KMR-sein. Die onlangsgerapporteerde stabilisering (betekenisvole verlenging van leeftyd) van Grubbs-katalisator **2a** deur die byvoeging van fenol en $SnCl_2$, en 'n begrip van die vorming en algemene gedrag van die dimeriese intermediêr,

45, het gelei tot die voorstelling van die inhibering van die bimolekulêre ontbinding in $CDCl_3$ in teenwoordigheid van hierdie bymiddels.

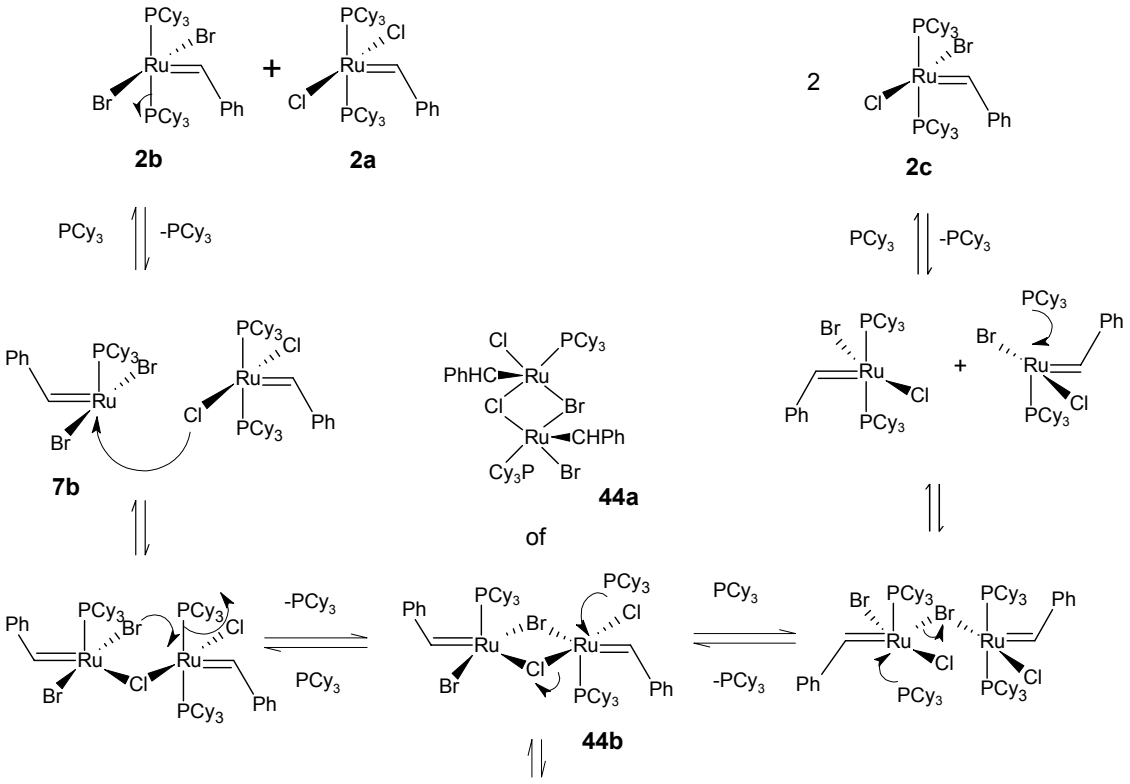

Bimolekulere ontbinding

*Voorgestelde meganisme vir die intermolekulêre halieduitruiling tussen die Grubbs-katalisator **2b** en Grubbs-katalisator **2a***

Ten einde die vorming van die dimeriese intermediêr, **45**, te verhoed, is die byvoeging van vaste en opgeloste soute bestudeer. ^{31}P en ^{1}H KMR-studies het getoon dat in teenwoordigheid van $(Bu_4N)Br$, opgelos in $CDCl_3$, haliedverplasing op Grubbs-katalisator **2a** $[Ru(Cl)_2(PCy_3)_2CHPh]$ induseer en die vorming van die gemengde haliedspesie, **2c** $[RuBrCl(PCy_3)_2CHPh]$ en uiteindelik die dibromospesie, Grubbs-katalisator **2b** $[Ru(Br)_2(PCy_3)_2CHPh]$. Verhoogde omskakeling en selektiwiteit is gevind wanneer vaste of opgeloste haliedsoute by die reaksiemengsel in die selfmetatesereaksie van 1-okteen gevoeg is. Modellering het aangetoon dat daar 'n moontlikheid van 'n

eteengeïnduseerde ontbinding van die Grubbs-katalisator metilideen **4a** $[Ru(Cl)_2(PCy_3)_2CH_2]$, met gepaardgaande propeenvorming, bestaan.

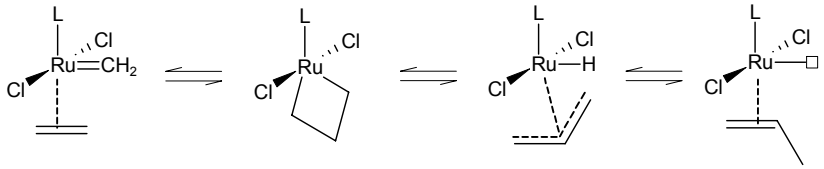

Die eteengeïnduseerde β-hidried ontbindingsroete

^1H KMR eksperimente in C_6D_6 (oornag) het duidelik die vorming van alfa-olefiene aangedui, wat die voorgestelde β-hidried ontbindingsroete bevestig het. Hierdie roete sluit ook die vorming van 'n hidriedspesie in wat moontlik isomerisasie kan ondergaan, en dus die afname in selektiwiteit wat eksperimenteel verkry word, kan verklaar.

'n Verdere deel van die studie het die eteengeïnduseerde ontbinding in $CDCl_3$ ingesluit, waar addisie van $CDCl_3$ oor die dubbelbinding geskied het (Kharasch-reaksie) in plaas daarvan dat propeen gevorm is. Hierdie toon dat die β-hidriedroete deur gechlorineerde oplosmiddels inhibeer word, wat moontlik kan verklaar hoekom beter selektiwiteite in hierdie oplosmiddles waargeneem word.

Chapter 1: Introduction and Aim

1.1 Introduction

Olefin metathesis is one of the few fundamentally novel organic reactions discovered in the last 40 years. This discovery has opened up new routes to important petrochemicals, polymers, oleo-chemicals and fine chemicals.[1]

Richard Schrock and Robert Grubbs pioneered homogeneous metathesis catalysts[2,3] and Yves Chauvin[4] proposed the metallacycle mechanism for metathesis (1970) involving carbenes long before any stable carbenes had been detected. This trio have recently been awarded the Nobel Prize for Chemistry in 2005 for their work in the field of olefin metathesis.[5] It is hoped that homogeneous metathesis will usher in a new era for the production of drugs and plastics that are more efficient and less harmful to nature than the traditional processes.

The metathesis reaction involves the reaction of two olefins in a disproportionation reaction *via* a metallacyclobutane intermediate **1** as depicted in ***Scheme 1.1*** below.

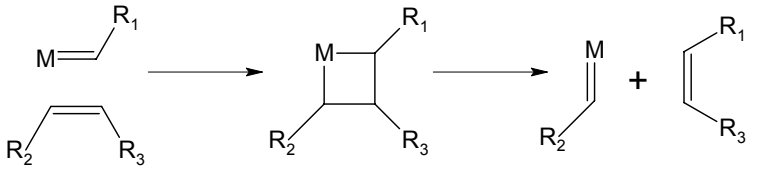

1

Scheme 1.1: *The Olefin Metathesis reaction*

The major industrial scale uses of metathesis are the production of propene *via* the reaction of ethylene and 2-butene over a heterogeneous catalyst, and the Shell Higher Olefin Process (SHOP)[6] which involves homogeneous

ethylene oligomerisation followed by metathesis over a heterogeneous catalyst.[7]

Homogeneous metathesis has become an extremely useful tool in organic synthesis due to the well defined metathesis catalysts, Grubbs catalyst **2a** $[Ru(Cl)_2(PCy_3)_2CHPh]$ and the second generation catalyst **2a** $[Ru(Cl)_2(PCy_3)(NHC)CHPh]$, introduced by the Grubbs group[8] in the mid 1990's (***Figure 1.1***). The homogeneous metathesis reaction has found application in the production of pharmaceutical products where small volume, high value products are produced and the cost of the catalyst is not a major factor in the process economics. In these processes the catalyst is not recycled, and decomposition of the catalyst is not a serious issue.

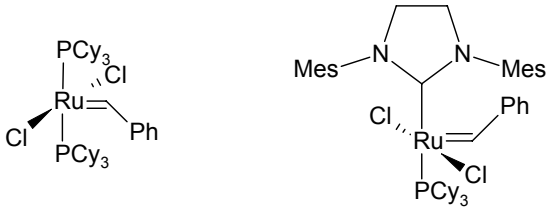

2a **3**

Figure 1.1: *Grubbs catalyst **2a** and the second generation Grubbs catalyst **3***

Although a few large scale metathesis processes have been investigated,[9] none have yet been implemented.

Major obstacles to the commercialisation of homogeneous metathesis technology for bulk chemical products include the relatively short lifetime of the catalysts, and side reactions (such as isomerisation) that take place concurrently with metathesis.

An example of a homogeneous cross metathesis reaction is the self-metathesis of 1-octene to yield 7-tetradecene and ethylene (***Scheme 1.2***). In

this reaction, the precatalyst **2a** is converted to propagating methylidene **4a** and the alkylidene species **5**. (***Scheme 1.3***).

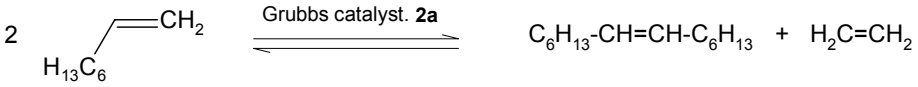

***Scheme 1.2**: Self metathesis of 1-octene to 7-tetradecene and ethylene*

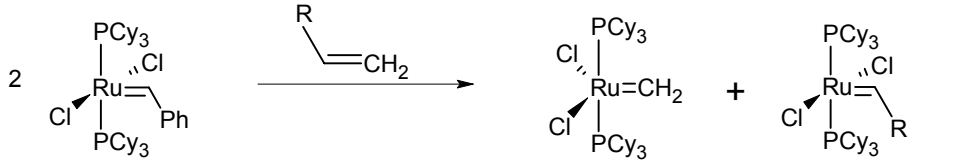

benzylidene (Grubbs catalyst) **2a**

methylidene **4a**

alkylidene **5**

R=C_6H_{13} **5a**

R= CH_2CH_3 **5b**

Scheme 1.3**: Catalytic species formed during the self-metathesis of any alpha olefin using Grubbs catalyst **2a

The decomposition of the methylidene **4a** and heptylidene **5a** (***Scheme 1.3***) under reaction conditions is of concern in the self-metathesis of 1-octene.

The methylidene **4a** and the propylidene **5b** are resting states of the catalyst in ring opening metathesis polymerisation (ROMP), ring closing metathesis (RCM) and acyclic diene metathesis (ADMET) reactions as well as cross metathesis (CM) reactions.[10]

Sanford and Love[11] have studied the thermal decomposition of the Grubbs catalyst propylidene **5b** extensively and it is thought that this decomposition occurs *via* a bimolecular pathway (***Scheme 1.4***). It was found by the same authors that the major decomposition products are trans-3-hexene, free PCy_3

and a mixture of unidentified ruthenium products. However, the exact mechanism of the reaction is still unclear.

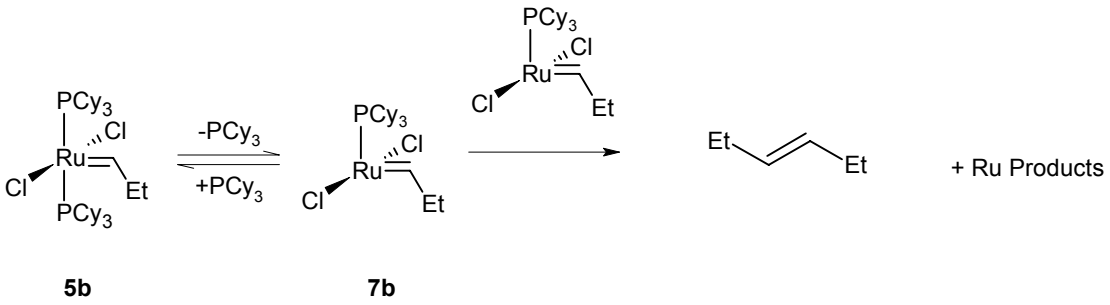

5b **7b**

Scheme 1.4**: Current suggested mechanism for decomposition of the propylidene **5b

The Grubbs benzylidene **2a** $[Ru(Cl)_2(PCy_3)_2CHPh]$ follows the same decomposition pathway as the propylidene,[12] with the formation of stilbene, presumably from the dimerization of the alkylidene fragment.

The methylidene **4a** $[Ru(Cl)_2(PCy_3)_2CH_2]$ clearly follows a different thermal decomposition pathway with all indications leading to decomposition *via* activation of the ligand.[11]

Thus far all decomposition studies have focussed on the thermal decomposition of the catalytic species[11,13] or specific reaction of the catalytic species with deactivators (for example, alcohols).[14,15] To the best of our knowledge, no decomposition studies carried out under reaction conditions have been reported.

1.2 Aims of the study

There are several opportunities for industrial scale implementation of homogeneous metathesis technology, for example the ethenolysis of 2-nonene for the production of 1-octene and the ethenolysis of methyl oleate.[16] However the economics of the processes become unfavourable due to the short lifetime of the catalyst. [16]

It is clear that the commercialisation of any homogeneous metathesis process will require a deeper understanding of the decomposition of the catalytic species formed in the reaction, especially under reaction conditions. The following were investigated in this study:

- Bimolecular decomposition of the Grubbs catalyst **2a** benzylidene $[Ru(Cl)_2(PCy_3)_2CHPh]$ *via* halide exchange between Grubbs catalyst di-bromide **2b** $[Ru(Br)_2(PCy_3)_2CHPh]$ and Grubbs catalyst **2a** (see Chapter 4).

- The halide exchange reaction between Grubbs catalyst **2a** or Grubbs catalyst methylidene **4a** $[Ru(Cl)_2(PCy_3)_2CH_2]$ and a salt (see Chapter 5).

- Ethylene induced decomposition of the methylidene species **4a** and **6** $[Ru(Cl)_2(PCy_3)(NHC)CH_2]$ formed from Grubbs catalyst **2a** and the second generation Grubbs catalyst **3** $[Ru(Cl)_2(NHC)(PCy_3)CHPh]$, in chlorinated and non chlorinated solvents (see Chapter 5). (NHC = 1,3-dimesityl-4,5-dihydroimidazole-2-ylidene).

Chapter 2: General Aspects of Relevance to the Metathesis Reaction

2.1 General Introduction to Catalysis

The systematic study of catalysis began early in the 19th century. In 1815, Davy[17] began working on the newly discovered Pt metal and invented the Davy lamp for use in the mines. This lamp contained Pt gauzes that glowed (catalytic combustion) in the presence of 'fire damp' (i.e. methane), warning miners that they were in a dangerous area.

The term catalysis was coined in 1836 by Berzelius.[18] He realised that there were species that could cause the formation of other species without themselves being part of the composition of the product and called this hitherto unknown power, catalytic power.

Catalysis has been misunderstood in the past, when scholars were taught that a catalyst does not take part in the reaction! Today catalysis can be defined as follows - "Catalysis is a process whereby a reaction occurs faster than the uncatalysed reaction, the reaction being accelerated by the presence of a catalyst".[17] Although a catalyst does not appear in the stoichiometric equation for an overall reaction, it is directly involved in the conversion and appears in individual mechanistic steps and in the rate law.

Today we depend on catalysis in varying forms for the production of plastics and fuel, for modification of food (e.g. margarine production[19]), for the removal of pollutants emitted from engines (catalytic converters) and for many processes in nature, the most impressive being the reactions in photosynthesis, without which life on earth as we know it would simply not exist. As much as 90% of our chemicals and materials use catalysis in at least one stage of their production.[17]

Requirements for a catalyst to be useful to industry today are that it be fast, selective, robust, cheap and easily separated from the reaction mixture.

2.2 Heterogeneous Catalysis

Heterogeneous catalysts are ill-defined catalysts, meaning that the active species itself cannot be easily identified. In heterogeneous the catalyst is in a different phase (either solid or liquid)[20] to the reagents. Usually, the catalyst is a solid that is (preferably) evenly distributed on a support such as alumina or silica and the reaction occurs on the surface or in the pores of the catalyst. The reactants and products are usually gases or liquids which are passed through the catalyst bed in the reactor. Continuous processes are thus fairly easy to design and operate, and separation of the catalyst from the reaction mixture is easily accomplished. Conditions for heterogeneous catalysis are generally harsher (higher temperatures, higher pressures, higher catalyst loading) than for homogeneous catalysis.

There are numerous examples of heterogeneous catalysis processes in industry, ranging from the Fischer Tropsch processes (HTFT,[21] LTFT,[22] SSPD,[23] CTL[24]), to unit operations in oil refineries, to modification of food. In fact, most industrial processes today involve heterogeneous catalysis at one stage or another.

2.3 Homogeneous Catalysis

In homogeneous catalysis, the catalyst is in the same phase as the reactants, usually dissolved in the reaction mixture.

2.3.1 Advantages of Homogeneous Catalysis

The main advantage of homogeneous catalysis over heterogeneous catalysis is that high selectivity and purer products can be often achieved using milder conditions. In heterogeneous catalysis there are different kinds of reaction sites on a surface (for example, Lewis and Brønsted acid sites) leading to a

number of different reactions and therefore products, whereas in a homogeneous reaction there is a single well defined active species at which the reaction takes place, leading to one product only. In homogeneous catalysis all active sites are accessible, therefore lower concentrations of catalyst can be used, which lowers operating cost.

Homogeneous reactions are often carried out under the pressure of reactive gases (for example, syngas in hydroformylation). A homogeneous system can be studied under reaction conditions using techniques such as high pressure (HP) NMR and high pressure infra-red (HPIR) spectroscopy.[25] Often the ligands used contain phosphorus, and thus HP ^{31}P NMR can be used as a direct probe to observe the catalytic species formed under reaction conditions. Previously, the exact species formed under pressure were difficult to identify or observe. HP NMR and HPIR spectroscopy have given researchers a new window to observe the catalyst under reaction conditions, enabling the R&D time to be cut dramatically.[26]

2.3.2 Disadvantages of Homogeneous Catalysis

The metals and phosphorus ligands used to form the catalysts needed for homogeneous catalysis are costly and are generally not environmentally friendly, making recycling of the catalyst necessary. One of the major problems in homogeneous catalysis is the separation of the catalyst from the reaction mixture. The ideal case is where the products separate from the reaction mixture as in Shell's ethylene oligomerisation unit in the SHOP process (see Section 2.4.4). The oligomers formed in the reaction form a new phase and are easily removed *via* a phase separation step.[7] The use of ionic liquids[27] as solvents is attractive since the ionic liquid can be chosen so that the reaction occurs in the ionic liquid phase or at the interface between two phases and the products separate out into a new phase. This has been extensively studied but as yet no commercial plant using ionic liquid as a solvent is in operation. The use of supercritical CO_2 as a solvent is also attractive because this can be easily removed after the reaction.[28]

In a truly homogeneous reaction, distillation is commonly used to separate the products from the catalyst. This is done in Sasol and Davy Process Technology's hydroformylation plant for the production of detergent alcohols in Secunda, South Africa.

2.3.3 Complexes for Homogeneous Catalysis

Homogeneous catalysts can be formed *in situ* or a preformed organometallic complex can be used. An example of a catalyst formed *in situ* is the formation of the phosphine modified hydride ($HCo(CO)_3L$) in Sasol's ModCo^{TM} Process.[26] The cobalt species formed in this reaction are shown in ***Scheme 2.1***.

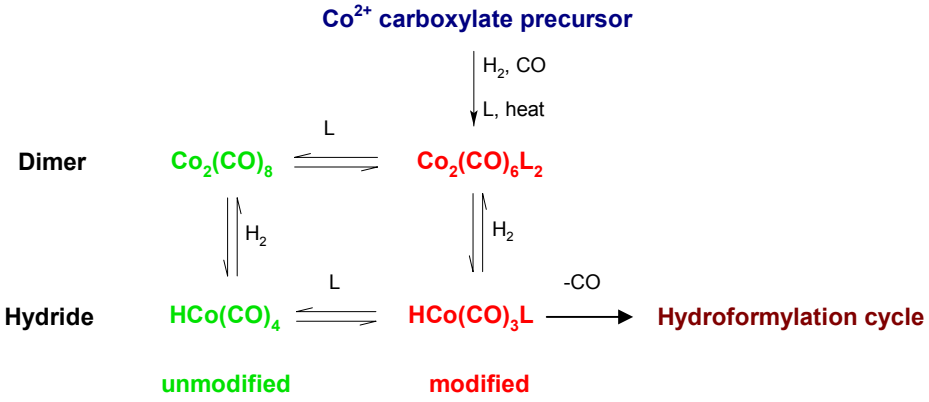

L = Phosphorus ligand of choice

Scheme 2.1: *Cobalt species formed in Sasol's ModCo^{TM} hydroformylation process*

In the ModCo^{TM} process a cobalt(II)carboxylate is co-fed with the phosphorus ligand of choice (L) dissolved in a hydrocarbon solvent. On heating in the presence of syngas (60 bar, 170 °C), the Co(II) is reduced to Co(I) and the modified hydride ($HCo(CO)_3L$) is formed, which is the precursor to the active species. The system has been extensively studied using HP NMR

spectroscopy.[26,29] Examples of the ligands studied are eicosyl phoban, Lim-C_{10} and Phoban-C_{10}.[30]

Although *in situ* generated catalysts are generally less costly, there is no general rule stating that either *in situ* or preformed catalysts are better or cheaper. When a new process is being developed, both types of systems are evaluated.

2.4 Olefin Metathesis

2.4.1 The Discovery of the Metathesis Reaction

At the Phillips Petroleum Company in 1964, Banks and Bailey[31] were investigating the use of alternative catalysts for the replacement of the HF acid catalyst for converting olefins into high octane paraffins by alkylation. When using a supported Mo catalyst, they found that instead of alkylation, the olefin molecules were split and they could convert propene to ethylene and 2-butene. This discovery was developed into the Phillips triolefin process and a small plant for the conversion of propene into 1-butene and ethylene was operated from 1966 - 1972 due to a demand for ethylene at the time.[32]

2.4.2 Olefins Conversion Technology® (OCT®)

64% of the propene produced today (March 2005) is used in the production of polypropylene.[33] At present, most propene is obtained from steam crackers, as a by-product of ethylene production. However, indications are that the demand for propene is outpacing the demand for ethylene and processes that produce propene 'on purpose' need to be investigated.[33]

OCT® uses the Phillips Triolefin Process in reverse, (i.e. the conversion of ethylene and 2-butene to propene) and this process is now offered for licence by ABB Lummus Global, Houston (USA).[7] The feed (a mixture of C4s and high purity ethylene) is heated and the reaction takes place in fixed bed reactors over two catalysts. In the first reactor, 1-butene is converted to 2-

butene (MgO catalyst) and the 2-butene reacts with ethylene over the WO_3/SiO_2 metathesis catalyst to produce propene in the second reactor. Naptha steam crackers, with an integrated OCT® unit, are being planned for the production of propene all over the world.[33]

There are several variants of the OCT® process. In the Lyondell[7] process, ethylene is dimerised to 2-butene using a homogeneous Ni catalyst, followed by heterogeneous metathesis with unreacted ethylene to produce propene. The Axens Meta 4® process[34] uses rhenium oxide on alumina to produce propene *via* the ethenolysis of 2-butene. Although this is a low temperature process, the catalyst is costly and undergoes rapid deactivation, hence this process was never commercialised.

2.4.3 Sasol Technology

Sasol Technology[35] has patented a heterogeneous autometathesis process where 1-butene is fed over a tungsten on silica catalyst. 1-Butene is isomerised *in situ* to 2-butene which undergoes metathesis with the remaining 1-butene to produce propene and 2-pentene. Self-metathesis of the 1-butene produces 3-hexene and ethylene. The ethylene formed undergoes metathesis with the 2-butene and 2-pentene to form more propene (see ***Scheme 2.2***).

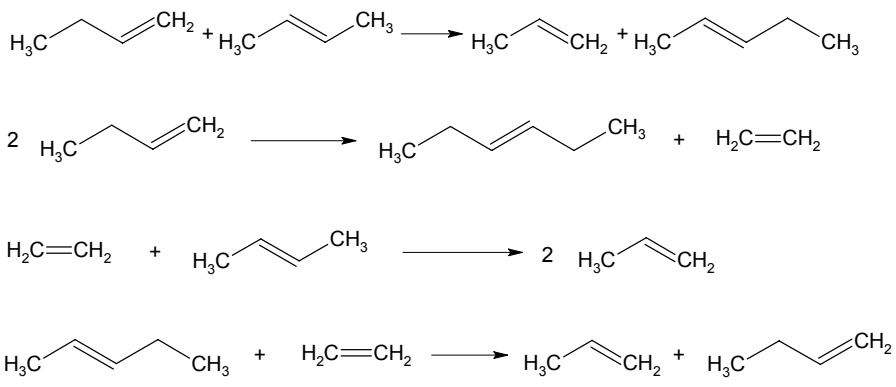

***Scheme 2.2**: Sasol's Technology for the production of propene via metathesis*

2.4.4 The Shell Higher Olefins Process (SHOP)

The Shell SHOP process[6] includes a heterogeneous metathesis reaction step for the production of α-olefins. A simplified flow scheme of the SHOP process is shown in ***Figure 2.1***.

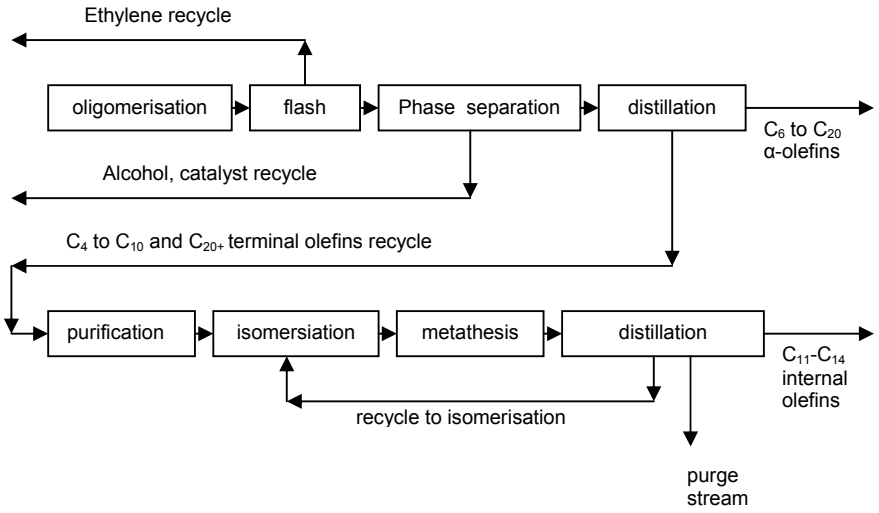

Figure 2.1: *Simplified flow scheme of the Shell Higher Olefin Process (SHOP)*

In the first step, ethylene is oligomerised in the presence of a homogeneous catalyst and a polar solvent, giving even-numbered α-olefins from C_4 to C_{40} with a Schultz-Flory distribution. The oligomerisation catalyst is a Ni hydride with a bidentate phosphine ligand. The Ni hydride is prepared from Ni salts using boron hydride as the reductant under ethylene pressure, after which the ligand is added. The Ni-hydride catalyst has surprisingly little isomerisation activity[36] and the major products are α-olefins. There are less than 3% branched or internal olefins in the product. The olefins formed are immiscible with the solvent (alcohol), providing easy separation and recycle of the catalyst. The desirable C_6 to C_{18} α-olefins are separated by distillation and fractionated into individual compounds for use as co-monomers for further processing into plasticizer and detergent alcohols, or synthetic lubricants.

The remaining lighter (<C_6) and heavier (>C_{18}) α-olefins undergo purification over an absorbent bed (to remove alcohol and ligand impurities) followed by double bond isomerisation to form internal olefins. The internal olefins formed are passed over an alumina supported molybdate catalyst where a mixture of odd and even-numbered internal olefins are formed *via* heterogeneous metathesis.

The product contains about 15% of olefins in the desired range ($C_{11}$to C_{14}) which are isolated by distillation. These C_{11} - C_{14} internal olefins are used as feed for a modified cobalt hydroformylation process for the production of detergent alcohols. The lights and heavies from the final distillation step are recycled to the isomerisation reactor (***Figure 2.1*** above). There is a purge stream from the distillation reactor to limit the build up of heavies, which can reach up to 50% due to the recycle to the isomerisation reactor.

2.4.5 Other Uses of the Metathesis Reaction

Sinopec has investigated the production of 1-hexene by self metathesis of 1-butene to 3-hexene (using AB Lummus technology)[7] and subsequent isomerisation of the 3-hexene to 1-hexene. This process was piloted but did not reach commercialisation.

3,3-Dimethyl-1-butene (Neohexene), an intermediate in the synthesis of musk perfume, is produced by the ethenolysis of 2,4,4-trimethyl-2-pentene (***Scheme 2.3***).[7]

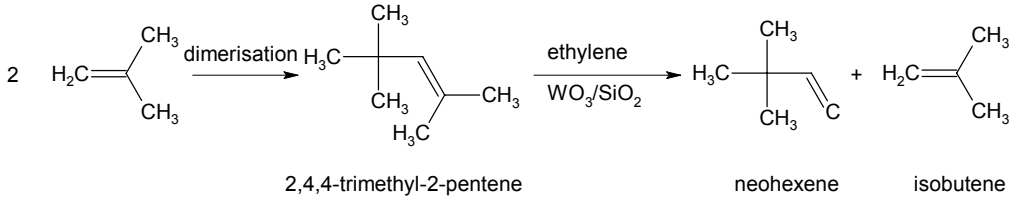

Scheme 2.3: *The production of neohexene from isobutene*

The first step is the dimerization of isobutene where a mixture of 2,4,4-trimethyl-2-pentene and 2,4,4-trimethyl-1-pentene is formed. The catalyst system used for the subsequent ethenolysis step is a mixture of WO_3/SiO_2 and MgO. The MgO isomerises the 2,4,4-trimethyl-1-pentene to 2,4,4-trimethyl-2-pentene which then undergoes ethenolysis. The isobutene produced in the reaction is recycled to the dimerization reactor. Chevron Phillips operates a neohexene unit with a capacity of 1400 tons per year. [7,37]

2.5 Early Homogeneous Catalysts for Metathesis

In the early years several ill-defined homogeneous systems were developed for the metathesis reaction. Typically the systems were Group 6 metal chlorides combined with an alkylating agent with Lewis acid properties, for example WCl_6 combined with $EtAlCl_2$.[38] The active species and the mechanism of activation were unknown for these systems, hence there was a drive to develop discrete organometallic pre-catalysts whose behaviour could be more readily understood and manipulated.

2.5.1 The Tebbe Complex

A well defined metathesis catalyst[2] is one where (i) the complex itself essentially resembles the active species in terms of metal oxidation state and ligand coordination sphere, (ii) is stable enough to be characterised using spectroscopic means and X-ray analysis and where (iii) reaction with an olefin yields a persistent new alkylidene from that olefin. The first well defined alkylidene complex to exhibit metathesis activity was the Tebbe complex **6** [39] (***Scheme 2.4***), which was generated by the reaction of Cp_2TiCl_2 with excess $AlMe_3$. It was shown that the Tebbe complex **6** could serve as a source of the methylidene (carbene) complex Cp_2TiCH_2.[40] The Tebbe complex was shown to react with deuterated methylene cyclohexane to produce the deuterated Tebbe complex and methylene cyclohexane in 1978.[41] This was the first time that a well defined alkylidene species had reacted with an olefin to form a propagating alkylidene that could be characterised.[39]

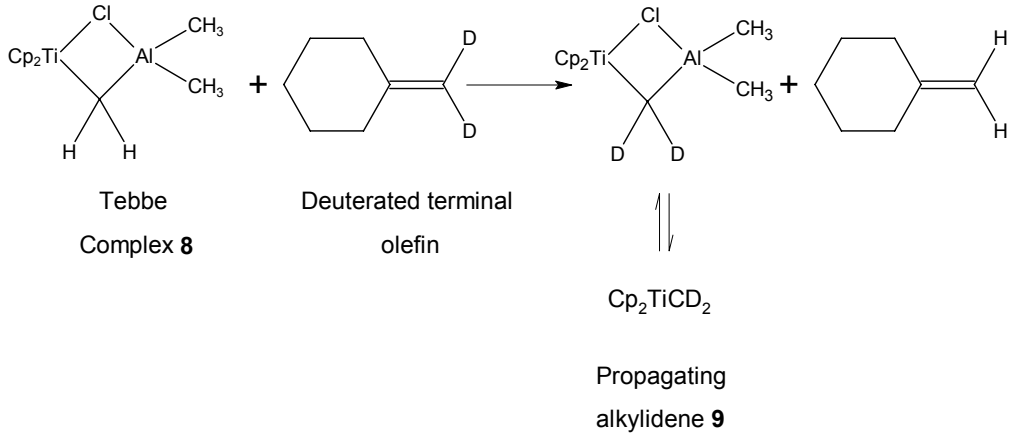

***Scheme 2.4**: Reaction of the Tebbe complex **8** with a deuterated terminal olefin*

Deuterium labelling experiments[39] (***Scheme 2.4*** above) using the Tebbe complex, showed that the kinetic products were also the thermodynamically favoured products (i.e. no deuterium scrambling took place, pairs of hydrogen or deuterium atoms were transferred). These results, as well as those from the study of Fischer carbenes (see Section 2.5.2), were best explained by the metallacycle mechanism proposed by Chauvin[4] and not by the favoured mechanism of the day[42]. The mechanism Chauvin proposed involves the coordination of an olefin to a metal carbene, followed by formation of the metallacycle **1** by 2+2 cycloaddition. Subsequent decomposition of the metallacycle then forms the new metal carbene (2+2 retro-cycloaddition) and the desired products as shown in ***Scheme 2.5***.

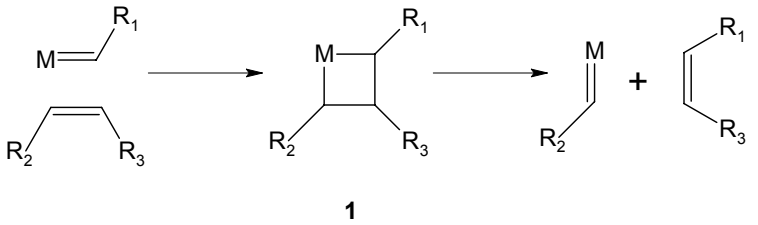

1

***Scheme 2.5:** Chauvin's mechanism for metathesis reactions*

This is remarkable because at the time that the mechanism was proposed (1970), the only systems available were ill-defined and no carbene intermediates had been detected.

2.5.2 Fischer Carbenes

Metal carbenes of type $M(=CRR^1)L_n$ can be divided into two categories, the Fischer type, where a heteroatom is attached to the carbene carbon, or the Schrock type, which contains only carbon atoms at the carbene carbon.

Various forms of Fischer carbenes were shown to have metathesis activity under varying conditions. The first isolable metal carbene **10** (***Scheme 2.6***) was made by Fischer[43] in 1964, but only reacted with strained cycloalkenes.[38] The diphenyltungstencarbonyl complex **11** was synthesised by Casey[44] in 1973 and is more reactive than the methoxyphenylcarbonyl complex **10** because the methoxy group is replaced with a phenyl group which has lower electron-donating capability. The diphenyltungstencarbonyl complex **11** was found to initiate metathesis on a number of olefins, including straight chained alkenes, for example, the metathesis of 2-pentene to 2-butene and 3-hexenes. This complex required no Lewis acid co-catalyst suggesting that tri-substituted alkenes (for example 1-methylcyclobutene) could undergo metathesis to form the translationally invariant unsaturated polymer polyisoprene, with perfect (within the limits of analysis) head to tail order.[45] For the same reaction, the ill-defined WCl_6 and $EtAlCl_2$ system resulted in the formation of mainly saturated polymers[45] because of the formation of tertiary cations during acid catalysed additions to the double bond.

However, the diphenyltungstencarbonyl complex **11** yielded only substoichiometric quantities of metathesis products, in addition to other products (for example, cyclopropanes). Although the initial carbene could be defined, no propagating metal carbene was detected and this is therefore still an ill-defined system. [38]

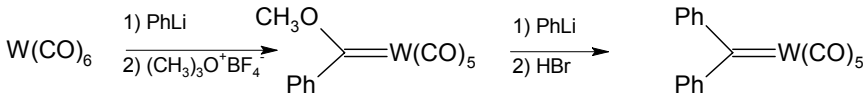

10 **11**

***Scheme 2.6**: Synthesis of the first isolable carbenes*

During the subsequent 8 years *ca.* 300 Fischer carbene complexes were prepared. [46]

The Fischer carbenes are also used for the polymerisation of acetylene. Although the methoxy phenyl complex **10** alone cannot polymerise alkenes,[44] complex **10** in the presence of a small amount of phenylacetylene effects this polymerisation.[38] This is because the phenylacetylene reacts first, resulting in the removal of the methoxy group from the metal center (***Scheme 2.7***).[38]

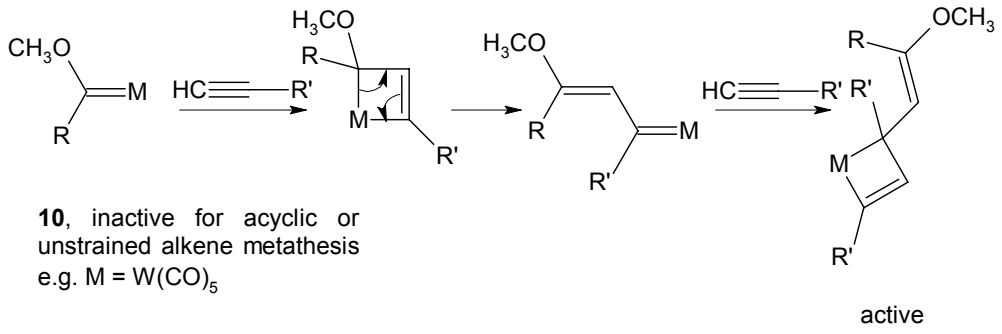

.

***Scheme 2.7**: Reaction of the methoxyphenyl complex **10** with alkylacetylene to produce a metathesis active catalyst*

The Fischer carbenes are also used for the rearrangement of enynes to dienes. [38]

2.6 The Nobel Prize for Chemistry 2005

It was announced recently that Robert Grubbs, Richard Schrock and Yves Chauvin were awarded the Nobel Prize for chemistry in 2005 for the

development of the homogeneous metathesis method in organic synthesis.[5] It is hoped that this new methodology (i.e. homogeneous metathesis) will usher in a new era for the production of drugs and plastics that are more efficient and less harmful to nature than traditional processes.

2.7 Schrock Carbene Complexes

Schrock's catalysts are characterised by the use of CHR alkylidenes. The first stable M=CHR complex synthesised was [Ta=CH-t-Bu(CH_2-t-Bu)$_3$] **12** (***Scheme 2.8***),[47] which was obtained by accident, during an attempt to synthesise Ta(CH_2-t-Bu)$_5$. This compound is sensitive to water and a variety of functional groups including aldehydes and ketones, with which it reacts to give polymeric (t-BuCH_2)$_3$Ta=O and an olefin.[48] It was later found that the trimethylphosphine complex [Ta=CH-t-BuCl$_3$(PMe_3)$_2$] **13** reacted with terminal olefins to produce four rearrangement products from a metallacyclobutane species.[49,50] [Ta=CH-t-BuCl(t-BuO)$_2$(PMe_3)$_2$] **14** reacted with styrene to produce [Ta=CHPhCl(t-BuO)$_2$(PMe_3)$_2$] **15** and also initiated the slow metathesis of 2-pentene.[49,50] However the ethylidene and propylidene intermediates formed in the metathesis of 2-pentene rearranged to give ethylene and propene respectively and so could not be observed.[49,50]

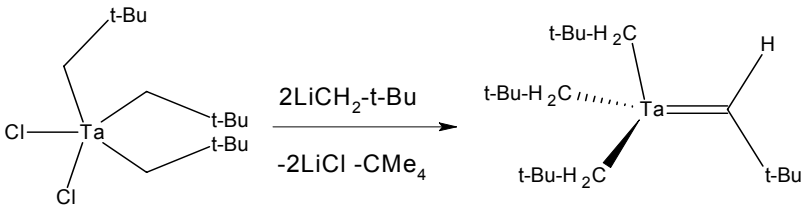

12

Scheme 2.8*: Formation of the first stable M=CHR complex*

The first tungsten Schrock alkylidene to be prepared was the 18 electron species [W(O)(=CH-t-Bu)(PEt_3)$_2$$Cl_2$] **16**, which could metathesise terminal olefins, albeit very slowly.[51] The rate of reaction was dramatically increased in

the presence of a trace amount of $AlCl_3$ and the propagating species $[W(O)(=CHEt)(PEt_3)_2Cl_2]$ **17** was observed for the first time.[50,51]

Complexes of the type [W≡ C-t-butyl$(OR)_3$] **18** were found to be highly active for alkyne metathesis.[2] The expected alkylidynes could be observed only when bulky electron withdrawing alkoxides were present, and were not observed when the alkoxide groups were replaced by chlorides. This indicates that for the tungsten Schrock catalysts, the alkoxide ligands promote metathesis while the chlorides promote side reactions that destroy the alkylidene.[52]

Complexes bearing the N-2,6-i-$Pr_2C_6H_3$ (NAr) imido ligands[53] were synthesised in 1986 to maximise steric protection at the metal center and to limit the ability of the imido ligand to form bridges between two metal centers, thereby preventing bimolecular decomposition. Some 14 electron $[W(NAr)(CH\text{-}t\text{-}Bu)(OR)_2]$ species **19** were isolated and were stable towards bimolecular decomposition due to the four sterically demanding ligands, all covalently attached to the metal center. [54]

The first Mo based catalysts, based on the W(NAr) catalysts above, were reported in 1987.[55] However, a practical synthesis of these catalysts was not reported until 1990 (***Scheme 2.9***).[56]

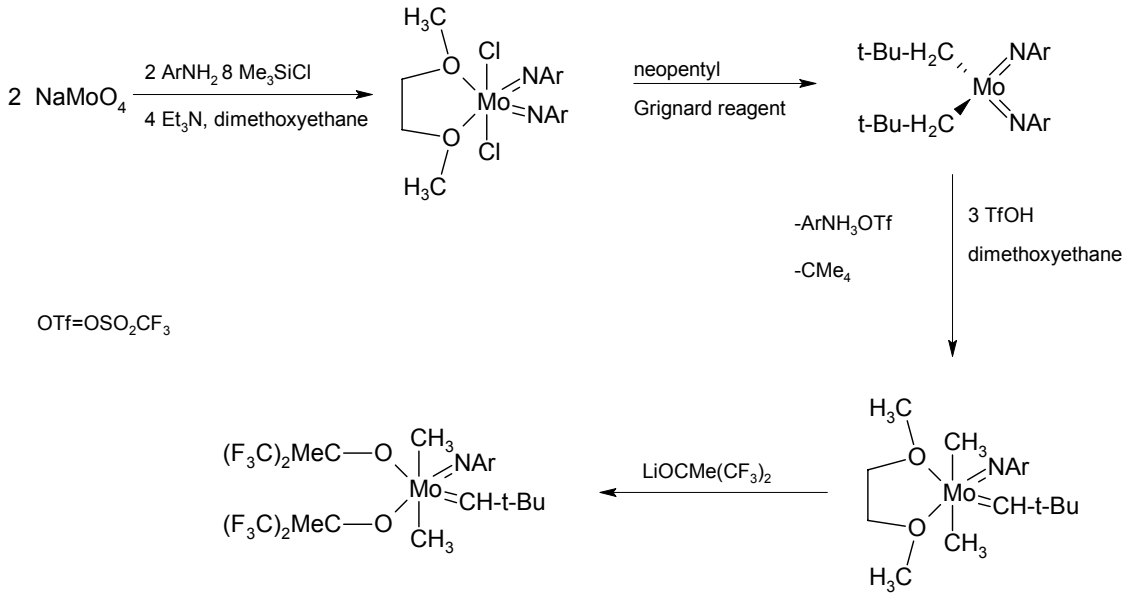

***Scheme 2.9**: Synthesis of Mo imido alkylidene catalysts*

The Mo based bis(alkoxy)arylimido alkylidenes are stable as long as the alkoxide ligand has sufficient bulk to prevent bimolecular decomposition. Many Mo based complexes were isolated and lists of stable compounds were reported.[54,57] It was discovered that the alkylidene complex can exist in two forms that interconvert *via* rotation about the M=C bond by 180°. The rate of rotation depends on the nature of the imido and alkoxide ligands and can vary from slow (10^{-5} s^{-1}) to fast (100 s^{-1}) at room temperature. [57]

Two primary routes for decomposition have been established, one being rearrangement of metallacyclobutanes to olefins, and the other being the bimolecular decomposition of the methylene complexes. Bimolecular decomposition was demonstrated for the 18 electron [$Ta{=}CH_2Cp_2(CH_3)$] **20** species. It is thought that an ethylene complex is formed from an intermediate that contains two bridging methylenes.[58,59]

The latest advances are concerned mainly with imidoalkylidene Mo and W complexes that contain chiral biphenolates or binaptholates. These complexes are used in asymmetric olefin metathesis.[2]

There has been some success with supported Schrock type catalysts. Catalysts have been prepared that can be linked chemically to a styrene backbone to prevent the bimolecular decomposition of the methylene complex.[60] However there was still some decomposition of the methylene species, leading to lifetimes that are shorter than expected. If no methylene complex is generated, then the catalysts are as efficient as those in solution.

Tungsten based chiral catalysts were also developed.[60] When compared to the molybdenum based catalysts it was found that a higher temperature was needed to obtain similar conversions, in spite of what appeared to be a higher rate of reaction. This is because the tungstacyclobutane formed is relatively stable with respect to dissociation to yield the product and the alkylidene.

Supported metal carbenes or carbynes of Mo, W or Re have been prepared which exhibit selectivities, activities and lifetimes close to those achieved using typical heterogeneous and homogeneous metathesis catalyts.[60]

2.8 Ruthenium Alkylidene Complexes

Homogeneous metathesis has become an extremely useful tool in organic synthesis due to the well defined and relatively stable metathesis catalysts introduced by Grubbs, $[Ru(PCy_3)_2Cl_2CHPh]$ **2a** and the second generation analogue $[RuCl_2(=CHPh)(H_2IMes)(PCy_3)]$ **3**.[8] The major advantage of the ruthenium alkylidene catalysts over Schrock's catalysts is that they are thermally more stable and much less sensitive to poisoning by polar and protic functionalities, including water. This means that the ruthenium catalysts can be used under much less stringently controlled reaction conditions.[28] However, the active catalyst is still sensitive to oxygen. Various ruthenium alkylidene complexes are shown in ***Figure 2.2***.

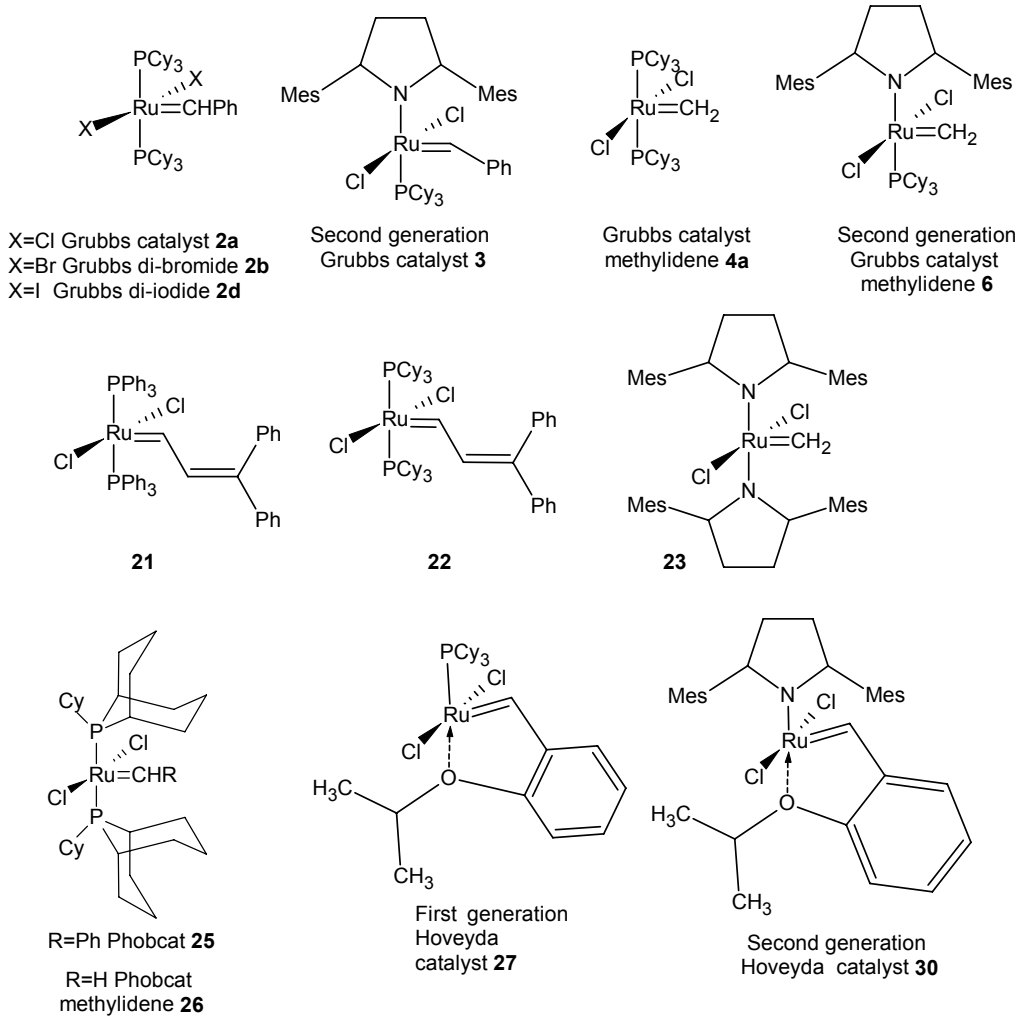

***Figure 2.2**: Ruthenium alkylidene catalysts used for homogeneous metathesis*

2.8.1 Mechanism of the Homogenous Metathesis Reaction using Ruthenium Alkylidenes

The accepted mechanism for the metathesis reaction involving carbenes and the formation of a metallacyclobutane was proposed by Chauvin[4] (see ***Scheme 2.5***).

Much effort went into determining whether the homogeneous metathesis reaction with ruthenium alkylidene species takes place *via* an associative or dissociative mechanism. Sanford, Love and Grubbs[61] studied the system extensively with several ruthenium alkylidene catalysts using ^{31}P

magnetisation transfer NMR and 1D ^{1}H NMR techniques. The study showed that the rate of metathesis is inversely proportional to the amount of free phosphine present, and that the rate of phosphine dissociation is independent of phosphine concentration. Thus the homogeneous metathesis reaction takes place *via* a dissociative mechanism. A study of initiation rates by the same authors supports this conclusion.[61]

Therefore the accepted mechanism for homogeneous metathesis reactions using ruthenium alkylidene complexes is as depicted in ***Scheme 2.10***. The first step is the dissociation of one phosphine ligand to form a 14 electron intermediate **7a**, followed by the coordination of an olefin. This is followed by formation of a ruthenium metallacyclobutane ring by 2+2 cycloaddition which breaks up (2+2 retrocycloaddition) to form the product olefin and a 14 electron ruthenium species that is ready for coordination of more olefin or free phosphine. Initiation, the formation of the propagating methylidene **4a** and alkylidene **5a** from the precursor (Grubbs catalyst **2a**), is shown in brown. Unproductive metathesis, where the same olefin is eliminated to what was coordinated, is shown in blue. Productive metathesis, where a different olefin is eliminated to that was coordinated, is shown in green.

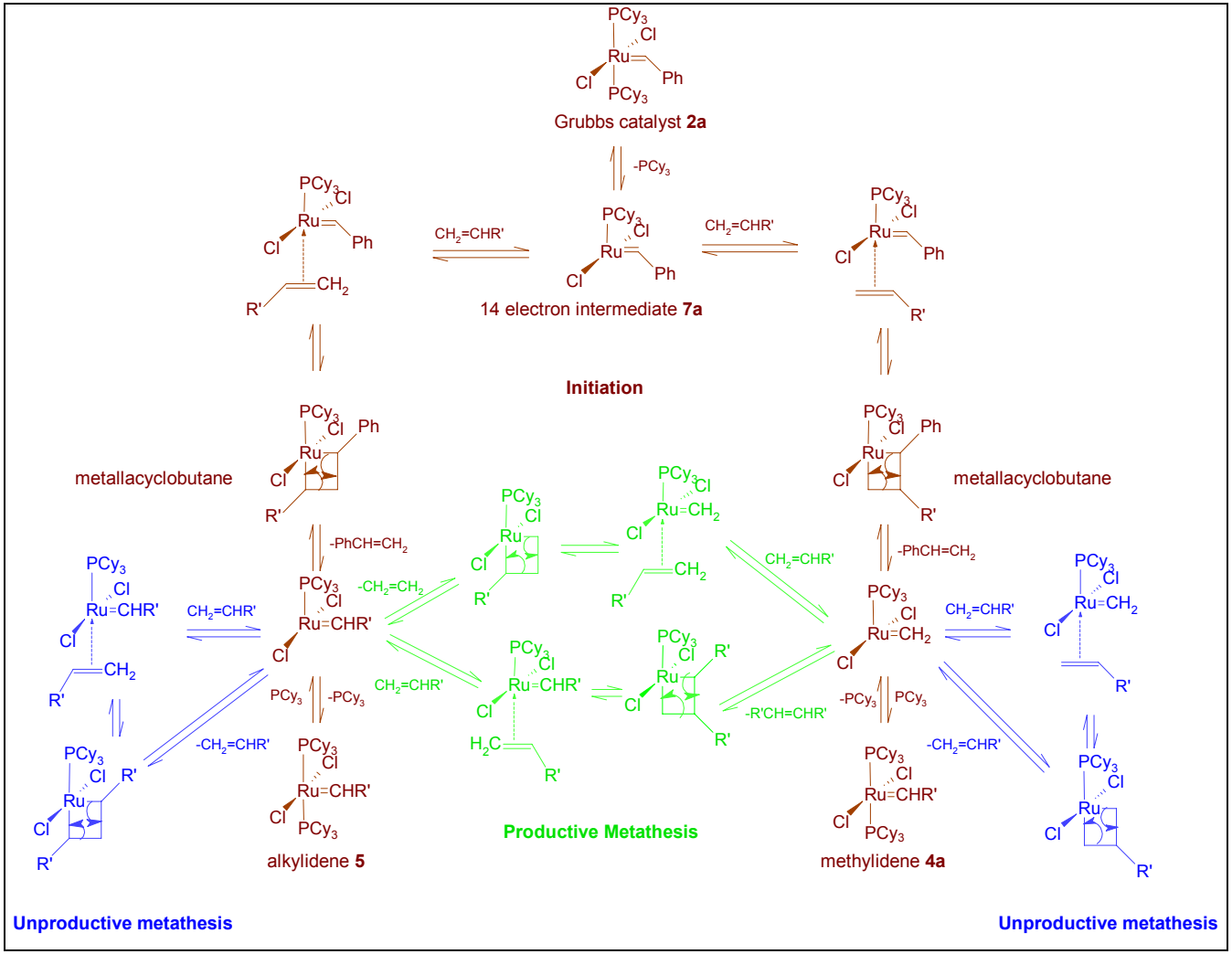

Scheme 2.10: *Accepted mechanism for the homogeneous metathesis reaction catalysed by ruthenium alkylidene complexes*

Recently, Piers *et al.* synthesised a catalyst where a Ru-cyclobutane intermediate **1b** was observed using low temperature ^{1}H NMR.[62] In this study a catalyst precursor was used where no phosphine dissociation was required (***Scheme 2.11*** below) making the formation of the Ru-cyclobutane **1b** the rate determining step.

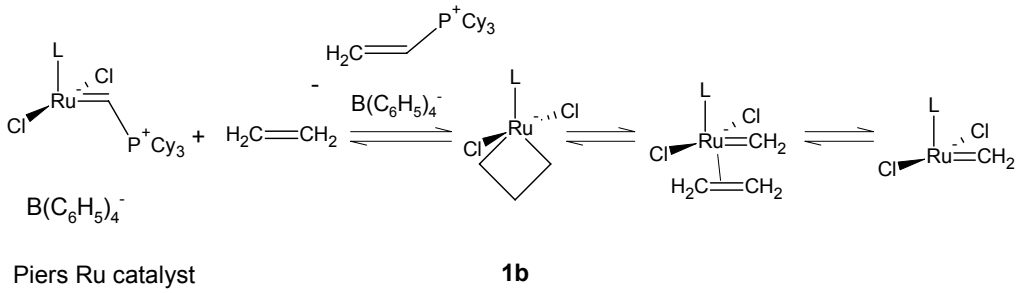

Scheme 2.11: *Piers ruthenium catalyst that does not require phosphine dissociation prior to metathesis*

This catalyst decomposes at -10 °C with the production of propene, probably because of the lack of excess phosphine to stabilise the active species.

2.8.2 1st Generation Grubbs Catalyst 2a [$Ru(Cl)_2(PCy_3)_2CHPh$]

The first phosphine ruthenium alkylidene to be discovered was the result of synergy and good communication within the Grubbs group. Johnson and Grubbs[63] had studied the reaction of diphenylcyclopropenes with W(VI) precursors to form W(VI) vinylalkylidene in an effort to make Schrock alkylidenes. This methodology was applied to $[Cl_2Ru(PPh_3)_3]$ in 1992 and the result was the formation of complex **20** (***Scheme 2.12***).[3, 64]

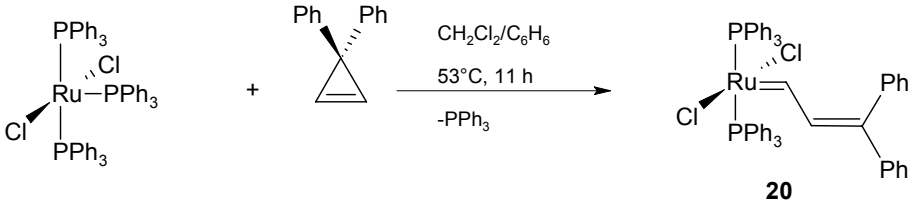

20

***Scheme 2.12**: Synthesis of the first metathesis active ruthenium alkylidene*

However, the bistriphenylphosphine complex **20** could only metathesise highly strained cyclic olefins, and attempts to replace the chlorides with several other electron-withdrawing anionic ligands met with limited success. In the Schrock systems the more electron-withdrawing the anionic ligands are, the higher the activity of the catalyst is, and it was thought that similar trends would apply for the Ru(II) catalysts. Eventually, in desperation and forsaking the previous logic, phosphine exchange was carried out, replacing the PPh_3 with the most electron donating phosphine in the stockroom, PCy_3. This resulted in the formation of the bis(tricyclohexylphosphine) complex **21** (***Figure 2.2***), which was found to catalyse the metathesis of 2-pentene, to effect RCM on a number of substrates, and to find use in a number of polymer applications.

In the search for a bulk synthesis of the new carbene ligands, phenyldiazomethane was used as the alkylidene precursor at -78 °C which lead to the synthesis of Grubbs catalyst **2a**. This methodology (***Scheme 2.13***) is used to produce kilogram quantities of Grubbs catalyst **2a**, which is now commercially available.

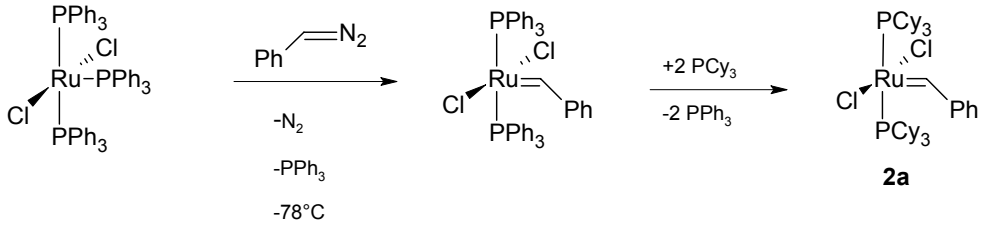

2a

Scheme 2.13**: Bulk synthesis of **2a

Large quantities of polymerisation catalysts are produced *via* the rearrangement of vinyl or propargyl halides (***Scheme 2.14***). This eliminates the use of the potentially explosive diazoalkanes and also the need for phosphine exchange in the synthesis of the ring opening metathesis polymerisation (ROMP) catalysts.

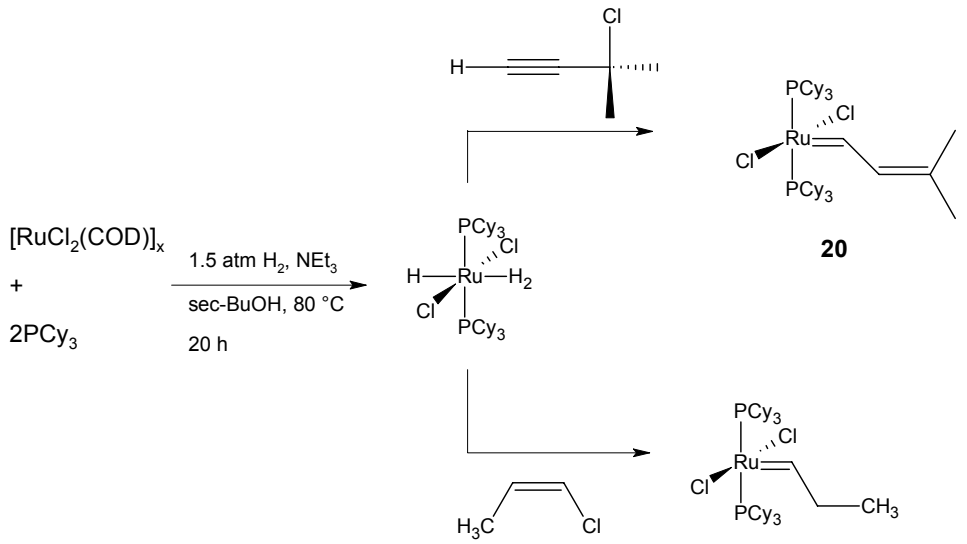

***Scheme 2.14**: Synthesis of ruthenium catalysts used for ROMP*

Both Grubbs di-bromide **2b** and Grubbs di-iodide **2d** (***Figure 2.2*** on page 22) have been synthesised by the Grubbs group,[61] using Finkelstein chemistry,[65] by reaction of Grubbs catalyst with LiBr in a mixture of THF and dichloromethane. The Finkelstein reaction is used in organic chemistry to exchange Cl or Br with I. This is possible because NaI is more soluble in acetone, tetrahydrofuran or crown ethers than NaBr and NaCl, thus any NaBr or NaCl that forms preciptates out and is removed from the equilibrium, thus allowing more exchange to take place. The Finkelstein reaction is now also used in organometallic chemistry to carry out halide exchange on various organometallic complexes, using halide salts in tetrahydrofuran or in acetone.[66,67,68]

Grubbs and co-workers[61] tested the di-bromide **2b** and the di-iodide **2d** and concluded that both are less active and less stable metathesis catalysts than

the chloride. The rate of phosphine dissociation was measured using magnetisation transfer NMR experiments and increases dramatically from Cl to Br to I.

2.8.3 2nd Generation Grubbs Catalyst 3 [$Ru(Cl)_2(PCy_3)(NHC)CHPh$]

The bis-N-heterocyclic carbene (NHC) complex **23** (***Figure 2.2*** on page 22) is formed by the reaction of Grubbs catalyst **2a** with two equivalents of N-heterocyclic carbene (NHC = 1,3-dimesityl-4,5-dihydroimidazole-2-ylidene). Hermann and coworkers showed that this complex showed little improvement on Grubbs catalyst **2a**.[69] Grubb's group then attempted to make the monophosphine, believing that the NHC may enhance phosphine dissociation from Grubbs catalyst **2a**, thereby increasing rates of reaction while still showing tolerance to water and air. The monophosphine N-heterocyclic carbene complexes **3** and **24** (***Scheme 2.15***) were successfully synthesised and showed improved rates and good stability. However, the rate of phosphine dissociation is actually decreased.[70] Although more active, the second generation Grubbs catalyst, **3** shows significant side reactions such as isomerisation in cross metathesis and ring closing metathesis (RCM) reactions.[71]

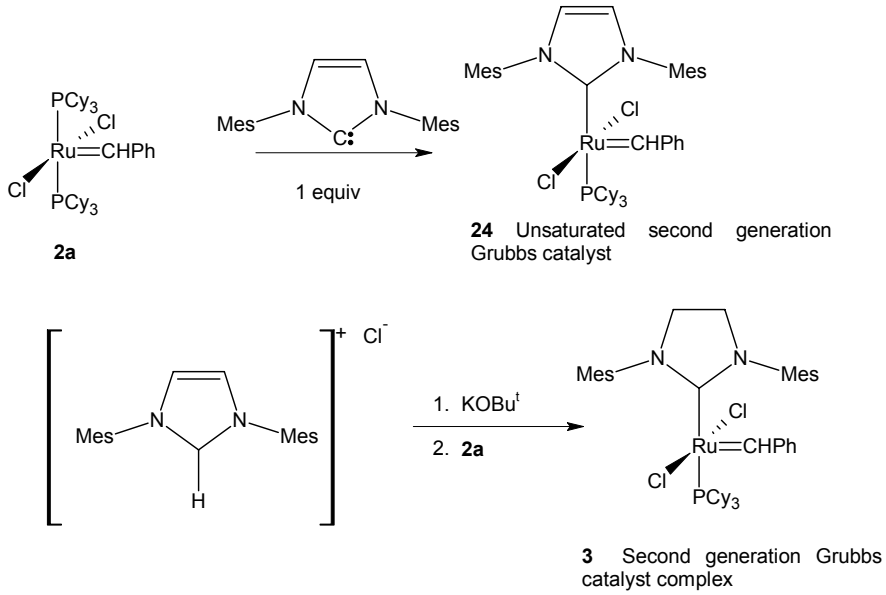

Scheme 2.15**: Synthesis of the second generation Grubbs catalysts **3** and **24

2.8.4 Phobcat 25 [Ru(Cl)$_2$(cyclohexyl[3.3.1]phoban)$_2$CHPh]

With the advent of the highly active NHC ruthenium alkylidene catalysts, most recent development efforts have focussed on these systems. However, a new bisphosphine ruthenium alkylidene metathesis catalyst, Phobcat **25**, was developed at Sasol Technology R&D in South Africa.[72,73] Here, a highly basic 2-phosphabicyclononane (phobane) ligand, similar to those employed in hydroformylation technology,[74] was used to make a new metathesis catalyst. Although hydroformylation technology generally makes use of straight chained phobanes (for example phobane-C_{10}, eicosyl phobane), it was decided to use a cyclohexylphoban ligand to maximise the bulk on the ruthenium center. Phobcat is synthesised as depicted in ***Scheme 2.16***.

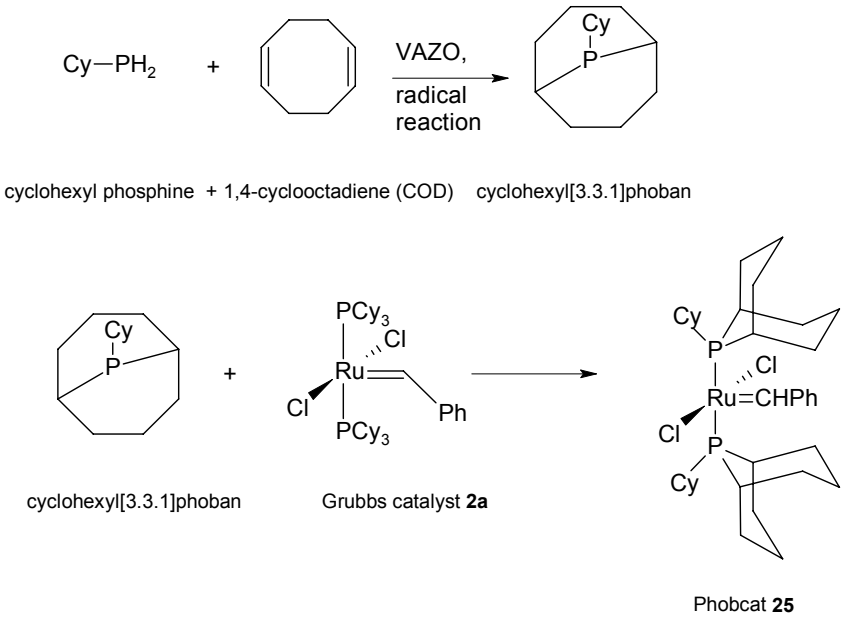

Scheme 2.16**: Synthesis of the Sasol homogeneous metathesis catalyst, Phobcat, **25

Phobcat **25** enjoys an improved lifetime and is useful for cross metathesis (CM), ring-closing metathesis (RCM) as well as ring-opening metathesis polymerisation (ROMP).[72] Replacement of the Cl ligands with Br ligands results in a catalyst with lower initial activity but much better stability. Both catalysts have been extensively studied using ^{31}P NMR and show interesting rotational isomerism in solution.[75] Very little isomerisation occurs when using Phobcat in cross metathesis reactions. Phobcat methylidene **26** (***Figure 2.2*** on page 22) appears to be more stable than Grubbs catalyst methylidene **4a**, possibly due to a different decomposition mechanism (see Section 2.11.3).

2.8.5 1st Generation Hoveyda Catalyst 27 [$Ru(Cl)_2(PCy_3)CH(C_6H_4O\text{-}iPr)$]

In 1997 Hoveyda noted that ROMP reactions with Grubbs catalyst **2a** were inhibited by the presence of isopropoxy vinyl ether, and the first generation Hoveyda catalyst **27** was suspected to be present. The Hoveyda catalyst **27** was synthesised by reaction of isopropoxy vinyl ether with Grubbs catalyst **2a** and the product formed was found to be catalytically active.[76] It was thought

that it would be more efficient and cheaper to synthesise the Hoveyda catalyst **27** directly from $[RuCl_2(PPh_3)_3]$ and thus the alternative synthesis in ***Scheme 2.17*** was developed. This follows the same protocol used in the synthesis of Grubbs catalyst **2a**. However, the synthesis of the required diazoalkane is a multistep process, making this route rather long and therefore more expensive.

The Hoveyda catalyst **27** is reported to be so robust that it can be recovered after the reaction by column chromatography and used again.[76] However, this could be because the catalyst is highly active but slow to initiate. Thus in each reaction only a small amount of active catalyst is formed and in the column separation the deactivated catalyst is removed and 'new' catalyst initiates in the next reaction.

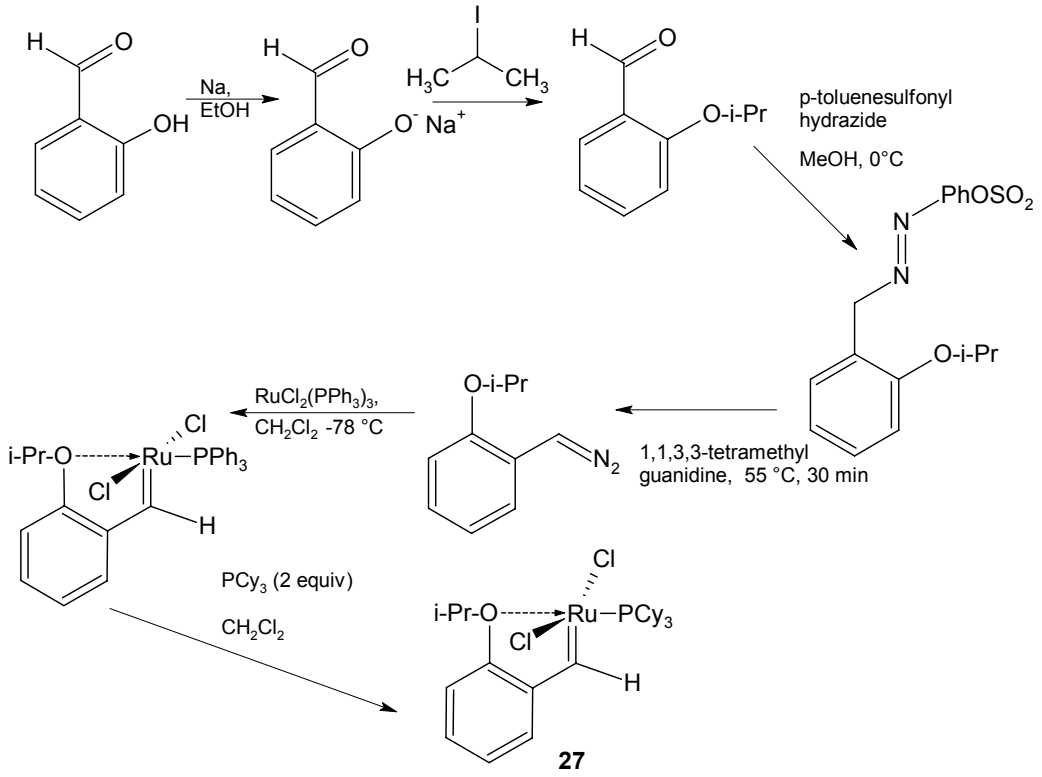

Scheme 2.17**: Alternative synthesis of 1st generation Hoveyda catalyst **27

Hoveyda and co-workers[77] attempted to synthesise complex **28**, where the isopropyl group has been substituted with a methyl group, using the synthetic route shown in ***Scheme 2.17***. This resulted in formation of a metathesis inactive doubly chloride bridged Ru triphenylphosphine dimer **29** which was isolated and characterised with X-ray crystallography (see ***Figure 2.3***). The stability of the unwanted dimer confirms the necessity for bulky ligands on the ruthenium center. The desired catalyst **28** was successfully synthesised but proved to be a less effective catalyst and was not recoverable by column chromatography.

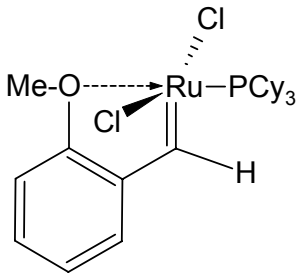

28

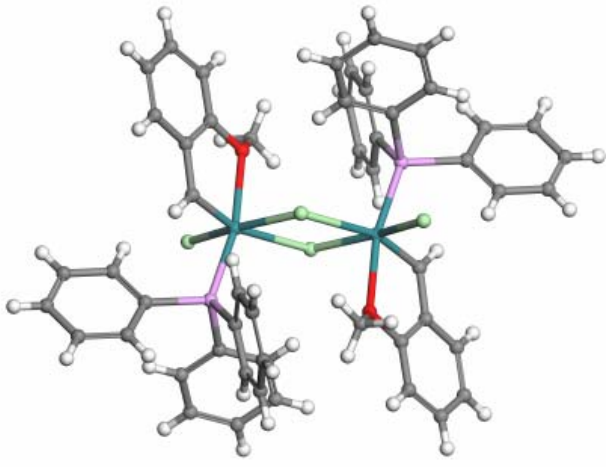

29

Figure 2.3: *Crystal structure[77] of the Ru triphenylphosphine dimeric complex **29** isolated en route to the first generation Hoveyda catalyst with the isopropyl group substituted with a methyl group, **28***

2.8.6 2nd Generation Hoveyda Catalyst 30 [Ru(Cl)$_2$(NHC)CH(C$_6$H$_4$O-iPr)]

The second generation Grubbs Hoveyda catalyst **30** (***Figure 2.2*** on page 22) is formed by reaction of the isopropoxy vinylstyrene ether with the second generation Grubbs catalyst **3** [Ru(Cl)$_2$(PCy$_3$)(NHC)CHPh] as shown in ***Scheme 2.18***.[77]

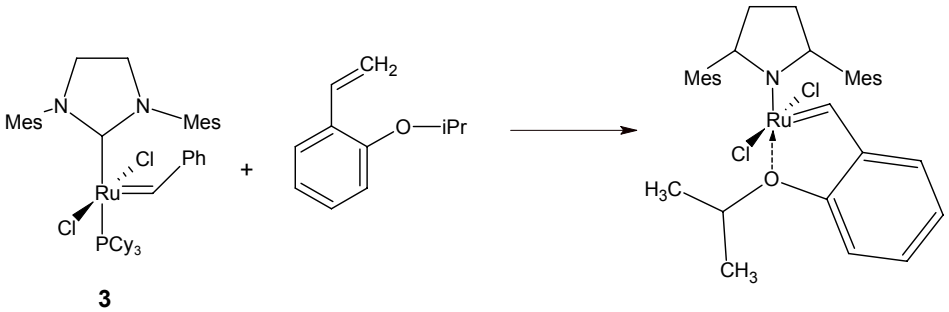

3 **30**

Scheme 2.18: *Synthesis of the second generation Hoveyda Catalyst **30***

The second generation Hoveyda catalyst **30** contains no phosphine and therefore cannot be studied with ^{31}P NMR. Again, recovery of the used catalyst by column chromatography is claimed.

Blechert[78] developed an improved synthesis and patented the catalysts formed by reaction of the second generation Grubbs catalyst **3** (or Grubbs catalyst **2a**) with a number of phenyl vinyl ethers with various substitution patterns on the aromatic ring, for example, complex **31.** (***Scheme 2.19***).

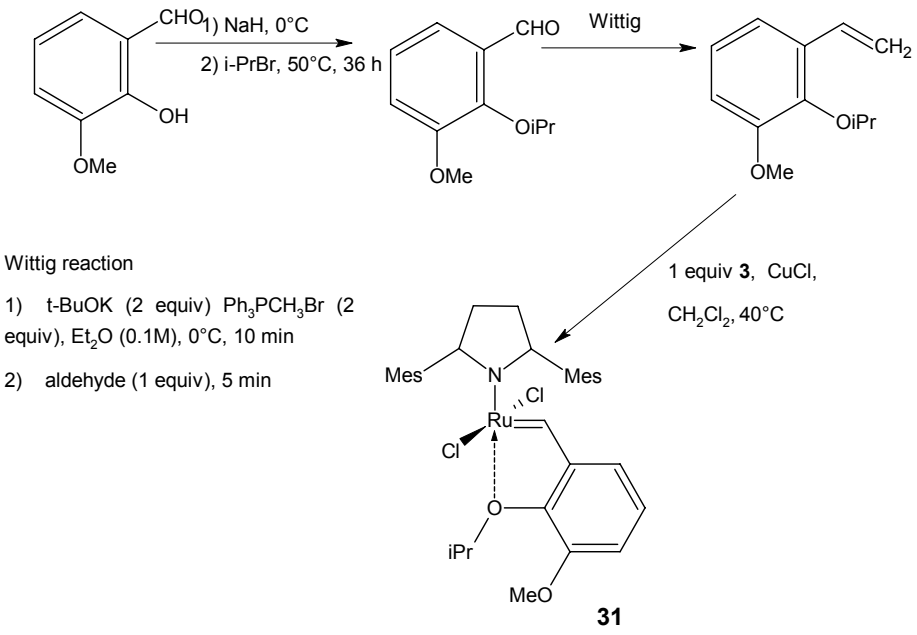

***Scheme 2.19**: Blechert's synthesis of second generation Hoveyda catalysts*

2.8.7 Cationic Dimeric Ruthenium Complexes

The dinuclear Ru dihydride **32** (***Scheme 2.20***) is a good precursor for cationic ruthenium alkylidene dimers. The neutral ruthenium alkylidene complex **33** is formed by reaction of the dihydride with propargyl or vinyl chlorides.[79,80] The catalytic activity of these complexes is increased significantly by reaction with trimethyl silyl triflate which abstracts a chloride and forms the cationic chloride bridged dimer **34** which can be isolated as the air stable dinuclear triflate. Three cationic chloride bridged ruthenium alkylidene dimers have been synthesised and characterised with NMR and X-ray crystallography.[79,80] The chelate effect severely decreases the lability of the phosphines. Initiation involves dissociation of the chloride bridge to form the 14 electron monocation **35** (***Scheme 2.21***) which is the active species. The monocation coordinates olefin and enters the catalytic cycle. The activity depends on the dimer/monomer equilibrium as well as the olefin coordinated complex.

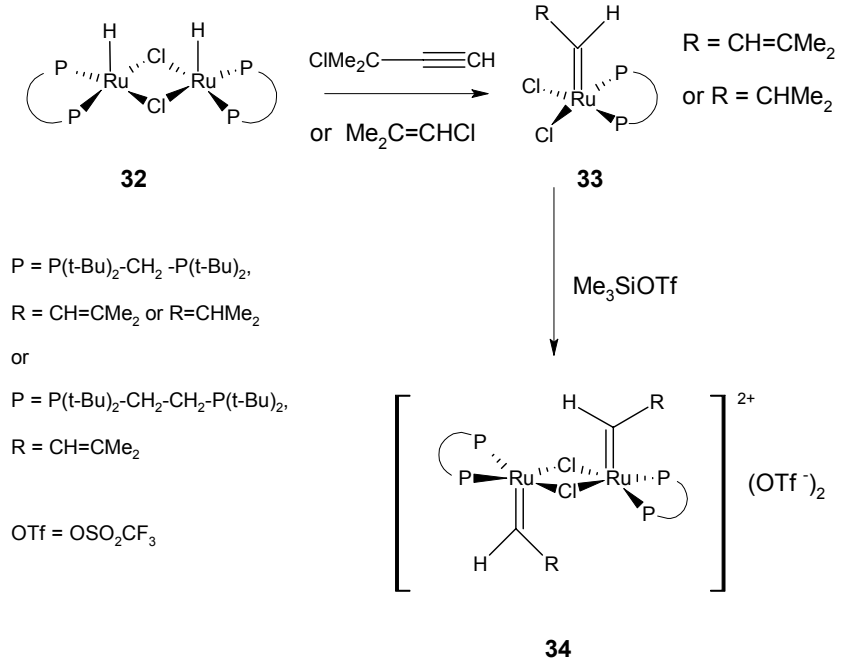

***Scheme 2.20**: Formation of ruthenium alkylidenes with cis chelating phosphines and their conversion into cationic dimers*

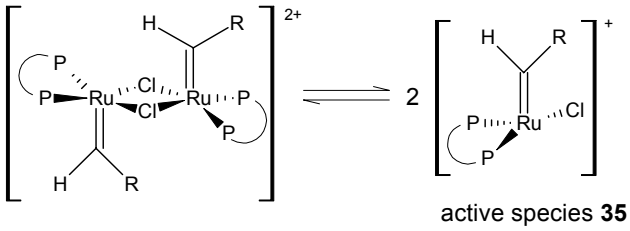

Scheme 2.21**: Dissociation of the cationic ruthenium dimer to form the 14 electron metathesis active monocation **35

The authors attempted to replace the chlorides with bidentate anionic ligands in an attempt to stop dimerization and hence form a more active catalyst. This resulted in complexes exhibiting low metathesis activity because the formation of the active species by dissociation of the anionic ligand was slow and

possibly also because the intrinsic reactivity of the active monocation formed was lower than that of the chloride.

2.8.8 The *In-situ* Homogeneous System

Ruthenium alkylidene complexes are expensive to make because they require multistep processes from $RuCl_3$. An alternative is to make the complex *in situ*. A metathesis system was patented by Nubel and Hunt[81] where $RuCl_3$, propargyl chloride, and a phosphine are mixed and heated with 1-octene in an inert atmosphere. Better conversions and selectivity are obtained if the reaction is sparged with hydrogen. This system was further studied and optimised by Vosloo *et al*.[82]

2.8.9 Immobilisation of Ruthenium Alkylidene Metathesis Catalysts

The immobilisation of homogeneous ruthenium catalysts on polymer beads has been attempted in order to facilitate separation of the catalyst from the reaction mixture for recycling. This would result in the selectivity of a homogeneous catalyst with the ease of separation of the catalyst for recycle, a feature of heterogeneous catalysis. [83]

Supported ruthenium metathesis catalysts, where one phosphine is bound to the support, are available.[84] However, both the phosphines are labile, thus binding a phosphine to the support results in leaching when phosphine dissociation occurs. If both phosphines are bound to the support,[85] then the activity is reduced.[83]

The alkylidene of the first generation Grubbs catalyst[86] can be bound to the support. This catalyst effectively dissipates into the reaction medium because it is freed after just one cycle, but after the reaction is complete the catalyst binds to the resin again, in a system known as the boomerang system.[87] The spent catalyst resin is easily separated from the reaction mixture and can be recycled.

Second generation Hoveyda 'boomerang' systems have been successfully synthesised, have good activity and can be recycled.[88,89,90,91] However, it is possible that the activity may be due to a small amount of $(NHC)X_2Ru=CHR$ which is freed after the first turn over cycle, which propagates very quickly.[83] As the initiation of the second generation catalyst is slow, these systems may be simply a slow release reservoir of active catalyst.

Reaction of a functionalised polystyrene resin with silver nitrate to form a supported silver salt, which is then reacted with Grubbs catalyst **2a** results in an immobilised catalyst where one chloride is replaced with an O-R group (R = functionalised resin).[92] The catalyst prepared in this way was easily separated from the reaction products and can be recycled. The products were free from ruthenium.

Dendrite and polymer-supported complexes of the first and second generation Hoveyda catalysts **27** $[Ru(Cl)_2(PCy_3)CH(resin\text{-}C_6H_3\text{-}O\text{-}iPr)]$ and **30** $[Ru(Cl)_2(NHC)CH(resin\text{-}C_6H_3\text{-}O\text{-}iPr)]$[93] have been made, but studies show that the ruthenium is released during the metathesis cycle and activity is diminished after recycling of the catalyst.

Second generation Grubbs catalysts where one mesityl group has been replaced with an $R\text{-}Si(OEt)_3$ group have been successfully synthesized and bonded to a silica surface.[94] These catalysts were active for ring closing metathesis and could be recycled up to 5 times without losing significant activity.

2.9 Applications for Ruthenium Homogeneous Metathesis Catalysts

Ruthenium alkylidenes have been applied to a number of different substrates resulting in the well known metathesis reactions. An intriguing facet of

metathesis is that the same catalysts can be used with varying substrates and conditions to perform the entire spectrum of different metathesis reactions.

2.9.1 ROMP (Ring Opening Metathesis Polymerisation)

ROMP (***Scheme 2.22***) is the major driving force behind the homogeneous metathesis catalyst development and has been extensively studied.[95] The polymers formed are unsaturated and therefore allow direct incorporation of functionality into the backbone.

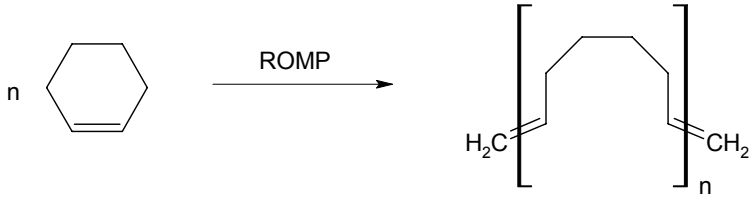

Scheme 2.22*: Ring opening metathesis polymerisation*

The chain growth can be controlled by chain termination or the adjustment of monomer/catalyst ratio. Block polymers may be synthesised because the propagating species remains at the end of the chain, so addition of more (or different) monomer results in further chain growth. This kind of polymerisation is known as living polymerisation, because there is no termination of the chains. If a mixture of monomers is used, the reactivity of the two monomers plays an important role in the composition of the product. In the extreme case, the more reactive monomer will react first, followed by the less reactive monomer, resulting in a perfect block copolymer, or a tapered block copolymer where only the middle section contains both monomer units.

Secondary metathesis reactions resulting in intermolecular or intramolecular chain transfer within the growing chain must be significantly retarded. Intermolecular chain transfer is the metathesis between two growing polymer chains resulting in transfer of the metathesis active transition metal to other chains. This causes deactivation of some chains and leads to a broadening of

the molecular weight distribution. Intramolecular chain transfer, known as backbiting, results in the formation of cyclics and macrocyclics. Highly strained cyclic olefins like cyclobutene and norbonene are suitable for living ROMP because the strained cyclic olefins are far more reactive than the olefin units in the resulting polymer chains.

There are several transition metals that have been used as ROMP catalysts including Ti, W, Mo and, of course, ruthenium catalysts. The great advance in this area came with the development of the well defined ROMP catalysts (initiators), as these facilitated the development of living ROMP. Although the first block copolymers made consisted of non-polar segments only, recent advances have lead to functional group tolerant well defined ruthenium ROMP catalysts with which block copolymers with pendant polar functional groups have been synthesized.

ROMP can be used for the formation of alternating copolymers by ring-opening insertion metathesis polymerisation (ROIMP). The treatment of diacrylates and cycloalkenes with the second generation Grubbs catalyst **3** $[Ru(Cl)_2(PCy_3)(NHC)CHPh]$ yielded a highly AB alternating polymer in high isolated yield. However, the creation of an alternating copolymer with similar monomers has not yet been achieved.

2.9.2 CM (Cross Metathesis)

In CM, two olefins react to form two different olefins as shown in ***Scheme 2.23***. This has been extensively reviewed by Cannon and Blechert.[96]

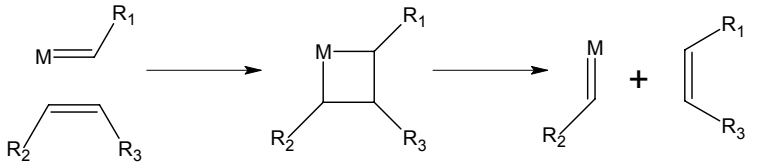

Scheme 2.23*: The cross metathesis of two olefins*

An example of a cross metathesis process is the self-metathesis of 1-heptene to 6-dodecene which can be further processed using the Sasol ModCo™ hydroformylation process to produce detergent alcohols.[7] The ethenolysis and self-metathesis of methyl oleate have also been studied extensively.[16]

2.9.3 ADMET (Acyclic Diene Metathesis)

ADMET polymerisation (***Scheme 2.24***) is a self-metathesis reaction of a terminal diene to form high molecular weight polymers with narrow molecular weight ranges, with the evolution of ethylene. Any mono-olefin present will act as a chain capping reagent, thus the purity of the monomers is important. This reaction has been extensively studied.[97]

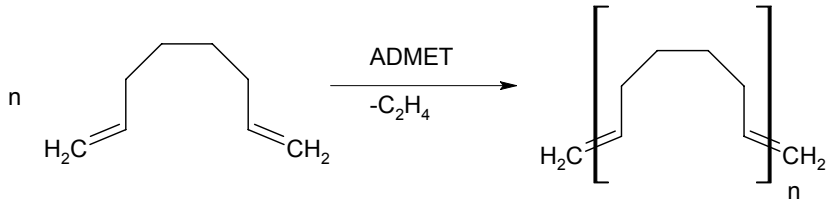

***Scheme 2.24**: ADMET reaction*

2.9.4 RCM (Ring-Closing Metathesis)

RCM (***Scheme 2.25***) is the most prominent field of olefin metathesis for organic synthesis.[98] This is one of the most straightforward and reliable methods for the formation of small, medium sized and large ring systems.

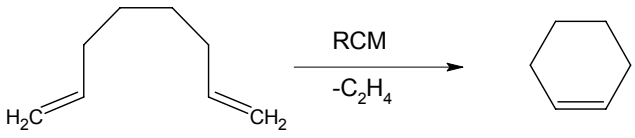

***Scheme 2.25**: Ring closing metathesis*

The main competing reaction in RCM is thought to be oligomerisation *via* ADMET. The rate of oligomerisation can be reduced by lowering the concentration of the diene in solution by adding the substrate slowly. High temperatures favour ring closure above oligomerisation, but at these higher temperatures there is more catalyst decomposition. However, recent studies show that the ADMET products found in an RCM process may be intermediates rather than by-products, and the stringent procedures designed to reduce ADMET (high dilution, higher temperatures) may not be necessary.[28]

2.10 Non-Metathesis Reactions of Bisphosphine Ruthenium Alkylidene Complexes

2.10.1 Isomerisation

One of the major side reactions in metathesis is isomerisation. This often hampers selectivity towards the desired products. Sworen[99] and Lehman[71] both report extensive isomerisation when using the second generation Grubbs catalyst **3** [$RuCl_2(PCy_3P(NHC)(CHPh]$.

2.10.2 Degenerate Alkylidene Proton Exchange of the Carbene Proton

Grubbs and Lynn[100] reported that there is degenerate deuterium exchange with solvent-derived deuterium atoms when water soluble ruthenium alkylidenes are dissolved in protic solvents such as D_2O and CD_3OD. The rate of exchange is independent of phosphine concentration, showing that phosphine dissociation does not occur in this reaction. The rate of exchange is inversely proportional to the concentration of added chloride in aqueous solution. The postulated mechanism for this reaction is *via* the dissociation of a Cl ligand as shown in ***Scheme 2.26***.

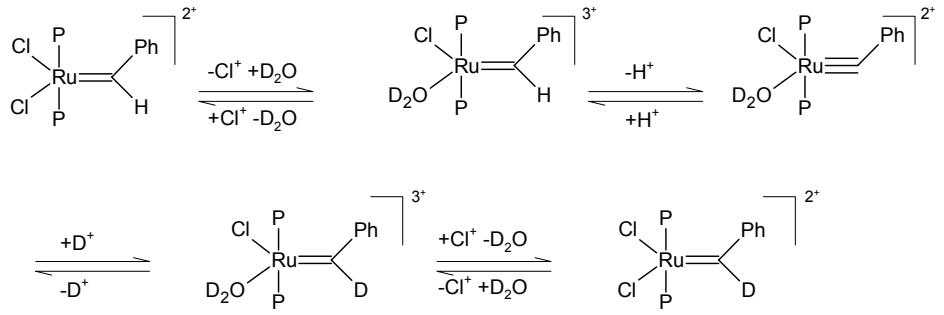

P = $PCy_2(Et)N(Me)_3^+$ Cl^-

***Scheme 2.26**: Degenerate deuterium exchange of water soluble ruthenium alkylidenes in deuterated protic solvents*

2.10.3 Halide Exchange

There is dissociation of the chloride in protic media (***Scheme 2.26*** above) hence halide exchange between complexes with different coordinated halogens may occur, although the possible halide exchange has not been studied in detail to our knowledge.

There has been some interest in modification or replacement of the halides in ruthenium bisphosphine alkylidene complexes in aprotic media. In the Schrock catalysts, replacement of the Cl ligands with other anionic donors resulted in much greater capability to tune activity and selectivity. This prompted Fogg and co-workers[101] to make halide free stable ruthenium metathesis catalysts using aryl oxides. Initial results showed low activities but progress has now been made using a variant of the second generation Hoveyda catalyst, where the chlorides have been replaced by O_2CCF_3, reaching a turnover number of 1400 in 2 hours, with a catalyst loading of 0.5 mol%, at 45 °C.[102]

Demonceau *et al.*[103] found that in the early stages of the ATRP reaction, using Grubbs catalyst **2a,** and ethyl-2-bromo-2-methylpropanoate as initiator,

[$Ru(PCy_3)_2Br_2CHPh$] **2b** as well as a new carbene complex tentatively identified as [$Ru(PCy_3)_2BrClCHPh$] **2c** were formed.

However, although the Grubbs group have synthesized the di-bromide **2b**, and the di-iodide, [$Ru(PCy_3)_2I_2CHPh$] **2d**, as part of a mechanistic study, little work has been undertaken on varying the halogens on Grubbs catalyst **2a** *in situ*. In this study it is demonstrated that the halogens are readily exchanged *in situ* and in fact, that halide exchange occurs continuously in any solution of ruthenium bisphosphine alkylidene complexes.

2.10.4 Kharasch Reaction

The Kharasch reaction is the addition of $CHCl_3$ across a double bond (***Scheme 2.27***). Snapper *et al.*[104] used Grubbs catalyst **2a** to catalyse the addition of $CHCl_3$ to a variety of 1,1-disubstituted olefins. Styrene was exposed to chloroform (10 equivalents) for 2 hours at 65 °C in the presence of 2.5 mol% Grubbs catalyst **2a** [$Ru(Cl)_2(PCy_3)_2CHPh$] which resulted in quantitative conversion to the Kharasch product. This is achieved using milder conditions than those used for the conventional Kharasch catalyst [$RuCl_2PPh_3$]. The reaction was severely inhibited in the presence of 2,6-di-*tert*-butyl-4-methylphenol (BHT), which is a free radical scavenger, thus it is thought to occur *via* a free radical mechanism. No reaction occurred in the presence of only the phosphine or the phosphine oxide, supporting the assumption that the reaction is ruthenium mediated.

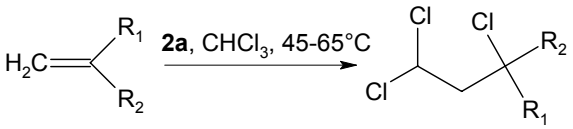

R_1=Ph, hexyl, COOMe, Bu, COOEt

R_2=H, Me

Scheme 2.27: *Reaction of $CHCl_3$ across a double bond via the Kharasch reaction in the presence of Grubbs catalyst **2a***

2.11 Decomposition of Ruthenium Alkylidene Catalysts

The major obstacle to the large scale commercialisation of homogeneous cross metathesis technology is generally the short lifetime of the catalyst. Commercial scale processes (for example, the ethenolysis of methyl oleate) are being investigated, but the turnover numbers achieved are still not high enough to justify the building of a plant due to catalyst poisoning and/or decomposition.[16] Also, side reactions such as double bond isomerisation hamper selectivity to the desired products.[71,105] The understanding of decomposition pathways may lead to the development of improved catalysts, additives or processes that overcome these problems.

2.11.1 Substrate Induced Decomposition

There has been growing interest in the deactivation of Grubbs type catalysts because of the possibilities for commercialisation of homogeneous metathesis technology. Recent studies at Sasol[106] revealed the possibility of substrate induced decomposition of the Grubbs catalyst methylidene **4a** $[Ru(Cl)_2(PCy_3)_2CH_2]$ and the second generation Grubbs catalyst methylidene **6** $[Ru(Cl)_2(PCy_3)(NHC)CH_2]$ under ethenolysis conditions *via* β-hydride transfer from the ruthenacyclobutane intermediate with the formation of propene amongst other short chained hydrocarbons. This forms part of the current study and is discussed in Chapter 5.

2.11.2 Bimolecular Decomposition of the Alkylidene

The decomposition of the propylidene **5b** $[Ru(Cl)_2(PCy_3)_2CHCH_2CH_3]$ has been extensively studied as a model reaction for bimolecular decomposition.[11] This was chosen because ruthenium alkylidenes (as modelled by the propylidene) are resting states in ROMP, RCM, CM and ADMET reactions. The major decomposition products are free PCy_3, trans-3-hexene (presumably from dimerization of the alkylidene fragment) and unidentified ruthenium products, including several hydrides. The decomposition follows

second order kinetics and is severely inhibited by the addition of excess PCy_3. As the reaction progresses, the increasing isomerisation activity of the catalyst results in the conversion of the trans-3-hexene to several hexene isomers. The suggested mechanism is shown in ***Scheme 2.28***. Note that the decomposition actually proceeds from the 14 electron intermediate **7a** that is required for the metathesis reaction to take place. Thus any attempt to increase the rate of the reaction by increasing the amount of the 14 electron intermediate **7a** in solution (for example, by addition of a phosphine scavenger such as CuCl) will result in increased decomposition *via* this route.

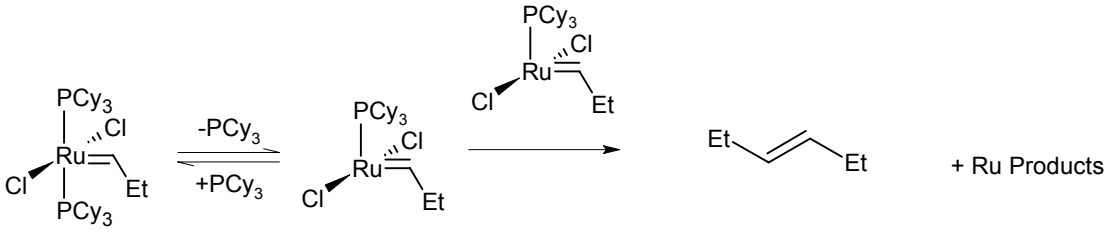

Scheme 2.28**: Current suggested mechanism of decomposition of the propylidene **5b

The Grubbs catalyst benzylidene **2a** follows the same pathway as the propylidene.[12] Stilbene is detected, presumably from the dimerization of the alkylidene fragment. [12]

Fogg and co-workers[107] synthesised the monoalkylidene triple chloride bridged dinuclear Ru species **38**. This was achieved by reaction of 3,3-dimethyl butyne with the triply chloride bridged Ru species **36** (***Scheme 2.29*** on page 46).

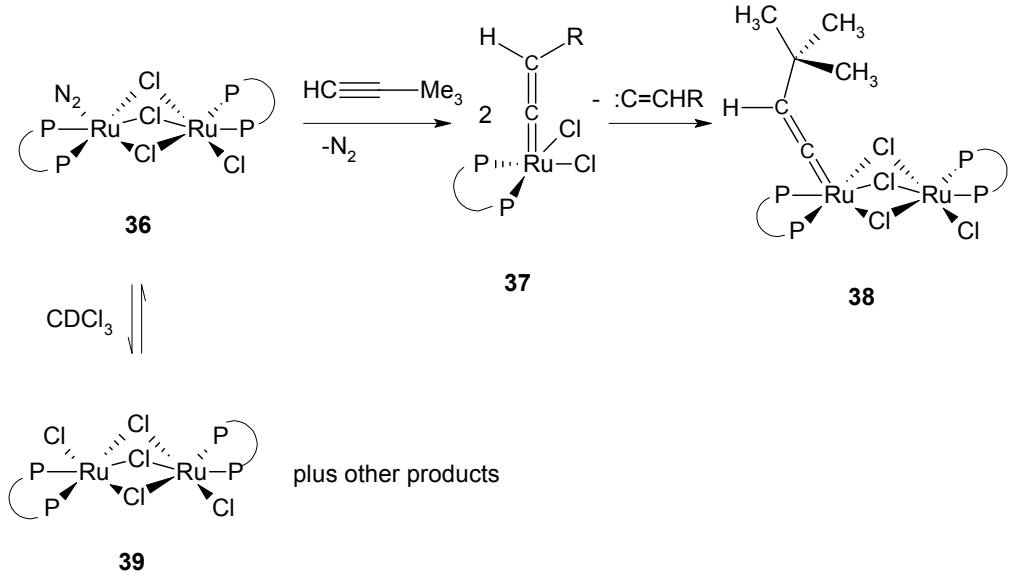

***Scheme 2.29**: Formation of the triple chloride bridged monoalkylidene dimeric species **38,** using a cis phosphine chelating ligand*

The formation of complex **38** could either take place *via* cross dimerization, homodimerization or reaction at the site vacated by the N_2 ligand. The reaction was found to take place *via* homodimerization of **37** with extrusion of the alkylidene as $Me_2C{=}CHCH{=}CHCH{=}CMe_2$. The dimer was isolated and a crystal structure and NMR data were obtained.[107]

Similar chemistry is thought to occur for the Grubbs triphenylphosphine precursor $[Ru(PPh_3)_2Cl_2CHCH{=}CMe_2]$ **40**.[108] The dimer formed cannot be isolated but has similar NMR spectra to that of the dimer with the cis chelating phosphine ligand, showing that the triphenylphosphine dimer formed also contains two phosphine ligands per ruthenium center.

Fraser *et al.* have isolated and characterised the triply chloride bridged ruthenium dimer **41** using crystallography.[109] This dimer is similar in structure to **40** except that the benzylidene has been replaced by a C=S group. This shows that the proposed dimer **40** is probably possible, even if it cannot be isolated.

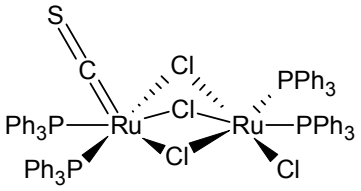

41

Scheme 2.30: *Fraser's triply bridged stable ruthenium dimer*

The starting complex **36** (***Scheme 2.29***) decomposed to a mixed valence $[Ru_2Cl_5(dycpb)_2]$ complex **39** in $CDCl_3$ which showed no ^{31}P NMR signals due to paramagnetism. Complex **39** was isolated and characterised with X-ray crystallography.

The isolated dimer **38** shows very little activity and Fogg[107] speculated that a related process with loss of one bulky phosphine ligand may occur for Grubbs catalyst in chlorinated solvents. The proposed reaction for the bimolecular decomposition of Grubbs catalyst where the more labile phosphine ligand is lost in preference to the carbene is depicted in ***Scheme 2.31***.

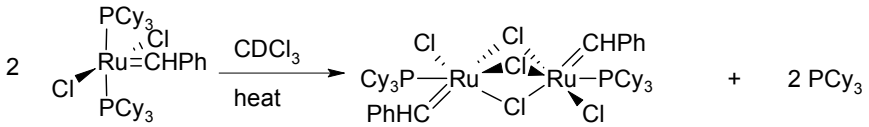

2a **42**

Scheme 2.31*: Possible decomposition pathway for Grubbs catalyst* ***2a*** *in chloroform*

2.11.3 Thermal Decomposition of the Methylidenes 4a, 6 and 26

The thermal decomposition of the Grubbs catalyst methylidene **4a** $[Ru(Cl)_2(PCy_3)_2CH_2]$ has been studied extensively.[11] The decomposition of **4a** is first order with respect to phosphine concentration and is not inhibited by

excess phosphine. Deuterium labelling experiments show that the deuterium from the methylidene fragment is incorporated in the phosphine ligand of the decomposition products. All evidence points to a unimolecular reaction involving intramolecular activation of the phosphine ligand.

Grubbs[13] and co-workers have studied the thermal decomposition of the second generation Grubbs catalyst methylidene **6** $[Ru(Cl)_2(PCy_3)(NHC)CH_2]$ in benzene to form methyltricyclohexylphosphonium chloride as well as an isomerisation active dinuclear ruthenium carbyne complex which was isolated and characterised.

Forman *et al.* [72] studied the thermal decomposition of phobcat methylidene **26** $[Ru(Cl)_2(cyclohexyl[3.3.1].phoban)_2CH_2]$ and report the formation of ethylene. This is significant because it indicates a bimolecular decomposition pathway while a unimolecular decomposition pathway has been reported for Grubbs catalyst methylidene **4a** $[Ru(Cl)_2(PCy_3)_2CH_2]$, the second generation Grubbs catalyst methylidene **6** $[Ru(Cl)_2(PCy_3)(NHC)CH_2]$ and variants thereof.[11]

2.11.4 Reaction with Water, Alcohols and Oxygen

Mol and co-workers[14] identified $[Ru(PCy_3)_2ClPhCO]$ which forms on reaction of Grubbs catalyst **2a** with primary alcohols, water and oxygen. This is the often present metathesis inactive impurity at δ 25.4 in the ^{31}P NMR spectrum in solutions of Grubbs catalyst **2a**. Further studies showed the second generation Grubbs catalyst **3** also reacts with primary alcohols, water and oxygen, forming carbonyl ruthenium complexes.[15] Ki-Won Jun *et al.*[110] recently reported that ruthenium benzylidenes react with water to produce benzaldehyde and an aqua ruthenium complex. All of these studies underline the necessity for a dry, inert atmosphere for metathesis reactions in order to avoid deactivation of the active species *via* these routes.

2.12 Additives

Forman *et al.*[111] discovered that the addition of phenol to a metathesis reaction using Grubbs catalyst **2a** [$Ru(Cl)_2(PCy_3)_2CHPh$] greatly improves the conversion and selectivity obtained. High pressure ^{31}P NMR studies prove that the lifetime of the catalyst with added phenol is greatly improved in both chlorinated and non-chlorinated solvents under catalytic conditions. ^{31}P NMR studies over time showed that this improvement in lifetime of the propagating species is not seen in the absence of olefin.

The peaks corresponding to phenol in the ^{1}H NMR spectrum shift when Grubbs catalyst **2a** is added to the solution, indicating that there is a definite interaction between the two species.[111] Both PCy_3 and $O{=}PCy_3$ interact with phenol with marked changes in the chemical shift in the presence of phenol. Molecular modelling indicates that the phenol is hydrogen bonded to the complex *via* the chloride ligand. It is also possible that the phenol acts as a free radical scavenger and inhibits free radical decomposition pathways.

Meyer *et al.*[112] report the formation of a Sn-Ru dinuclear ruthenium complex when $SnCl_2$ is added to a solution of Grubbs catalyst **2a** [$Ru(Cl)_2(PCy_3)_2CHPh$] in CD_2Cl_2. In the key experiment, CuCl was added to Grubbs catalyst in CD_2Cl_2 which resulted in a green solution which showed no metathesis activity and no ^{31}P NMR signal. $SnCl_2$ was then added which resulted in the return of the NMR signal (peak at δ 28, with Sn satelites) and the formation of an orange solution from which crystals were isolated and found to be the Ru-Sn dimer **43** shown in ***Figure 2.4***.

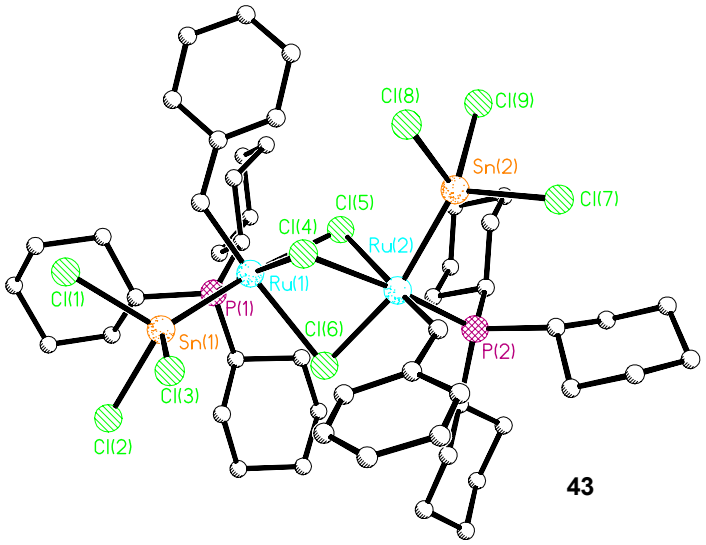

Figure 2.4: *Crystal structure of the diruthenium complex* ***43*** *$[HPCy_3][Ru_2Sn_2(PCy_3)_2(=CHPh)_2Cl_9]_4$ ($[HPCy_3]$+ omitted for clarity).*

The crystals[112] obtained for **43** were tested for metathesis activity and found to be highly metathesis active, in contrast to the low activity ruthenium dimers reported by Fogg *et al*.[107] The authors speculate that it is possible that a free site becomes available *via* the dissociation of two of the chloride bridges, thus this is a catalyst that does not require phosphine dissociation before metathesis can occur. However, it could also be that this dinuclear complex is in equilibrium with the monomer, which is in fact the active species. It is interesting to note that reaction with the solvent is likely because there is more chloride in the product than would be expected. $SnCl_2$, $SnBr_2$, $FeCl_2$ and $FeBr_2$ were tested as additives in the self metathesis of 1-octene using Grubbs catalyst **2a** and were found to be highly beneficial in both chlorinated and non-chlorinated solvents, suggesting the formation of the Ru-Sn dinuclear ruthenium complex *in situ.*

Chapter 3: Synthesis and Characterization of Complexes

This study focuses on the use of NMR and GC/MS to study the decomposition of Grubbs catalyst **2a** $[Ru(Cl)_2(PCy_3)_2CHPh]$ *via* the halide exchange reaction. An additional topic is the decomposition of the Grubbs catalyst methylidene **4a** $[Ru(Cl)_2(PCy_3)_2CH_2]$ and the second generation catalyst methylidene **6** $[Ru(Cl)_2(PCy_3)(NHC)CH_2]$ under ethenolysis conditions (NHC = 1,3-dimesityl-4,5-dihydroimidazole-2-ylidene). Thus these complexes as well as Grubbs catalyst di-bromide **2b** $[Ru(Br)_2(PCy_3)_2CHPh]$ and Grubbs catalyst di-iodide **2d** $[Ru(I)_2(PCy_3)_2CHPh]$ had to be obtained or synthesised.

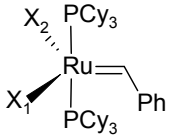

2

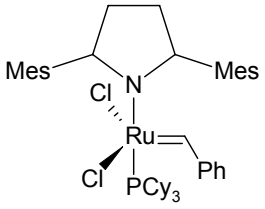

3

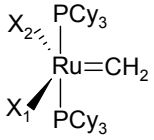

4

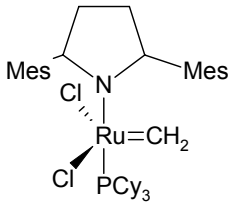

6

2a $X_1=X_2=Cl$

2b $X_1=X_2=Br$

2c $X_1=Br$ $X_2=Cl$

2d $X_1= X_2=I$

2e $X_1=Cl$, $X_2=I$

4a $X_1=X_2=Cl$

4b $X_1=X_2=Br$

4c $X_1=X_2=I$

4d $X_1=I$, $X_2=Cl$

4e $X_1=Br$, $X_2=Cl$

***Figure 3.1**: Selected ruthenium alkylidene complexes*

3.1 Grubbs Catalyst 2a [$Ru(Cl)_2(PCy_3)_2CHPh$]

Grubbs catalyst **2a** was obtained from Aldrich, stored under argon at 4 °C and used without further purification.

The structure and ^1H numbering of Grubbs catalyst **2a** is as shown below:

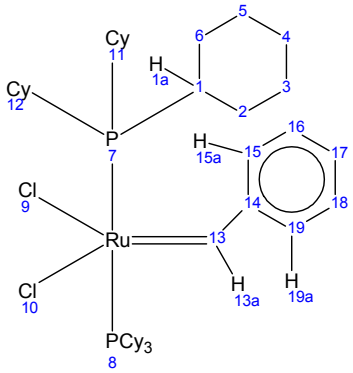

Figure 3.2**: Structure and ^1H numbering of Grubbs catalyst **2a

Grubbs catalyst **2a** (24 mg) was dissolved in 0.6 mL $CDCl_3$. ^{31}P NMR, ^1H NMR and HMBC[113] (heteronuclear multiple bond correlation, J = 8 Hz, ni = 128, nt = 4) spectra and were recorded at 30 °C. The purity of the final complex was determined to be 92.9% using ^{31}P NMR.

HMBC spectra of the carbene region and the aliphatic region of Grubbs catalyst in $CDCl_3$ were recorded and the ^{31}P NMR spectra and ^1H spectra are shown as traces on the HMBCs in ***Figure 3.3***. The ^{31}P NMR spectrum of the complex shows three peaks. Grubbs catalyst resonates at δ 37, tricyclohexylphosphine oxide resonates at δ 52 and an impurity at δ 25.

The HMBC of the carbene region is significant because until now, it was not known whether the carbene proton (H_{13a}) couples to the ^{31}P nucleus. The ^1H-^{31}P HMBC clearly shows coupling between the carbene proton (H_{13a}) and the ^{31}P nucleus. This is evidence that the resonance seen in the ^{31}P NMR spectrum is indeed a carbene species.

A ^{31}P-^{1}H HMBC of the aliphatic region was used to identify the protons closest to the ^{31}P nucleus (***Figure 3.3***). The HMBC shows long range coupling between the ligand protons (δ 0.8 to δ 2.6) and the ^{31}P nucleus for Grubbs catalyst (δ 37). H_{1a} is expected to be slightly more deshielded than the rest of the ligand protons due to close proximity to the ^{31}P nucleus, thus the peak at δ 2.6 in the ^{1}H NMR spectrum is assigned to H_{1a}. The other ligand protons were not assigned due to the number of conformations that the cyclohexyl ring can adopt.

The resonance at δ 25 in the ^{31}P NMR spectrum is $[Ru(PCy_3)_2ClPhCO]$ which is formed by reaction of Grubbs catalyst **2a** with primary alcohols, water and/or oxygen.[14] (see Section 2.11.4 on page 48). This resonance shows coupling to signals from δ 1.2 to δ 2.4, thus the PC<u>H</u> from $[Ru(PCy_3)_2ClPhCO]$ is assigned to the signal at δ 2.4 in the proton spectrum for the same reason as above.

The signal for tricyclohexylphosphine oxide at δ 52 (^{31}P NMR) shows long range correlation to the proton signals from δ 1.2 to δ 2.0, which represent the protons in the cyclohexyl ring.

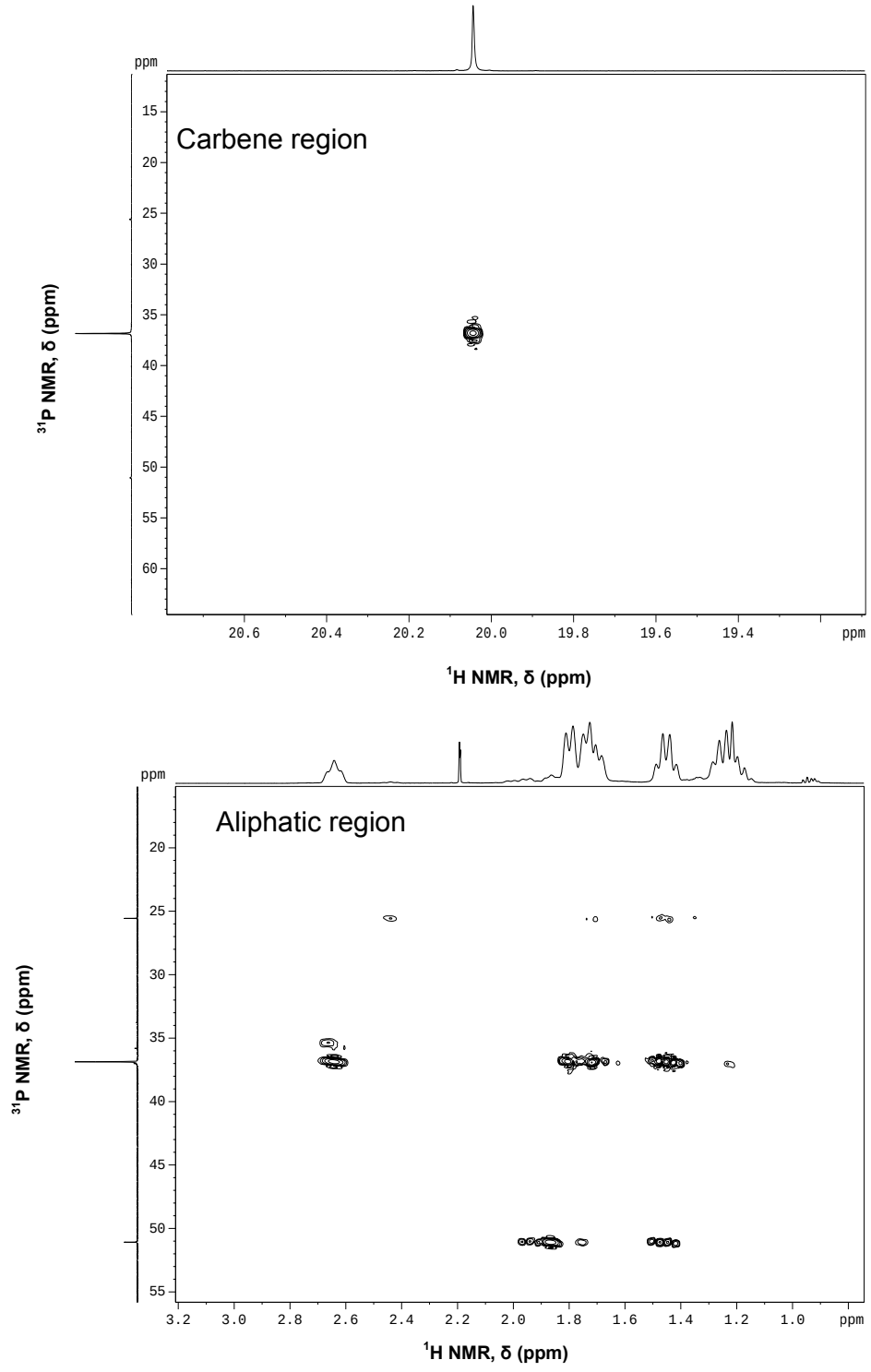

Figure 3.3: *^{1}H-^{31}P HMBC of the carbene region and the aliphatic region of Grubbs catalyst **2a***

3.1.1 Low Temperature Characterisation of Grubbs Catalyst 2a [$Ru(Cl)_2(PCy_3)_2CHPh$]

Low temperature ^1H NMR (-40 °C) of Grubbs catalyst **2a** in $CDCl_3$ (***Figure 3.4***) showed the presence of a broad hump in the aromatic region, which is typical of a spectrum of two species in equilibrium with each other. For species in equilibrium, the signals obtained can be two separate signals (slow exchange), one very broad signal (coalescence) or one sharp signal (fast exchange), depending on the rate of exchange and the strength of the magnet used to record the NMR spectra.[114] The rate of exchange increases as temperature increases, thus a system may be in slow exchange at low temperature, progressing to fast exchange with an increase in temperature.[114] The rate constant for the exchange can be determined from the point where the two signals first coalesce as follows:

$$k_{coalescence} = \frac{\pi(dv)}{\sqrt{2}}$$

$$\frac{1}{k_{chem}} = T = \frac{p_b}{k_{coalescence}} = \frac{1}{2} x \frac{\sqrt{2}}{\pi(dv)}$$

$$\therefore k_{chem} = 2k_{coalescence} = \frac{2\pi}{\sqrt{2}}(dv)$$

where dv = difference (Hz) in chemical shifts in slow exchange, T = average lifetime of each state, p_b is the population of site B, (in this case $p_a = p_b = 0.5$) k_{chem} is the true rate of reaction between the two species.[115]

The signal for the ortho protons on the aromatic ring (H_{15a} and H_{19a}) at 30 °C is one sharp doublet, while at -40 °C, it is a very broad hump, indicating an exchange process may be present. A ^1H temperature study was carried out and coalescence was found at -45 °C (measured at 500 MHz, ***Figure 3.4***). The ortho protons on the benzene ring are well separated at -62 °C (delta = 612 Hz).

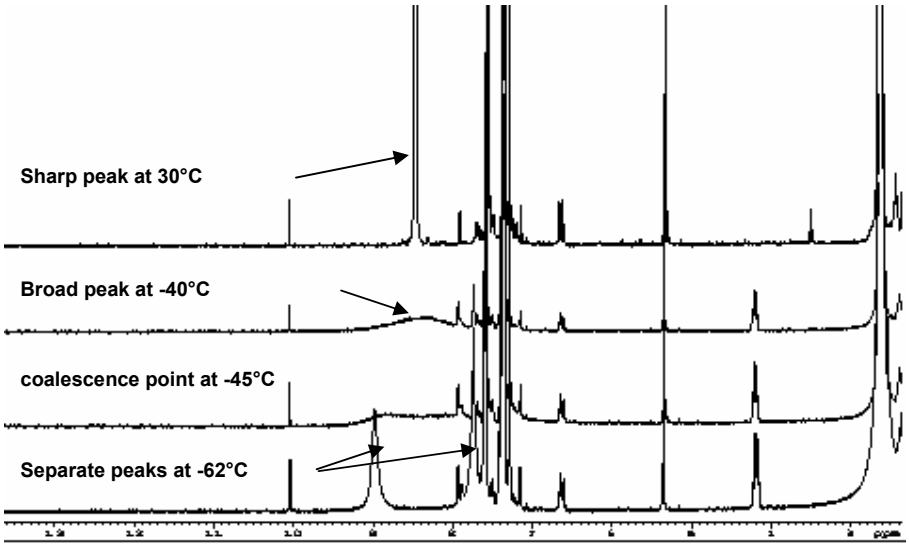

***Figure 3.4**: ^{1}H NMR spectra of **2a** at various temperatures in $CDCl_3$*

The rate constant for the process governing the equivalence of these two protons was calculated as shown below.

$$k_{chem} = \frac{2\pi(\mathrm{dv})}{\sqrt{2}} = \frac{2\pi(612)}{\sqrt{2}} = 2720 \ \mathrm{s}^{-1} \text{ at } -45°\mathrm{C} \text{ (measured at 500MHz)}$$

This equilibrium between the ortho protons could be caused by rotation of the entire benzylidene fragment or the rotation of the benzene ring only. As the carbene protons remain sharp throughout this exchange process, it is thought to be rotation of the benzene ring, around the HC-Ph bond.

The ^{31}P NMR spectrum of Phobcat **25** gives a very broad signal at 30 °C and is resolved into two singlets and one doublet at -40 °C, indicating an exchange process which is due to the presence of rotational isomers.[75] To check for similar behaviour, a ^{31}P spectrum of Grubbs catalyst **2a** was recorded at -40 °C and the ^{31}P NMR singlet remained sharp. Therefore it was concluded that there were no rotational isomers present that could be observed with ^{31}P NMR.

3.2 First Generation Grubbs Methylidene 4a [$Ru(Cl)_2(PCy_3)_2CH_2$]

Grubbs catalyst **2a** (300 mg) was dissolved in benzene (5 mL) and ethylene was bubbled through the mixture for 60 seconds. The reaction mixture was stirred for 15 minutes and the benzene was removed *in vacuo*. The precipitate was washed with 2 mL pentane and was dissolved in 5 mL benzene. Ethylene was again bubbled through for 60 seconds and the reaction mixture was stirred for 15 minutes, after which the benzene was removed *in vacuo*.

H_{1a} resonates at δ 2.6 as for Grubbs catalyst **2a** (see Section 2.8.7 on page 52). The carbene protons resonate at δ 18.9. The ^{31}P NMR chemical shift of the methylidene **4a** is δ 43.7.

The purity of the final complex was determined to be 88% by ^{31}P NMR. The desired complex is soluble in the pentane used to wash the product, thus the yield obtained is low (30%). Washing with pentane is necessary to remove the styrene that is formed on reaction of the benzylidene with ethylene.

3.3 First Generation Grubbs Catalyst di-bromide 2b [$Ru(Br)_2(PCy_3)_2CHPh$]

All manipulations were carried out under argon using schlenk techniques. Grubbs catalyst **2a** (250 mg) was reacted with LiBr (1.0g) in C_6H_6 (10 mL) and dry THF (5 mL) under argon for 4 hours. The solvent was removed *in vacuo* and 8 mL C_6H_6 was added. The salt was removed by centrifuging and the solvent was removed *in vacuo*. LiBr (1.0g),10 mL benzene and 5 mL dry THF were added and the process was repeated. The red-brown precipitate obtained was washed with pentane and dried *in vacuo* to afford the di-bromide **2b** in 50% yield. The purity of the product obtained was determined to be 93.5% (^{31}P NMR).

The major resonance at δ 38.1 in the ^{31}P NMR spectrum obtained represents the expected di-bromide Grubbs catalyst **2b** [$Ru(Br)_2(PCy_3)_2CHPh$. The ^{31}P NMR spectrum also shows the presence of $Ru(PCy_3)_2BrPhCO$ at δ 25.8. $Ru(PCy_3)_2BrPhCO$ is the halide exchange product of the often present $Ru(PCy_3)_2ClPhCO$ (see Section 3.1 on page 52). There is an unidentified peak at δ 36.2.

^{1}H-^{31}P HMBC spectra were recorded of the carbene region and the aliphatic region at 30 °C in C_6D_6. The ^{31}P NMR and ^{1}H NMR spectra are shown as traces on the HMBCs in ***Figure 3.5*** (carbene region) and ***Figure 3.6*** (aliphatic region). The protons are labelled exactly as for Grubbs catalyst **2a** (***Figure 3.2*** on page 52).

There is clear coupling between the carbene proton H_{13a} (δ 20.5 in the ^{1}H NMR) and the major ^{31}P NMR signal at δ 38 in the HMBC of the carbene region, confirming that this resonance represents a carbene complex and is Grubbs di-bromide **2b**.

Correlations are seen for protons signals between δ 1.6 and δ 3.2 ppm in the ^{1}H NMR for the resonance at δ 38 in the ^{31}P NMR spectrum. H_{1a} is therefore assigned to the resonance at δ 3.2 in the ^{1}H NMR spectrum.

On comparison with the ^{1}H NMR spectrum for Grubbs catalyst **2a**, H_{1a} is much more deshielded in the bromide complex **2b** than in Grubbs catalyst **2a** (δ 2.6). The carbene proton itself (complex **2b** δ 20.5, complex **2a** δ 19.6) is also more deshielded, as is the ^{31}P nucleus.

The halide exchanged impurity $Ru(PCy_3)_2BrPhCO$ resonates at δ 25.8 in the ^{31}P NMR and PC<u>H</u> of this complex resonates at δ 2.8 in the ^{1}H NMR spectrum.

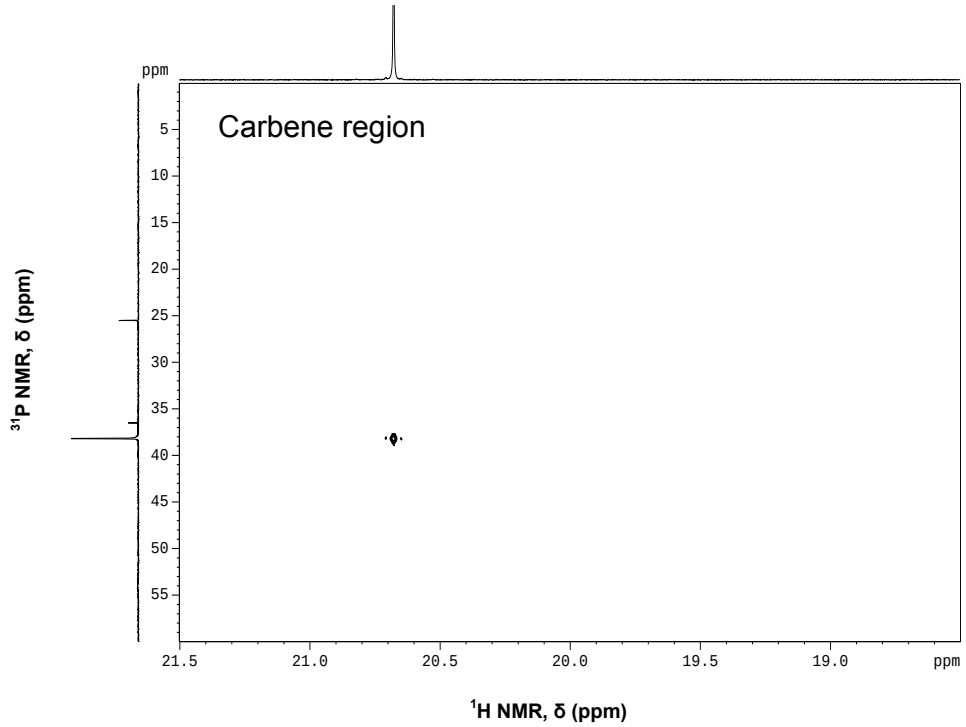

Figure 3.5: *^{1}H-^{31}P HMBC spectrum of the carbene region of Grubbs catalyst di-bromide **2b**, 30 °C, C_6D_6*

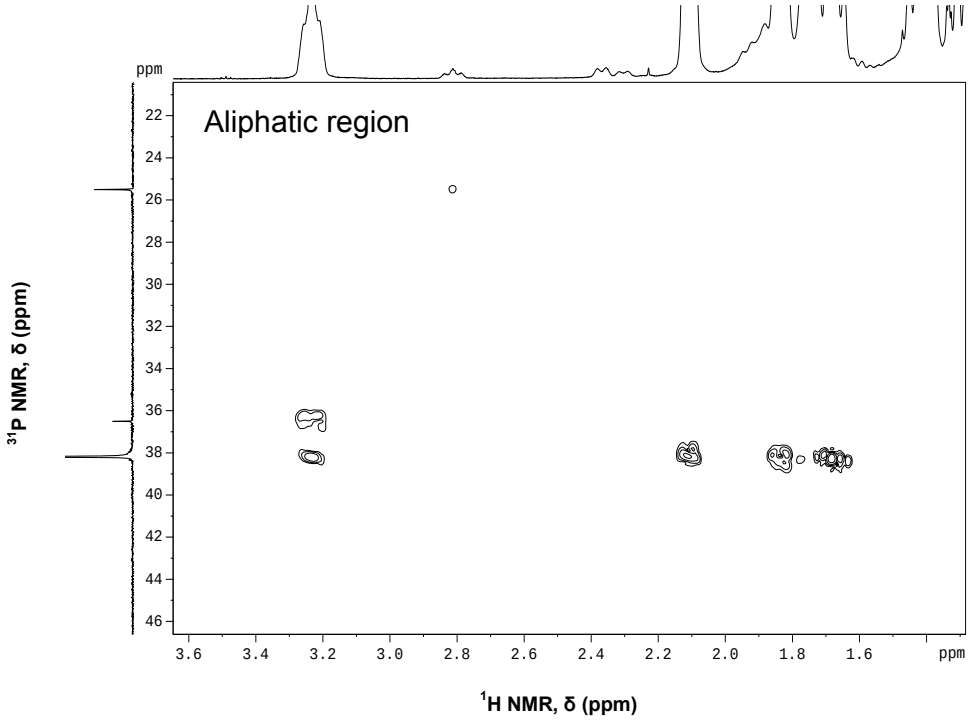

Figure 3.6: *^{1}H-^{31}P HMBC spectrum of the aliphatic region of Grubbs catalyst di-bromide **2b**, 30 °C, C_6D_6*

3.4 First Generation Grubbs Catalyst di-iodide 2d [$Ru(I)_2(PCy_3)_2CHPh$]

Grubbs catalyst **2a** (500 mg) was reacted with NaI (1.0g) in C_6D_6 (10 mL) and dry THF (5 mL) for four hours. The solvent was removed *in vacuo* and 8 mL of C_6H_6 was added. The salt was removed by centrifuging and the solvent was removed *in vacuo*. The dark green precipitate was washed with 5 mL pentane. NaI (1.0g) and 10 mL benzene and 5 mL dry THF were added and the reaction was repeated. The salt was removed *via* a whatmann syringe filter. A black precipitate was obtained after the solvent was removed.

It was attempted to record a ^{1}H-^{31}P HMBC in the carbene region and the aliphatic region, but no coupling was detected. However, from the ^{1}H NMR spectrum it was seen that H_{1a} and the carbene proton (H_{13a}) are again more deshielded than H_{1a} in the di-bromide **2b** or Grubbs catalyst **2a**.

The yield was not determined because it was suspected that the product had decomposed to a paramagnetic Ru(III) species which cannot be observed in the ^{31}P NMR spectrum. Sanford and Love report that the Grubbs catalyst di-iodide is unstable.[61]

3.5 Chemical Shifts for Grubbs Catalyst with the three Halides Studied

Table 3.1 summarises the chemical shifts of the carbene proton (H_{13a}), the ^{31}P nucleus and the CH (H_{1a}) attached to the ^{31}P nucleus in C_6D_6 for Grubbs catalyst **2a**, Grubbs catalyst di-bromide **2b** and Grubbs catalyst di-iodide **2d**.

***Table 3.1**: Chemical shifts for Grubbs catalyst **2a**, the di-bromide **2b** and the di-iodide **2d** in C_6D_6 and $CDCl_3$, 30 °C*

Complex	Solvent	δ (^{1}H) carbene proton H_{13a}	δ (^{1}H) H_{1a}	δ (^{31}P)
Grubbs catalyst **2a**	C_6D_6	19.6	2.6	36.1
Grubbs catalyst di-bromide **2b**	C_6D_6	20.5	3.1	38.0
Grubbs catalyst di-iodide **2d**	C_6D_6	20.5	3.5	38.1
Grubbs catalyst **2a**	$CDCl_3$	19.9	2.5	36.5
Grubbs catalyst di-bromide **2b**	$CDCl_3$	20.1	2.8	37.7
Grubbs catalyst di-iodide **2d**	$CDCl_3$	-	-	38.5

The ^{31}P nucleus is slightly more deshielded in the Grubbs catalyst di-bromide **2b** that Grubbs catalyst **2a** and even more deshielded in Grubbs catalyst di-iodide **2d**. Chloride is a good sigma donor, with decreased electron density being donated to the ruthenium center as the Cl is replaced with Br and then with I. Because there is less electron density at the ruthenium center, the ^{31}P ligands and the carbene CH donate more electron density and therefore more deshielded and resonate at lower field. A similar small effect is seen for the carbene proton.

The PCH proton shows a similar trend in the ^{1}H NMR spectra but the effect is much larger. It is thought that the larger Br and I ligands may cause polarization of the electron density around this proton, leading to the observed deshielding effects.

3.6 Second Generation Grubbs Methylidene 6 [$Ru(Cl)_2(PCy_3)(NHC)CH_2$]

The second generation Grubbs catalyst methylidene **6** was obtained from G. Forman at St Andrews University and was used without further purification. (NHC = 1,3-dimesityl-4,5-dihydroimidazole-2-ylidene)

The ^{31}P and ^{1}H NMR spectra of the second generation Grubbs catalyst methylidene **6** were recorded in C_6D_6. . The purity of the complex was 75% (^{31}P NMR).

Chapter 4: Insights into Bimolecular Decomposition *via* Halide Exchange

4.1 Introduction

The major obstacle to the commercialisation of homogeneous metathesis technology on a large scale is the short lifetime of the catalysts. Literature reveals that both the Grubbs catalyst alkylidenes and the benzylidene undergo thermal decomposition[116] *via* a bimolecular pathway,[11] possibly *via* the formation of a dimeric ruthenium intermediate species (see Section 2.11.2 on page 44). The detection of stilbene after the thermal decomposition of the benzylidene indicates a bimolecular decomposition pathway.

Several types of ruthenium dimers have been isolated and characterised. Cationic dichloride bridged ruthenium dimers are inactive but are in equilibrium with the highly active 14 electron intermediate (see Section 2.8.7 on page 34). This indicates the importance of the dimer/monomer equilibrium. Fogg *et al*.[107] have isolated triple chloride bridged monoalkylidene ruthenium dimers with very low metathesis activity and have suggested that dimerization represents a major bimolecular decomposition route for Grubbs catalysts (see Section 2.11.2 on page 44). Recently, Meyer *et al.*[112] have determined the crystal structure of a dimer-like Ru-Sn complex **43, (*Figure 2.4*** on page 50) that is very active for metathesis. This dimer was formed on addition of $SnCl_2$ to a decomposed solution of Grubbs catalyst **2a** in CD_2Cl_2.

In this study the halide exchange reaction was discovered during a study of the thermal decomposition of the di-bromide **2b** in deuterated tetrachloroethane (TCE). This observation represents a novel reaction of ruthenium alkylidene complexes that is relatively unknown in the literature.[117]

It is proposed that the intermolecular halide exchange reaction takes place *via* a dimeric ruthenium intermediate and that the study of this reaction gives

insight into the mechanism of the formation of such an intermediate, its structure, and possibly additives to slow down its formation.

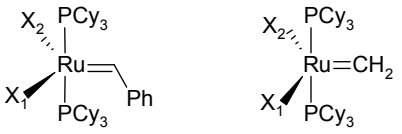

2 **4**

2a X_1=X_2=Cl **4a** X_1=X_2=Cl

2b X_1=X_2=Br **4b** X_1=X_2=Br

2c X_1=Cl X_2=Br **4c** X_1=Br X_2=Cl

2d X_1=X_2=I

2e X_1=I X_2=Cl

Figure 4.1: *Ruthenium alkylidene complexes relevant to the current halide exchange study*

4.2 Experimental

All chemical procedures and manipulations were carried out under argon using standard schlenk techniques.

4.2.1 General NMR methods

All NMR solvents were prepared by carrying out three cycles of the pump freeze thaw method. All NMR experiments were conducted on a Bruker Avance 500 MHz NMR fitted with a 5 mm QNP probe or a Varian Unity Inova 600 MHz NMR fitted with a 4 nucleus, switchable, pulsed field gradient (pfg) 5 mm probe.

^{31}P NMR spectra were recorded using a 30° pulse angle and a 2 second relaxation delay, with a spectral window from δ 200 to δ -200 ^{1}H NMR experiments were recorded using a 30° pulse angle and a 10 second relaxation delay, with a spectral window from δ -5 to δ 25.

4.2.2 Kinetic NMR experiments

Kinetic ^{31}P NMR experiments were recorded on a Bruker 500 MHz NMR using the pulse sequence 'kinetik', using a variable delay (VD) list, which was modified for ^{31}P NMR by P. Dvortsak from Bruker, Germany. Spectra were recorded every 30 seconds for the required period of time. Ten scans were recorded per spectrum.

Kinetic ^{31}P NMR experiments were recorded on a Varian 600 MHz NMR using the pre acquisition delay. Spectra were recorded every 30 seconds as above.

4.2.3 Halide Exchange of the di-bromide 2b $[Ru(Br)_2(PCy_3)_2CHPh]$ with $CDCl_3$

The Grubbs catalyst di-bromide **2b** $[Ru(Br)_2(PCy_3)_2CHPh]$ (20 mg, 21.9 x 10^{-2} mmol) was dissolved in 0.6 mL $CDCl_3$ and monitored with ^{31}P and ^{1}H NMR at 50 °C. The experiment was repeated in $CDCl_3$ that had been percolated though basic alumina, as well in the presence of phenol at 30 °C (0.24 g, 100 equivalents).

4.2.4 Halide Exchange of the di-bromide 2b $[Ru(Br)_2(PCy_3)_2CHPh]$ with HCl or CCl_4

The di-bromide **2b** $[Ru(Br)_2(PCy_3)_2CHPh]$ (20 mg, 21.9 x 10^{-2} mmol) was dissolved in 0.6 mL C_6D_6 and a substoichiometric amount of HCl gas was added after which ^{31}P NMR and ^{1}H NMR spectra were recorded.

Grubbs di-bromide **2b** (20 mg, 21.9 x 10^{-2} mmol) was dissolved in 0.5 mL C_6D_6 and 0.1 mL CCl_4 was added, after which ^{31}P NMR and ^{1}H NMR spectra were recorded. After the experiment, the reaction mixture was analysed with GC/MS using a PONA column as described in Section 4.2.8.1.

4.2.5 Intermolecular Halide Exchange between the di-bromide 2a [$Ru(Cl)_2(PCy_3)_2CHPh$] and Grubbs catalyst 2b [$Ru(Br)_2(PCy_3)_2CHPh$]

Equimolar quantities of **2a** [$Ru(Cl)_2(PCy_3)_2CHPh$] (12.0 mg, 1.32 x 10^{-2} mmol) and **2b** [$Ru(Br)_2(PCy_3)_2CHPh$] (10.3 mg, 1.22 x 10^{-2} mmol) were dissolved in 0.6 mL C_6D_6 and ^{31}P NMR spectra were recorded every minute for 30 minutes.

The experiment was repeated in the presence of excess phenol (20 equiv) or PCy_3 (3 equiv) or $O{=}PCy_3$ (3 equiv).

The experiment was repeated with half the concentration of catalyst **2a** (5.6 mg, 6.80 x 10^{-3} mmol) and Grubbs catalyst di-bromide **2b** (6.8 mg, 7.46 x10^{-3} mmol) and Grubbs in 0.6 mL C_6D_6.

4.2.6 Halide Substitution of Grubbs Catalyst 2a [$Ru(Cl)_2(PCy_3)_2CHPh$] *via* Dissolved Salt Addition

Grubbs di-bromide **2a** [$Ru(Cl)_2(PCy_3)_2CHPh$] (11.9 mg, 1.47 x 10^{-2} mmol) was mixed with 10 equivalents of Bu_4NBr in 0.6 mL $CDCl_3$. The interaction was monitored with ^{31}P NMR for 60 minutes.

The experiment was repeated twice using the following salts:

- 20 equivalents of Bu_4NBr in 0.6 mL $CDCl_3$
- 10 equivalents of Bu_4NI in 0.6 mL $CDCl_3$

4.2.7 Catalyst Testing Procedure

1-Octene was passed through a column containing basic alumina in order to remove any peroxides present. The 1-octene was degassed by sparging with argon to remove dissolved oxygen, and was then stored over a layer of basic alumina.

Reactions were carried out in three-necked flasks, fitted with a thermometer, a septum and a condenser. The cooling liquid through the condenser was set to 5 °C. The flasks were placed in oil baths that were heated using a thermocouple and a controller. The reactions were carried out with an argon sparge.

All liquid reagents were added to the flask with a syringe through the septum. All solid reagents were added by removing the condenser and adding the solid material to the flask while maintaining positive argon pressure. The setup was purged with argon for 10 minutes before 20 mL 1-octene and 10 mL $CHCl_3$ (if necessary) were added to the flask. The required amount of salt or other additive was added to the flask where necessary. Lastly, the required amount of Grubbs catalyst **2a** $[Ru(Cl)_2(PCy_3)_2CHPh]$ was added and the stopwatch was started.

Samples were taken at 2, 5, 10, 15, 20, 40, 60, 90, 120, 240, 300 and 360 minutes and at the end of the experiment (about 1200 minutes). Samples were analyzed using a GC fitted with a PONA column using the method GC-FID (catalyst testing) in Section 4.2.8.2.

4.2.8 Gas Chromatography

4.2.8.1 GC/MS (PONA column)

Samples were injected on an Agilent GC/MS (helium carrier gas, split/splitless inlet, split 1:100, inlet temperature 250 °C, injection volume 0.5 µL, PONA (50 m x 0.2 mm ID x 0.5 µm), 50 °C (1 min) to 320 °C (0 min) at a rate of 4 °C/min, ion source temperature 170 °C).

4.2.8.2 GC-FID (catalyst testing)

All samples were analysed on a 6890 Agilent GC (hydrogen carrier gas, inlet temp 250 °C, injection volume 0.2 µL, PONA (50 m x 0.2 mm x 0.5 µm), 100 °C (1.00 min), 15 °C/min to 190 °C, 3 °C/min to 195 °C, 50 °C/min to 300 °C (5 min), detector temperature 300 °C).

4.3 Halide Exchange of the di-bromide 2b [$Ru(Br)_2(PCy_3)_2CHPh$] with $CDCl_3$

Grubbs catalyst di-bromide **2b** (purity is 93.5%, see Section 3.3) was dissolved in $CDCl_3$ and monitored with ^{31}P and ^{1}H NMR at 50 °C as described in Section 4.2.3.

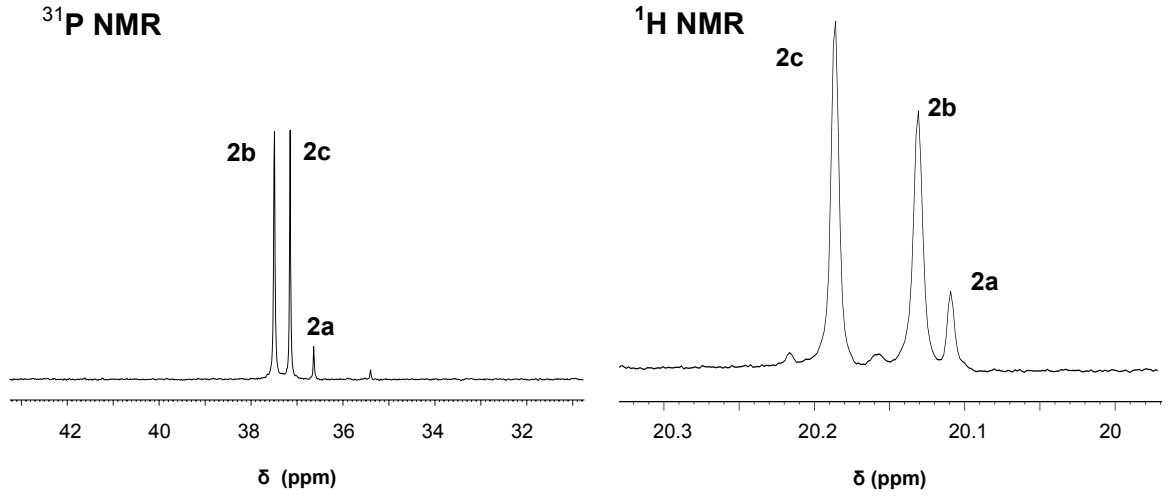

***Figure 4.2**: NMR spectra after 30 minutes, showing the reaction of the di-bromide **2b** with $CDCl_3$ ([**2b**] = 3.65 x 10^{-2} M, 30 °C, $CDCl_3$)*

With time, two carbene species appeared, one of which was positively identified as Grubbs catalyst **2a**, while the other is thought to be the mixed halide catalyst **2c** (***Figure 4.2***). The new species is a carbene (^{1}H NMR, δ 20.19) with a ^{31}P NMR chemical shift between Grubbs catalyst **2a** and the di-bromide **2b** (^{31}P NMR, δ 37.3). To further confirm this, the di-bromide **2b** was reacted with a substoichiometric amount of HCl gas and the same complex was formed (***Figure 4.3***).

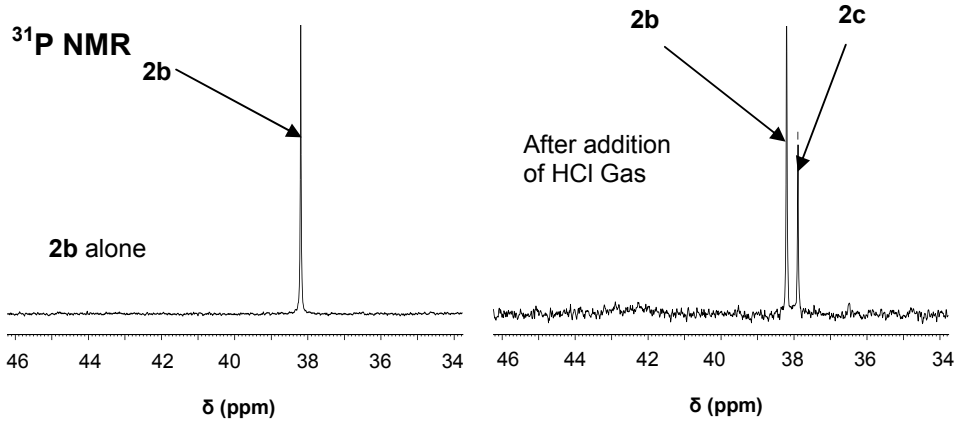

Figure 4.3: *^{31}P NMR of the di-bromide **2b** alone and after reacting a substoichiometric amount of HCl gas with **2b** ([**2b**] = 3.65 x 10^{-2} M C_6D_6, 30 °C)*

It is known that chlorinated solvents may contain trace amounts of HCl. To confirm whether the halide exchange was in fact due to reaction with the solvent and not HCl, the reaction was repeated in $CDCl_3$ that had been percolated though basic alumina, and the same reaction occurred.

To determine whether or not this is a free radical reaction, the experiment was repeated in the presence of 100 equivalents of phenol (a free radical scavenger) and it was found that the reaction was not inhibited. Therefore the reaction between Grubbs catalyst di-bromide **2b** and chloroform solvents does not appear to be a free radical reaction.

This should be repeated with a hindered phenol such as BHT (buylated hydroxytoluene) which is a better free radical inhibitor as phenol is known to have other roles in the system.[111]

4.4 Halide Exchange of the di-bromide 2b [$Ru(Br)_2(PCy_3)_2CHPh$] with CCl_4

For further evidence that the chlorinated solvent reacts directly with the catalytic species, the di-bromide **2b** was reacted with 0.1 mL CCl_4 (see

Section 4.2.4) and the same new complex was formed, but decomposition followed swiftly. In this case CCl_3Br is expected to be formed due to the halide exchange with the carbon tetrachloride. The chromatogram obtained from GC/MS analysis showed the presence of carbon tetrachloride (7.1 min) and C_6D_6 (6.9 min) and in addition, a small peak was observed at 9.8 minutes. The chromatogram and the MS spectrum for the peak at 9.8 minutes are shown in ***Figure 4.4***

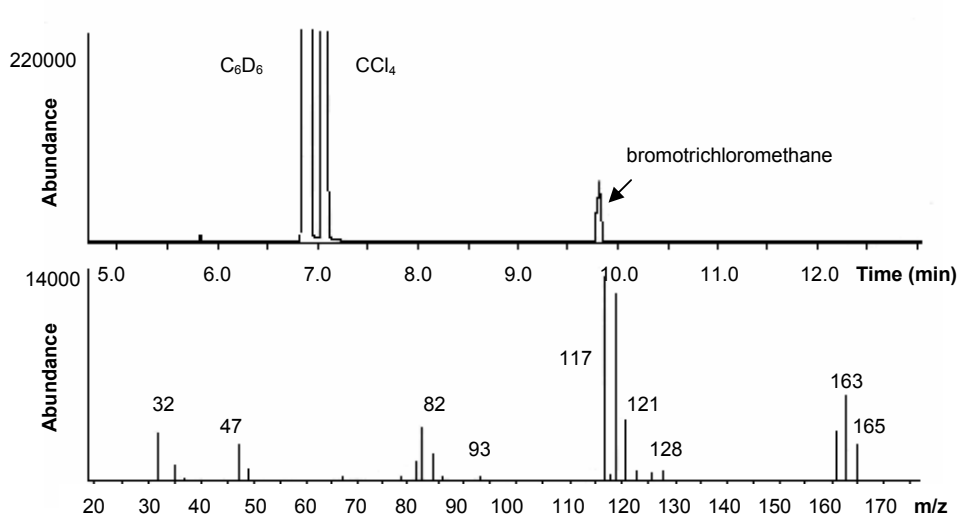

***Figure 4.4**: GC/MS Total ion chromatogram and spectrum of peak at 9.8 minutes of reaction mixture after reaction of **2b** ([**2b**] = 3.65 x 10^{-2} M) with 0.1 mL CCl_4*

The molecular ion of the peak at 9.8 minutes (196), is not visible, but the expected base peak due to the loss of a Br radical is present (117) and shows the expected pattern for a compound containing three chlorine atoms. The ion formed by loss of a Cl radical is also present (161) and shows the expected pattern for a compound containing two chlorine atoms and a bromine atom. Thus the peak was conclusively identified as CCl_3Br.

The detection of CCl_3Br in the reaction mixture proves that the reaction of the di-bromide **2b** $[Ru(Br)_2(PCy_3)_2CHPh]$ with chlorinated solvents is not due to reaction with small amounts of Cl^- in the chlorinated solvents, but rather a

halide exchange reaction with the solvent itself, possibly as shown in ***Scheme 4.1***.

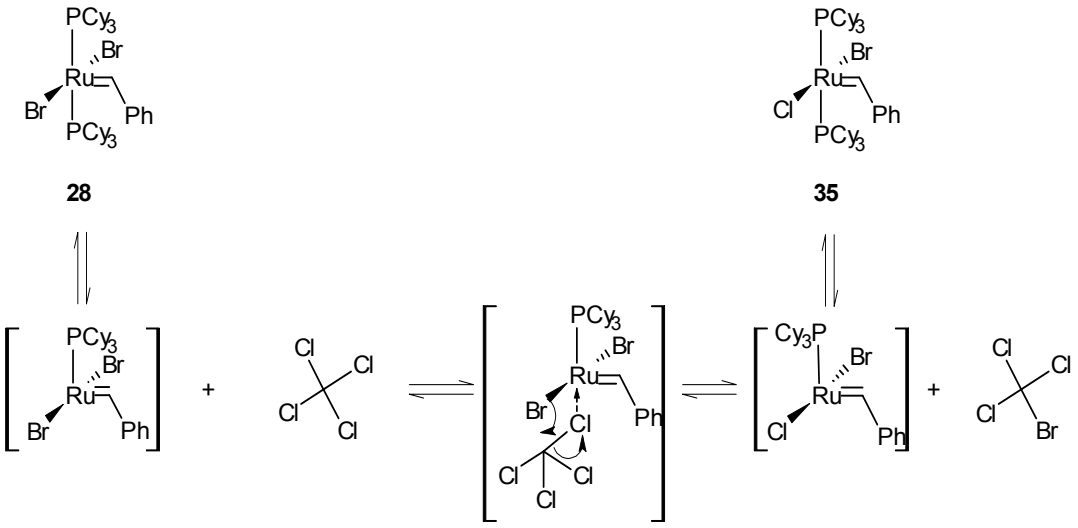

***Scheme 4.1**: Possible mechanism for reaction of the di-bromide **2b** with chlorinated solvents*

4.5 Intermolecular Halide Exchange between the di-bromide 2b [$Ru(Br)_2(PCy_3)_2CHPh$] and Grubbs Catalyst 2a [$Ru(Cl)_2(PCy_3)_2CHPh$]

4.5.1 Qualitative NMR studies

Considering the reaction of the di-bromide **2b** [$Ru(Br)_2(PCy_3)_2CHPh$] with chlorinated solvents, it was decided to determine whether or not the di-bromide **2b** reacts with Grubbs catalyst **2a** [$Ru(Cl)_2(PCy_3)_2CHPh$] to form the mixed halide **2c** (***Scheme 4.2***).

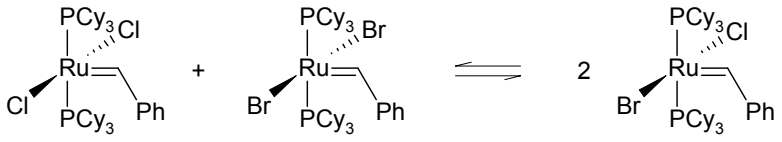

2a **2b** **2c**

Scheme 4.2**: Intermolecular halide exchange of Grubbs catalyst **2a** with the di-bromide **2b** to form the mixed halide complex **2c

Equimolar quantities of **2b** and **2a** were dissolved in 0.6 mL C_6D_6 (see Section 4.2.5) and a ^{31}P NMR spectrum confirmed that the two complexes reacted to form a species with the same chemical shift as the mixed species observed above (***Figure 4.5***). This is further proof of the ready halide exchange reactions these complexes undergo, as well as the identity of the mixed halide complex formed, **2c**. The species equilibrated within about 15 minutes at 30 °C (***Figure 4.8***).

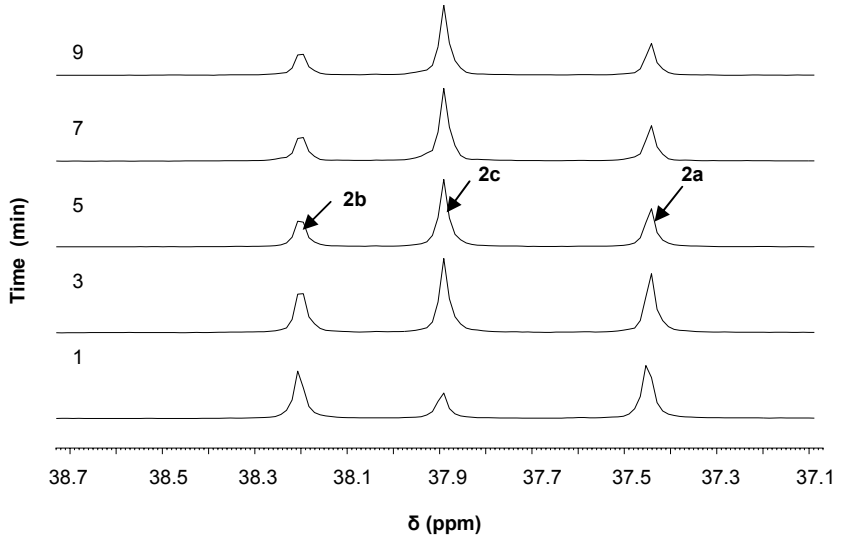

***Figure 4.5**: ^{31}P NMR stacked plot showing intermolecular halide exchange of Grubbs catalyst **2a** with the di-bromide **2b** to form the new mixed species **2c**. ([**2a**] = 2.09 x 10^{-2} M [**2b**] = 2.19 x 10^{-2} M, C_6D_6, 30 °C)*

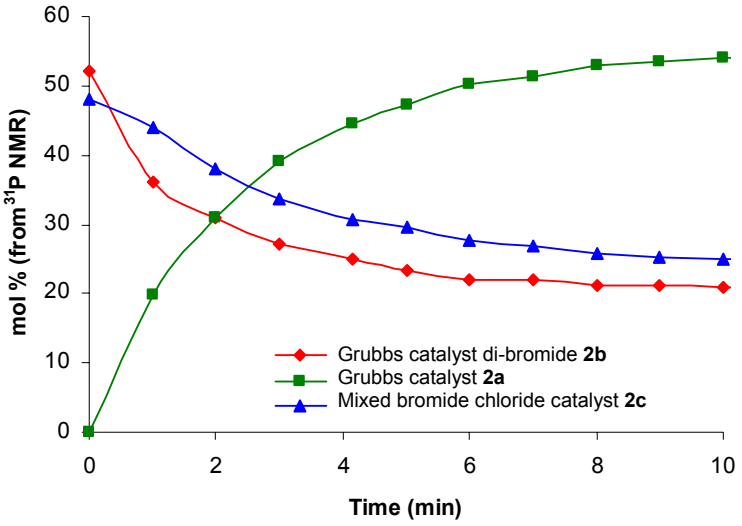

Figure 4.6: *Graph of mol % (from ^{31}P NMR data) catalytic species vs. time for the intermolecular halide exchange of Grubbs catalyst **2a** [Ru(Cl)$_2$(PCy$_3$)$_2$CHPh] with the di-bromide **2b** [Ru(Br)$_2$(PCy$_3$)$_2$CHPh] ([**2b**] = 2.19 x 10^{-2} M , [**2a**] = 2.09 x 10^{-2} M, C$_6$D$_6$, 30 °C)*

Addition of excess tricyclohexylphosphine and/or tricyclohexylphosphine oxide markedly inhibits the reaction of Grubbs catalyst **2a** with the di-bromide **2b**. In the presence of three equivalents of tricyclohexylphosphine, equilibrium is still not reached in 24 hours, showing that the first step is the dissociation of the phosphine.

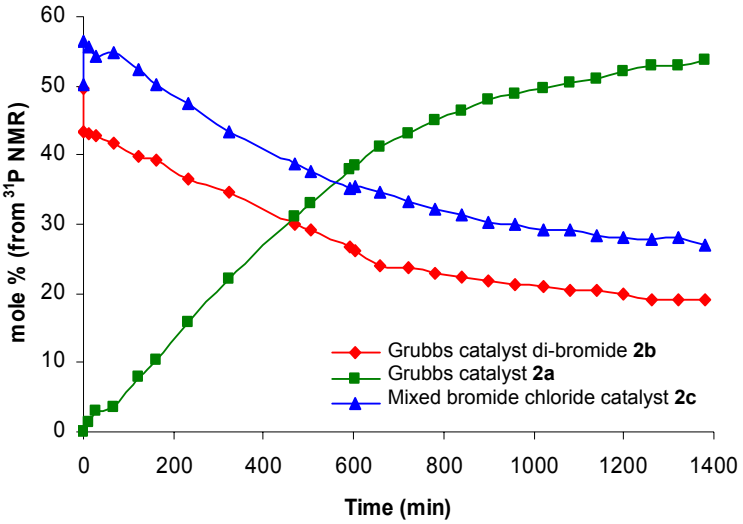

***Figure 4.7**: Graph of mol% catalytic species (from ^{31}P NMR data) vs. time for the intermolecular halide exchange of the di-bromide **2b** with **2a** in the presence of three equivalents of PCy_3 ([**2b**] = 2.47 x 10^{-2}M, [**2a**] = 2.50 x 10^{-2} M, C_6D_6, 30 °C)*

Addition of phenol (a free radical scavenger) does not alter the rate or equilibrium position of the halide exchange reaction between the Grubbs catalyst **2a** and the di-bromide **2b** (***Figure 4.8***).

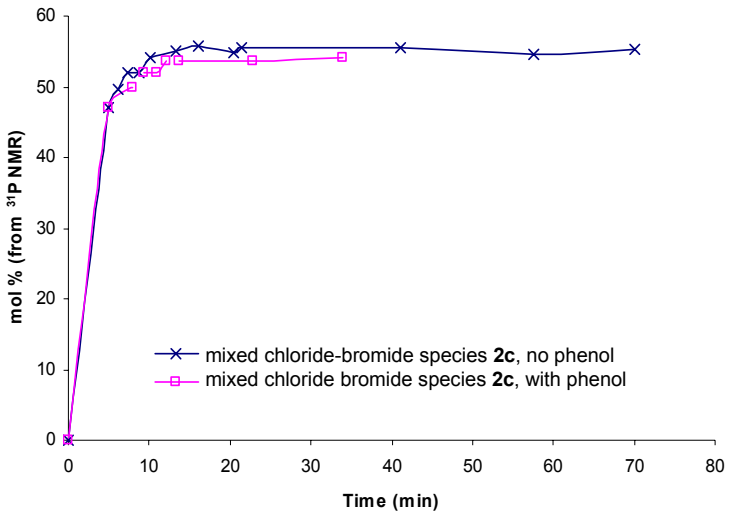

***Figure 4.8**: Graph of mol% catalytic species (from ^{31}P NMR data) vs time for the intermolecular halide exchange of Grubbs catalyst **2a** with the di-bromide **2b** in the presence of 20 equivalents of phenol, compared with a similar reaction in the absence of phenol, ([**2b**] = 2.19 x 10^{-2} M and [**2a**] = 2.09 x 10^{-2} M, 30 °C, C_6D_6).*

4.5.2 Mechanism of the Formation of the Mixed Species 2c

The halide exchange reaction between two ruthenium alkylidene complexes does not appear to occur *via* a radical mechanism because the addition of phenol, a free radical scavenger, does not retard the reaction. The addition of excess phosphine ligand slows the reaction dramatically, indicating that the first step is phosphine dissociation, thus there is no halide dissociation directly from the Grubbs catalyst itself. After loss of the phosphine ligand it is unlikely that there will be a further dissociation of the halide from the already coordinatively unsaturated metal center.

Fogg *et al.*[107] have isolated chloride bridged ruthenium dimers with *cis* chelated phosphine ligands which are formed by homodimerization of the monomer (see ***Scheme 2.29***). Similar chemistry was observed for the Grubbs precursor [$Ru(PPh_3)_2Cl_2CHCH{=}CMe_2$]. It is therefore proposed that the halide exchange reaction observed in this study takes place *via* a halide bridged dimeric intermediate **44** [$(Rh(PCy_3)_2BrClCHPh)_2$]. Such a species

(***Figure 4.9***) was modelled using density functional theory (DFT) by Meyer and two forms, **44a** and **44b**, could be optimised.[118] This dimeric intermediate is in equilibrium with the active 14 electron species, as is the case with cationic ruthenium dimers (see Section 2.8.7).[79,80] A possible mechanism for the formation of such a dimer is shown in ***Scheme 4.3***.

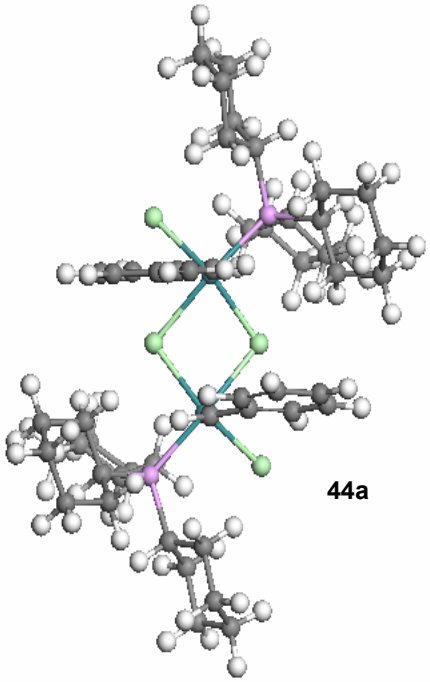

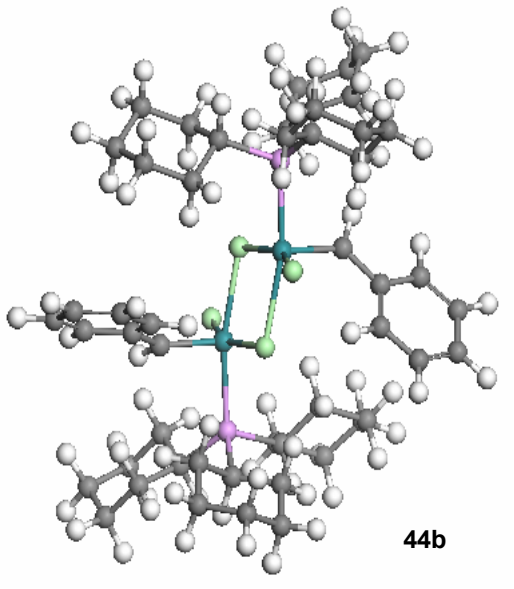

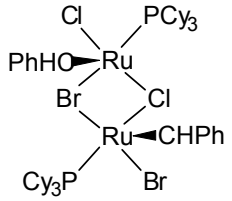

44a

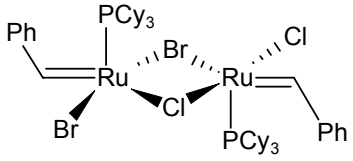

44b

Figure 4.9**: Possible dimeric intermediates in the halide exchange of Grubbs catalyst **2a** with the di-bromide **2b

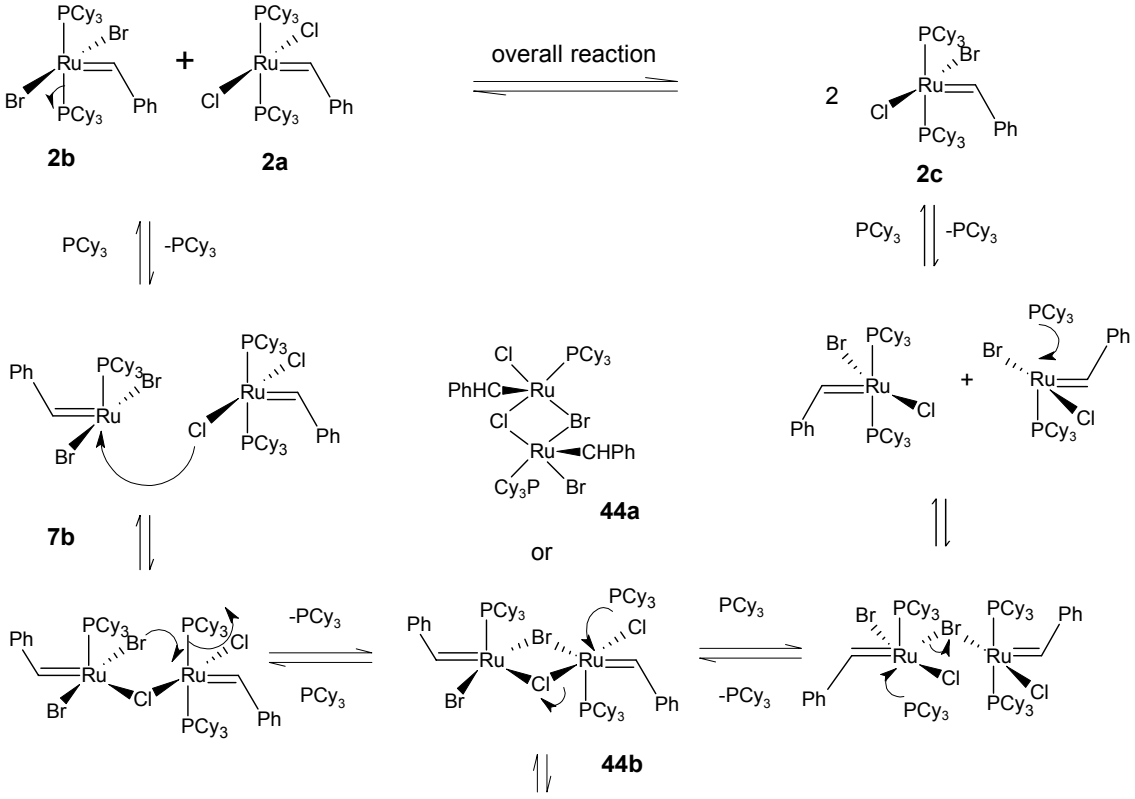

***Scheme 4.3**: Possible mechanism for the reaction shown in **Scheme 4.2** for the formation of the mixed halide **2c** via a dimeric intermediate*

The addition of excess phosphine slows the intermolecular halide exchange reaction dramatically, indicating that the first step is the dissociation of the phosphine to form the 14 electron intermediate **7b**. The dimeric intermediate is formed by reaction of the 14 electron intermediate **7b** [$Ru(Br)_2(PCy_3)CHPh$] with Grubbs catalyst itself, with the chloride of the Grubbs catalyst acting as a ligand. This is followed by dissociation of the tricyclohexylphosphine and coordination of the bromide to the ruthenium center resulting in the formation of the doubly halide bridged dimeric ruthenium species **44a** and **44b**. These dimeric ruthenium species are not stable and when the halide bridge breaks, they can again react with ligand resulting in the formation of the mixed halide species. The dimer itself is probably inactive for metathesis, although it is in equilibrium with the active 14 electron intermediate **7b** [$Ru(Br)_2(PCy_3)CHPh$].

4.5.3 Order of Reaction for the Intermolecular Halide Exchange between Grubbs catalyst 2a and Grubbs Catalyst di-bromide 2b

Two possibilities were considered for the determination of the order of the intermolecular halide exchange between Grubbs catalyst **2a** and Grubbs catalyst di-bromide **2b**.

- A second order reaction (bimolecular) where the rate is first order in both reagents, i.e. rate = k_{obs}[**2a**][**2b**]. Doubling both reagents will result in a four fold increase in rate.

- A slow unimolecular pre-equilibrium step (phosphine dissociation from **2b**) followed by fast reaction with **2a** to form **2c**, i.e. rate = k_{obs}[**2b**]. Doubling of the concentration of both reagents will result in a two fold increase in the rate.

The rate of formation of the mixed halide **2c** was measured using ^{31}P NMR (see Section 4.2.2 on page 64) at two different starting concentrations of the di-bromide **2b** and Grubbs catalyst **2a**, at 30 °C. In the second experiment the starting concentrations of the reagents were 1.9 times that used in the first experiment. The expected [**2c**] for a four fold (second order case) and two fold increase (first order case) in [**2c**] was calculated from the conversion obtained in the first experiment and is shown on the graph below (***Figure 4.10***).

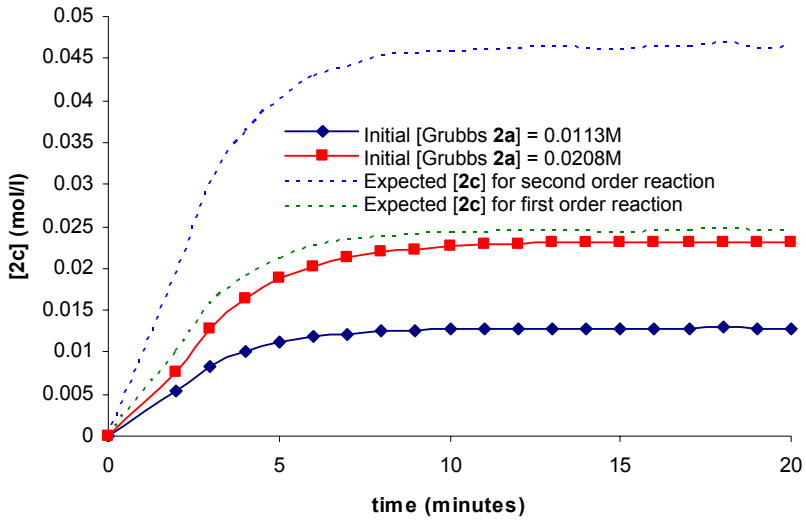

Figure 4.10: *Using 1.9 times the starting concentrations of both reagents results in 1.9 times the rate of formation of **[2c]**, for the intermolecular halide exchange between **[2a]** and **[2b]**. ([**2b**] = 1.24x 10^{-2}M, **[2a]** = 1.13 x 10^{-2} M, and **[2b]** = 2.19 x 10^{-2} M, **[2a]** = 2.09 x 10^{-2}M, C_6D_6, 30 °C)*

From the above graph it is clear that the intermolecular halide exchange is of the first order.

4.5.4 Equilibrium Constant *K* for the Intermolecular Halide Exchange between Grubbs Catalyst 2a and Grubbs catalyst di-bromide 2b.

A stepwise scheme (***Scheme 4.4***) for intermolecular halide exchange resulting in the formation of complex **2c** is shown here for clarity. The full scheme is shown in ***Scheme 4.3***.

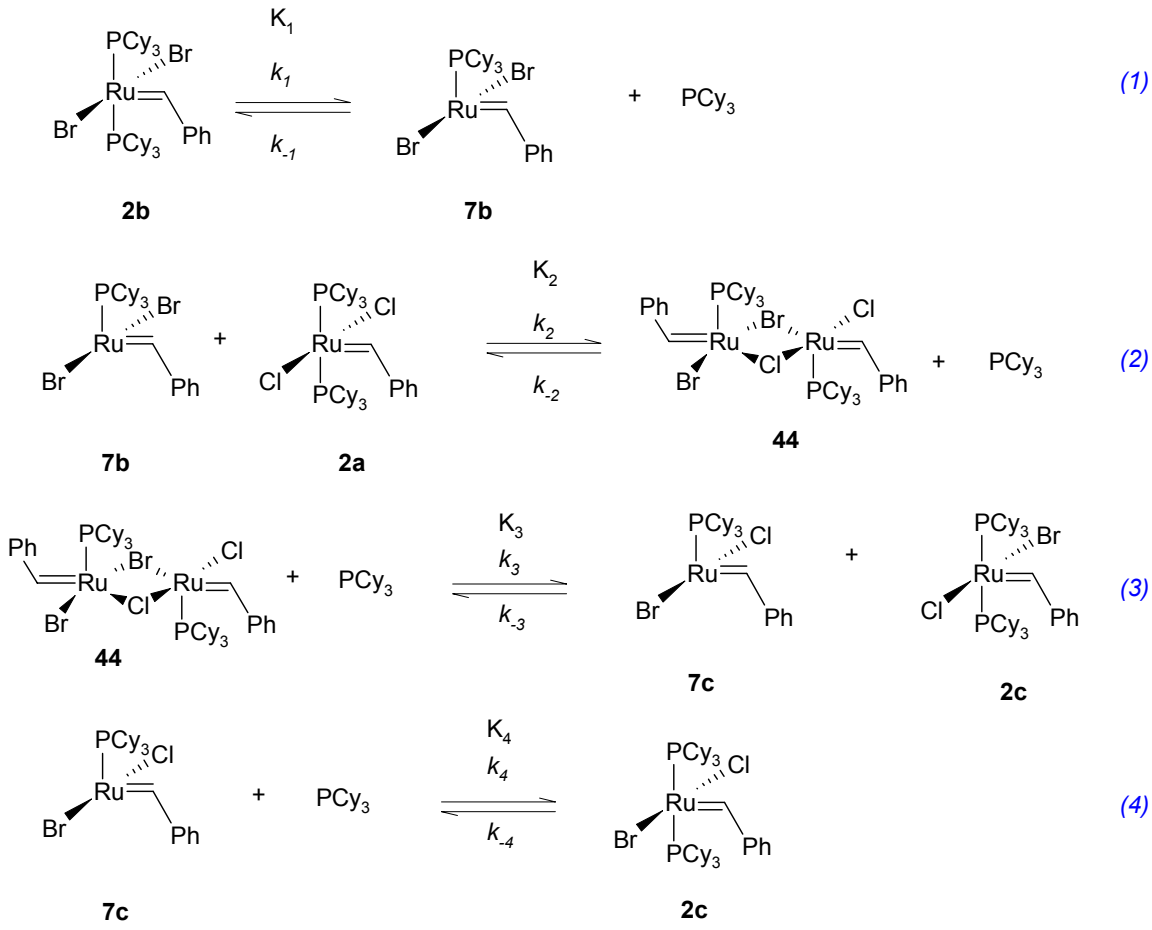

***Scheme 4.4**: Stepwise representation of the reaction of Grubbs catalyst **2a** with Grubbs catalyst di-bromide **2b** to form the mixed halide complex **2c**, as shown in **Scheme 4.3**.*

The overall equilibrium constant $K_{1\text{-}4}$ was calculated as follows:

$$K_{1\text{-}4} = K_1 \times K_2 \times K_3 \times K_4 = \frac{[PCy_3][\mathbf{7c}]}{[\mathbf{2b}]} \times \frac{[\mathbf{44}][PCy_3]}{[\mathbf{7c}][\mathbf{2a}]} \times \frac{[\mathbf{7c}][\mathbf{2c}]}{[\mathbf{44}][PCy_3]} \times \frac{[\mathbf{2c}]}{[\mathbf{7c}][PCy_3]}$$

$$= \frac{[\mathbf{2c}]^2}{[\mathbf{2a}][\mathbf{2b}]}$$

$K_{1\text{-}4}$ was calculated from the kinetic ^{31}P NMR experiments for the two experiments with different starting concentrations. $K_{1\text{-}4}$ was found to be

(5.58±0.13) x 10^{-2} for the reaction where the initial concentration of Grubbs catalyst is 0.0113 M, and (5.59±0.05) x 10^{-2} for the reaction where the initial concentration of Grubbs catalyst is 0.0208 M. Thus the values obtained for $K_{1\text{-}4}$ agree within experimental error.

4.5.5 Preliminary Kinetics of the Intermolecular Halide Exchange Reaction

Formation of species **2c** confirmed a first order rate law with rates at least one order of magnitude slower than the rate of dissociation of the phosphine measured by the Grubbs group.[119] This indicates a pre-equilibrium step favouring the reactants, confirming the first step in ***Scheme 4.4***.

It is necessary to carry out detailed kinetics to determine the values for all the rate constants. This could be achieved using stopped flow NMR techniques,[120] and applying the steady state approximation to the formation of [**7b**], [**7c**] and [**44**]. This information would further confirm the proposed mechanism for halide exchange.

4.5.6 Bimolecular Decomposition *via* the Dimeric Intermediate

Stilbene is one of the major decomposition products found after the thermal decomposition of Grubbs catalyst **2a**.[12] Stilbene, presumably formed by dimerization of the alkylidene fragment, can only be formed by the interaction of two catalyst molecules and thus indicates a bimolecular decomposition pathway.

It is proposed that intermolecular halide exchange occurs in any solution of Grubbs complexes, with the formation of dimeric intermediate **45**, which may be the start of a bimolecular decomposition process as shown in ***Scheme 4.5***.

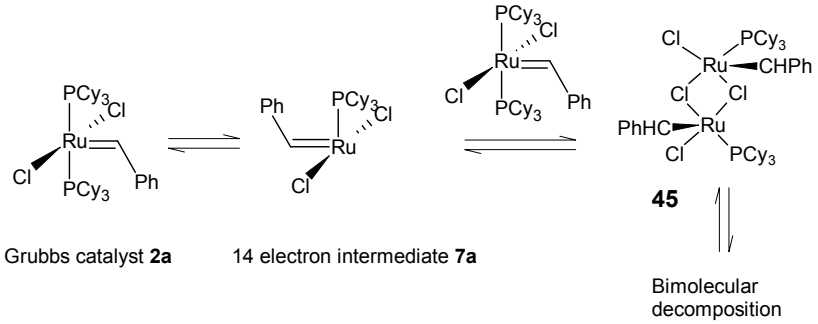

Scheme 4.5: *Formation of a dimeric intermediate **45** in any solution of Grubbs catalyst **2a***

Stilbene could possibly be formed from the dimeric intermediate **45** as shown in ***Scheme 4.6*** below. However, according to Fogg[121] this is unlikely as the two Ru centers cannot get close enough to form the required bonds. Detailed modelling is required to confirm this.

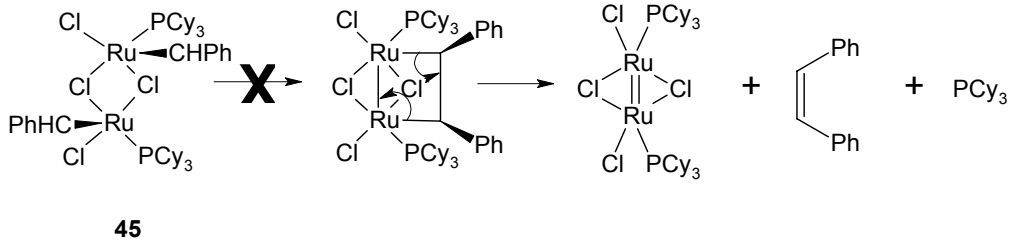

Scheme 4.6*:* *Considered pathway for bimolecular decomposition from the dimeric intermediate **45**, with the formation of stilbene*

Another option, suggested by Fogg *et al.*,[107] is depicted in ***Scheme 4.7***. Here a carbene is lost from dimeric intermediate **45** and a triple chloride bridged complex **46** is formed. The free carbene then causes the loss of a carbene from another molecule of **45**, resulting in the formation of stilbene. The final species **46** still contains a carbene proton. According to ^{1}H NMR, there is no carbene proton left after decomposition has taken place, thus this may not be the end of the decomposition route.

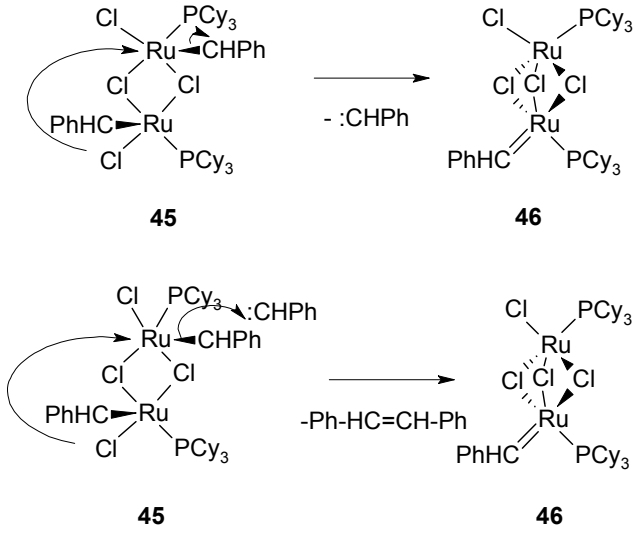

***Scheme 4.7**: Possible mechanism for bimolecular decomposition with the extrusion of stilbene (Ph-CH=CH-Ph)*

Fogg and coworkers[108] have reported the formation of a paramagnetic triple chloride bridged decomposition species in $CDCl_3$. Decomposition of Grubbs catalyst **2a** in chloroform may involve a free radical reaction with the dimeric intermediate **45** to form a mixed valent, paramagnetic species **42** as shown in ***Scheme 4.8***.

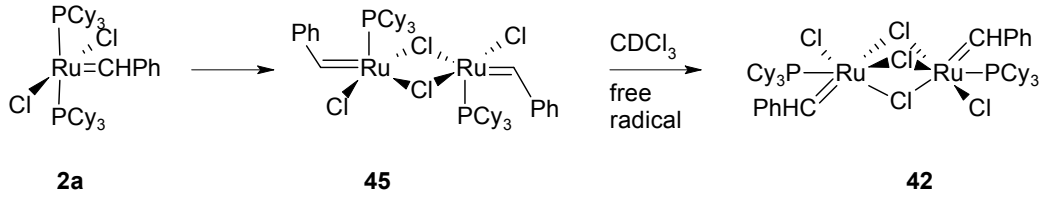

***Scheme 4.8**: Possible decomposition of the dimeric intermediate **45** into the mixed valent, paramagnetic complex **42** in $CDCl_3$.*

4.6 Halide Substitution at Grubbs Catalyst 2a *via* Salt Addition

4.6.1 Halide Substitution at Grubbs Catalyst 2a *via* Solid Salt Addition

After considering the reaction of Grubbs catalyst **2a** with the di-bromide **2b**, it was decided to determine if Grubbs catalyst **2a** reacts with another halide source. For this reason Grubbs catalyst **2a** was reacted with solid and dissolved salts. It was thought that the salt may react with the 14 electron intermediate **7a** preventing the formation of the dimeric intermediate **45** (***Scheme 4.8***), thus limiting bimolecular decomposition.

An attempt was made to carry out NMR experiments using solid salts, however this required that the experiment be carried out in the absence of spinning which meant that there was insufficient mass transfer leading to broad lines and very low conversions. However, batch reactions were carried out in the presence of a solid salt and monitored by GC, and showed an improvement in conversion and selectivity (see Section 4.7.2).

4.6.2 Halide Substitution at Grubbs Catalyst 2a *via* Addition of Bu_4NBr dissolved in $CDCl_3$

Reaction of Grubbs catalyst **2a** with an excess of Bu_4NBr dissolved in $CDCl_3$ resulted in the formation of both the di-bromide **2b** and the mixed halide complex **2c**. The reactions were monitored by recording ^{31}P NMR spectra every minute and were complete within about 15 minutes at room temperature as described in Section 4.2.2. The results are summarised in ***Figure 4.13*** and ***Figure 4.14*** on pages 88 and 89.

4.6.3 Equilibrium Constants for the Halide Substitution at Grubbs Catalyst 2a using Bu_4NBr dissolved in $CDCl_3$

The overall equilibrium constant $K_{5\text{-}6}$ was determined from ^{31}P NMR data by plotting K versus time and determining when K reached a constant value for 10 and 20 equivalents of Bu_4NBr (***Scheme 4.9*** and ***Table 4.1***).

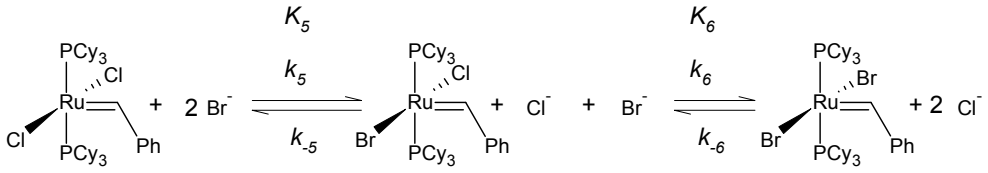

2a **2c** **2b**

Scheme 4.9: *Halide exchange of Grubbs catalyst **2a** with Bu_4NBr*

The equilibrium constants K_5, K_6 and $K_{5\text{-}6}$ were determined from the molar concentrations (from ^{31}P NMR data) as shown in ***Figure 4.11*** below. The concentration of Cl^- was calculated from the amount of **2b** and **2c** formed.

$$K_5 = \frac{[\mathbf{2c}][Cl^-][Br^-]}{[\mathbf{2a}][Br^-]^2}$$

$$K_6 = \frac{[\mathbf{2b}][Cl^-]^2}{[\mathbf{2c}][Cl^-][Br^-]}$$

$$K_{5\text{-}6} = \frac{[\mathbf{2c}][Cl^-][Br^-]}{[\mathbf{2a}][Br^-]^2} \times \frac{[\mathbf{2b}][Cl^-]^2}{[\mathbf{2c}][Cl^-][Br^-]} = \frac{[\mathbf{2b}][Cl^-]^2}{[\mathbf{2a}][Br^-]^2}$$

Figure 4.11: *Equations used to determine the required equilibrium constants for halide substitution at Grubs catalyst **2a** using Bu_4NBr*

***Table 4.1**: Equilibrium constants for the reaction of Grubbs catalyst **2a** with 10 or 20 equivalents of Bu_4NBr ([**2a**] = 2.16 x 10^{-2} M, $CDCl_3$, 30 °C (**Scheme 4.9**)*

	10 equivalents Bu_4NBr (x 10^{-2})	**Standard deviation, s (x 10^{-3})**	**20 equivalents Bu_4NBr (x 10^{-2})**	**Standard deviation, s (x 10^{-3})**
K_5	9.79	3.92	10.3	3.24
K_6	1.74	1.12	1.85	1.28
$K_{5\text{-}6}$	1.71	1.75	1.91	1.83

Thus the values of K_5, K_6 and $K_{5\text{-}6}$ obtained for the two experiments are the same within experimental error.

4.6.4 Order of Reaction for the Halide Substitution at Grubbs Catalyst 2a Using Bu_4NBr in $CDCl_3$

The reaction of Grubbs catalyst **2a** with Bu_4NBr dissolved in $CDCl_3$ involves a number of steps (***Scheme 4.9***). It is likely that the dissociation of the phosphine from Grubbs catalyst **2a** is the rate-determining step and that the kinetics is first order. This is supported by the fact that the reaction is severely inhibited in the presence of excess phosphine.

However, the situation is more complex because each of the complexes can undergo intermolecular halide exchange or react with the solvent as shown in Section 4.5.2. To simplify the situation it is assumed that there is no reaction with other complexes because of the excess salt used. It is also assumed that there is no reaction with the solvent for similar reasons.

Using the above approximations the reaction can be described as follows:

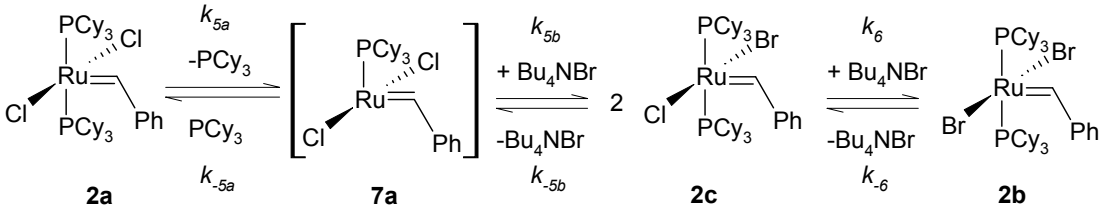

***Scheme 4.10**: The reaction of Grubbs catalyst **2a** with Bu_4NBr*

Considering only the first two steps, the application of the steady state approximation for the formation of [**7a**] leads to the following equations.

$$\text{rate} = \frac{k_{5a}k_{5b}[\text{2a}][\text{Bu}_4\text{NBr}]}{k_{-5a}[\text{PCy}_3] + k_{5b}[\text{Bu}_4\text{NBr}]}$$

$$\text{rate} = k_{5a}[\text{2a}] \quad \text{when } k_{-5a}[\text{PCy}_3] << k_{5b}[\text{Bu}_4\text{NBr}]$$

Two experiments were carried out, using 10 and 20 equivalents of Bu_4NBr respectively. Therefore $k_{-5a}[PCy_3] << k_{5b}[Bu_4NBr]$, the formation of [**2c**] is expected to be first order in [**2a**] and zero order in $[Bu_4NBr]$.

To verify the order of the reaction with respect to the bromide salt, two experiments were carried out where the same concentration of Grubbs catalyst was reacted with 20 and 10 equivalents of Bu_4NBr respectively (see ***Figure 4.13*** and ***Figure 4.14***). The first 5 minutes of the reaction were monitored because after this the formation of the di-bromide **2b** from the mixed chloride bromide **2c** is significant. There was little difference obtained in the rate of formation of **2c** with double the concentration of Bu_4NBr thus, as expected, the formation of [**2c**] is zero order with respect to Bu_4NBr.

4.6.5 Preliminary Kinetics of Substitution at Grubbs Catalyst 2a Using Bu_4NBr

From the above it is clear that the halide substitution at Grubbs catalyst in the presence of an excess of dissolved salt is a first order reaction which reaches equilibrium in about 15 minutes. The original scheme (***Scheme 4.4***) was simplified (***Scheme 4.1*** below) to allow determination of the rate constants for the formation of all complexes using a Microsoft Excel spreadsheet[122] that assumes first order behaviour of all components.

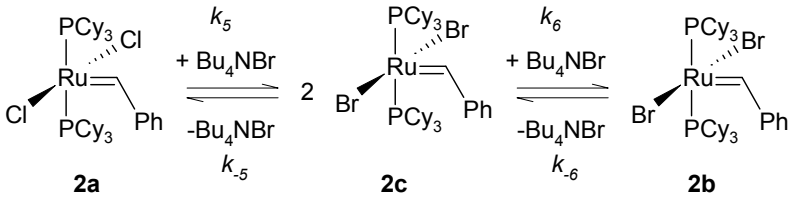

Scheme 4.11: *Simplified scheme for the reaction of Grubbs catalyst* ***2a*** *with* Bu_4NBr

The spreadsheet can handle up to 5 complexes, in equilibrium with each other. The solver function was used to vary k_5, k_{-5}, k_6 and k_{-6} until the sum of the square of the difference between the experimental data and the simulated data were at a minimum. The general equation for the rate constant simulation as well as the equations used to simulate the concentrations of **2a**, **2b** and **2c** throughout the experiment are shown in ***Figure 4.12***.

$$[\mathbf{A}] = [\mathbf{A}]_{\text{t-dt}} \;\; \text{dt}(\; \Sigma k_{\textit{loss of A}})[\mathbf{A}]_{\text{t-dt}} + \text{dt} * (\Sigma\; k_{\textit{formation of A}}) * [\text{species yielding } \mathbf{A}]_{\text{t-dt}}\;)$$

$$[\mathbf{2a}] = [\mathbf{2a}]_{\text{t-dt}} - \; \text{dt}(k_5) * [\mathbf{2a}]_{\text{t-dt}} + \text{dt}(k_{-5})[\mathbf{2c}]_{\text{t-dt}}$$

$$[\mathbf{2c}] = [\mathbf{2c}]_{\text{t-dt}} - \text{dt}(k_{-5} + k_6)[\mathbf{2c}] + \text{dt}(k_5 + k_{-6})([\mathbf{2a}]_{\text{t-dt}} + [\mathbf{2b}]_{\text{t-dt}})$$

$$[\mathbf{2b}] = [\mathbf{2b}]_{\text{t-dt}} - \text{dt}(k_{-6})[\mathbf{2b}] + \text{dt}(k_6)[\mathbf{2c}]_{\text{t-dt}}$$

Figure 4.12: *General and specific equations used in the general rate constant simulation Microsoft Excel spreadsheet for the reaction of Grubbs catalyst **2a** with Bu_4NBr*

The simulated data and experimental data for both cases are depicted in ***Figure 4.13*** and ***Figure 4.14***. The rate constants that were determined using the spreadsheet are summarised in ***Table 4.2***.

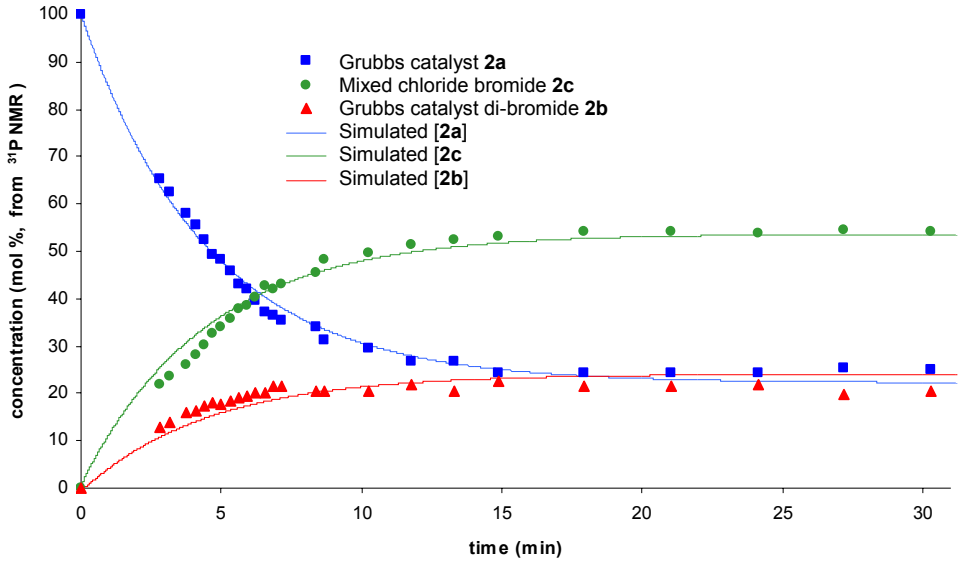

Figure 4.13: *Experimental data points and simulated data points for the reaction of Grubbs catalyst **2a** with 20 equiv Bu_4NBr ([**2a**] = 2.16 x 10^{-2} M, 30 °C, $CDCl_3$)*

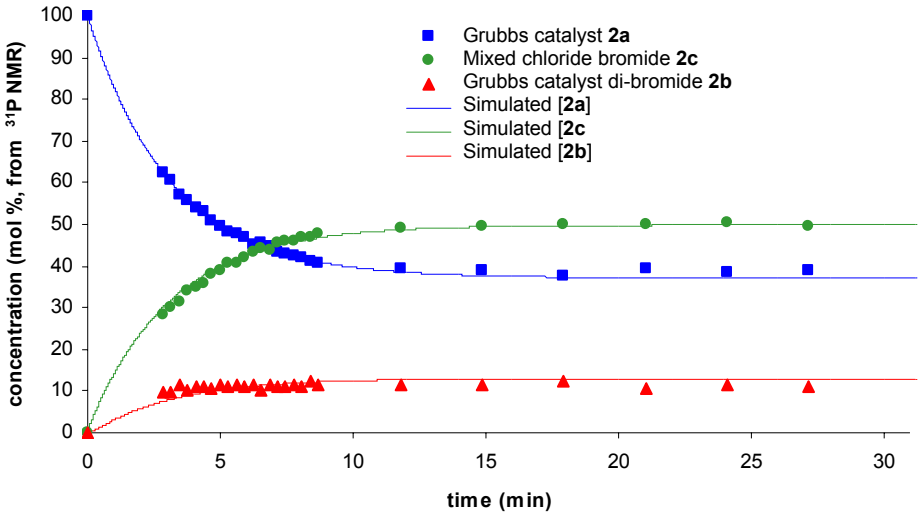

Figure 4.14: *Experimental data points obtained from ^{31}P NMR data and simulated data points for the reaction of Grubbs catalyst **2a** with 10 equiv Bu_4NBr ([**2a**] = 2.16 x 10^{-2} M, 30 °C, $CDCl_3$)*

Table 4.2: *Rate constants obtained for the reaction of Grubbs catalyst **2a** with 10 or 20 equivalents of Bu_4NBr ([**2a**] = 2.16 x 10^{-2} M, 30 °C, $CDCl_3$)*

Exp no.		k_5 s^{-1}	k_{-5} s^{-1}	k_6 s^{-1}	k_{-6} s^{-1}
1	Grubbs catalyst **2a**, + 10 equiv Bu_4NBr	3.3 x 10^{-3}	2.5 x 10^{-3}	2.2 x 10^{-2}	8.4 x 10^{-2}
2	Grubbs catalyst **2a**, + 20 equiv Bu_4NBr	2.9 x 10^{-3}	1.2 x 10^{-3}	3.6 x 10^{-2}	8.1 x 10^{-2}

The difference between the k_5 values obtained for the two different bromide concentrations is small (13%) and can probably be attributed to experimental error. The values for k_6 are not similar and reflect a larger amount of the mixed halide **2c** being converted to the di-bromide **2b** in the case of the second experiment. This also accounts for the slower rates for k_{-5} in the case of the second experiment.

The rate constant k_5 is an order of magnitude slower than that reported for the dissociation of the PCy_3, again showing significant rates for the recoordination of PCy_3 to the 14 electron intermediate **7a** (see Section 4.5.5).

The fit obtained for the experiment using 10 equivalents of Bu_4NBr is far better than that obtained for the experiment using 20 equivalents of Bu_4NBr, probably due to experimental error and because it was not possible to obtain data points within the first two minutes of the reaction.

It is possible to determine the equilibrium constant ($K_{5\text{-}6}$) from the kinetic data. The data determined from the kinetics is pseudo first order, thus the rate constants are observed rate constants and must be converted to real rate constants by multiplication with the molar concentration of the salt. This was done for the experiment where 10 equivalents of Bu_4NBr was reacted with Grubbs catalyst **2a** $[Ru(Cl)_2(PCy_3)_2CHPh]$.

$$K_{5\text{-}6} = \left(\frac{k_5 \times k_6}{k_{-5} \times k_{-6}} \right) \times [Bu_4NBr] = \frac{3.3 \times 10^{-3} \times 2.2 \times 10^{-2}}{2.5 \times 10^{-3} \times 8.4 \times 10^{-2}} \times [Bu_4NBr]$$

$$= 0.34 \times 0.025 = 0.008$$

The $K_{5\text{-}6}$ calculated from kinetic data is within a factor of 4 of the value obtained at equilibrium, 0.0017 (see Section 4.6.3). Thus reasonable agreement is obtained between the preliminary kinetic data and the equilibrium data, thereby supporting the proposed mechanism.

4.6.6 Dissolved Salt Addition - Halide Substitution at Grubbs Catalyst 2a Using Bu_4NI in $CDCl_3$

Grubbs catalyst **2a** was reacted with 10 equivalents of Bu_4NI in $CDCl_3$ (***Figure 4.15***), which resulted in the formation of a new species which resonates at δ 37.2.

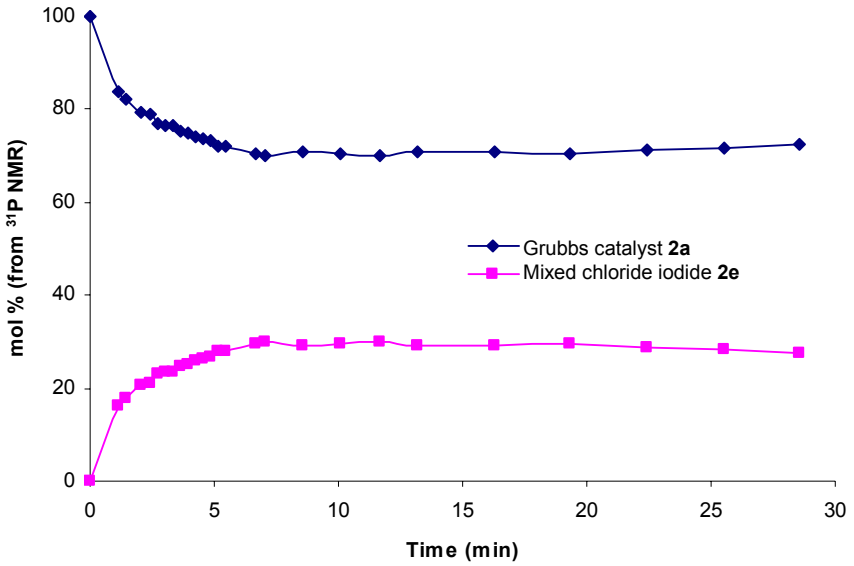

Figure 4.15: *Halide exchange of Grubbs catalyst **2a** with 10 equivalents of Bu_4NI ([**2a**] = 2.15 x 10^{-2} M 30 °C, $CDCl_3$)*

An attempt was made to synthesise the di-iodide **2d**, but it was found that the complex underwent some decomposition. Sanford and Love report that the bisphosphine ruthenium iodides can be unstable.[65] Nevertheless the ^{31}P NMR and ^{1}H NMR spectrum showed the chemical shifts of the di-iodide **2d** as expected. Grubbs catalyst **2a** was reacted with the di-iodide **2d** and the same new complex was formed. This indicates that a mixed complex, $[Ru(PCy_3)_2ICICHPh]$ **2e** was formed on reaction of Grubbs catalyst **2a** with Bu_4NI.

4.6.7 Low Temperature Behaviour of the Mixed Halide Grubbs Catalyst 2c

Low temperature ^{1}H NMR (-60 °C) showed the presence of four carbene species when Grubbs catalyst **2a** was reacted with Bu_4NBr in $CDCl_3$. (***Figure 4.16***). Two of these peaks were in equilibrium and broadened with increasing temperature before coalescing to one peak at -40 °C.

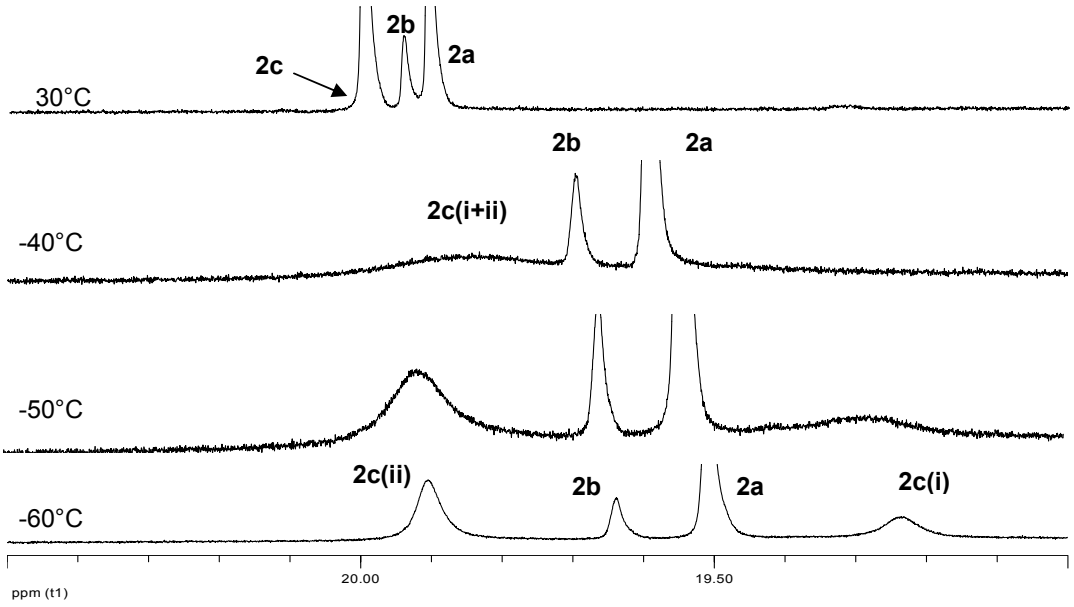

Figure 4.16: *^{1}H NMR showing that there are two forms of **2c** visible at low temperature, 1.46 x 10^{-2} mmol Grubbs catalyst **2a**, 10 equivalents Bu_4NBr in 0.6 mL $CDCl_3$*

The two resonances observed at -60 °C presumably reflect the two possible orientations of the halides. Molecular modelling[123] shows that there is not much difference in the energy required (2 kJ.mol^{-1}) to form these two species, thus indicating that both mixed species will form (***Figure 4.17***).

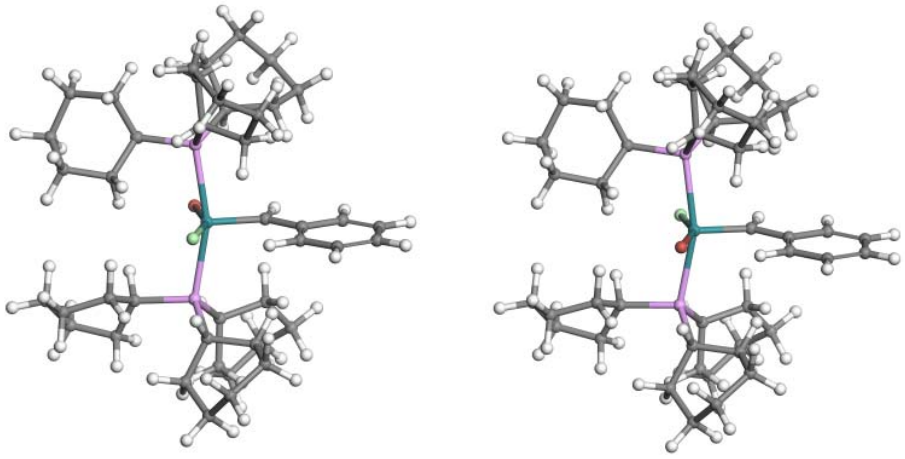

Figure 4.17: *Modelled structures of the two forms of the mixed bromide chloride Grubbs catalyst **2c***

The rate constant at the coalescence point was calculated as follows:

$$k_{chem} = 2 \times \frac{\pi(dv)}{\sqrt{2}} = 1781 s^{-1} \text{ at } \quad 40°C \text{ (measured at 600MHz)}$$

The factor of 2 is used to take into account the populations of the two sites in an AB system.[115] The broad coalesced peak corresponds to that of the mixed species **2c** at room temperature. This reaction is much faster than that of phosphine dissociation[119] and addition of extra ligand does not slow the rate of exchange between these two carbenes, indicating that phosphine dissociation is not required. Therefore the interconversion of the two mixed species represents an intramolecular rearrangement, without prior dissociation of the phosphine. This intramolecular rearrangement probably occurs in any solution of Grubbs catalyst.

Rotation around the Ru=C bond has been reported before for Schrock type methylidene complexes[57] (see Section 2.7 on page 18) and would explain the current results. However, this is unlikely to occur because of the bulk of the CHPh group.

4.7 Catalytic Evaluation

The self-metathesis of 1-octene was used to test the effect of the addition of solid and dissolved salts on conversion and selectivity. The desired products are *cis*- and *trans*-tetradecene. The side products, due to isomerisation are *cis* and *trans* 2-octene, 3-octene, 4-octene and tridecene. The experiments were carried out as described in 4.2.7. Conversion and selectivity were calculated from GC-FID data as follows:

$$\text{Conversion} = \frac{[\text{internal octenes}] + 2[\text{tridecene}] + 2[\text{tetradecene}]}{[1-\text{octene}] + [\text{internal octenes}] + 2[\text{tetradecene}] + 2[\text{tridecene}]} \times 100$$

$$\text{Selectivity} = \frac{2[\text{tetradecene}]}{2[\text{tetradecene}] + 2[\text{tridecene}] + [\text{internal octenes}]} \times 100$$

$$\text{where } [\text{internal octenes}] = [2-\text{octene}] + [3-\text{octene}] + [4-\text{octene}]$$

4.7.1 Self-metathesis of 1-Octene in the Presence of $CDCl_3$

Catalyst testing was carried out in the presence and absence of 10 mL $CDCl_3$. A much improved conversion and selectivity were obtained (***Figure 4.18***).

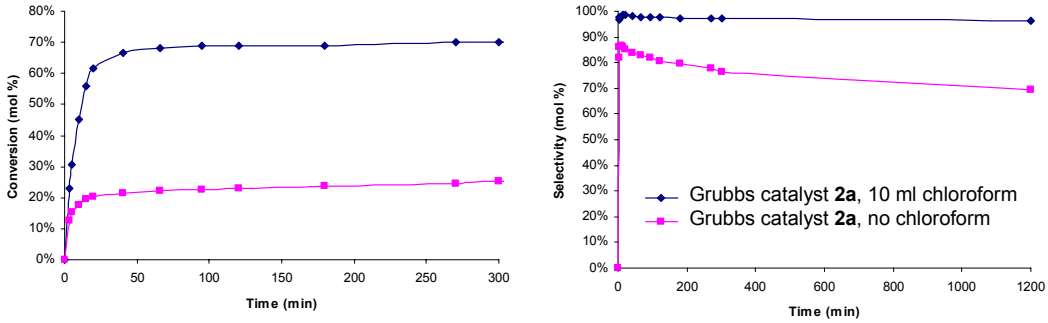

Figure 4.18: *Effect of the presence of 10 mL chloroform on the self metathesis of 1-octene using Grubbs catalyst* ***2a*** *(100 ppm Ru, [Ru] = 7.05 x 10^{-4} M (excluding $CDCl_3$) , 50 °C, 20 mL 1-octene)*

Others[124] have also shown much improved conversion and selectivity in the presence of chlorinated solvents. It is postulated in Section 4.3 that the 14 electron intermediate **7a** reacts with chlorinated solvents. Although other factors play a role, the improvement in conversion may be due to the reaction of the 14 electron intermediate **7a** with the chlorinated solvent, resulting in a reduction in formation of the dimeric intermediate and thus less bimolecular decomposition. Concentrations of ruthenium in the reaction were calculated

by excluding the added chloroform in order to keep the catalyst to substrate ratio constant.

4.7.2 Self-metathesis of 1-Octene in the Presence of a Solid Salt

Catalyst testing was carried out in the presence of a solid salt Et_4NCl as described in Section 4.2.7 and the results are shown below. A chlorinated salt was chosen so that there was no possibility of formation of a new catalyst. It is again clear that there is an improvement in conversion and selectivity in the presence of the salt.

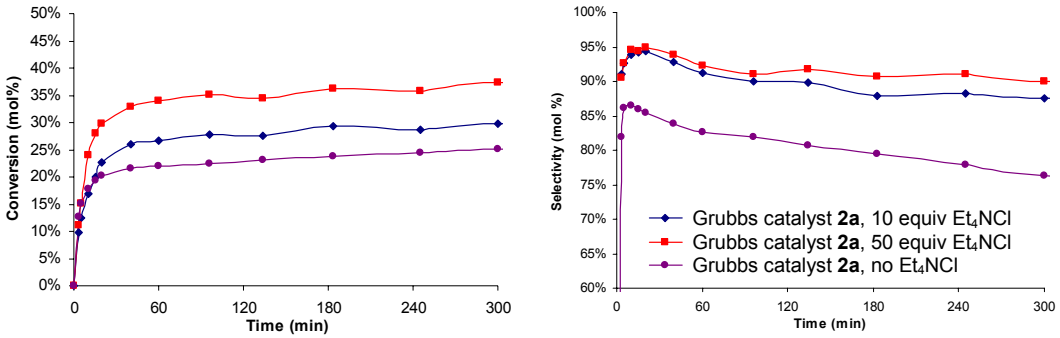

Figure 4.19: *Effect of the presence of solid Et_4NCl on the self metathesis of 1-octene using Grubbs catalyst **2a** (100 ppm Ru, [Ru] = 7.05 x 10^{-4} M, 50 °C, 20 mL 1-octene)*

Improved conversion and selectivity are also obtained if self-metathesis of 1-octene is carried out in the presence of solid NaI. However, in this case it is possible that a new catalyst is formed (the di-iodide **2d** or the mixed iodide chloride **2e**) which has different stability characteristics compared to Grubbs catalyst **2a**. According to Grubbs and coworkers,[61] the di-iodide **2d** is far less stable and less active than Grubbs catalyst **2a** and thus formation of the new catalyst should result in lower conversion and selectivity. Thus it is concluded that it is the presence of the salt that increases conversion and selectivity in this case.

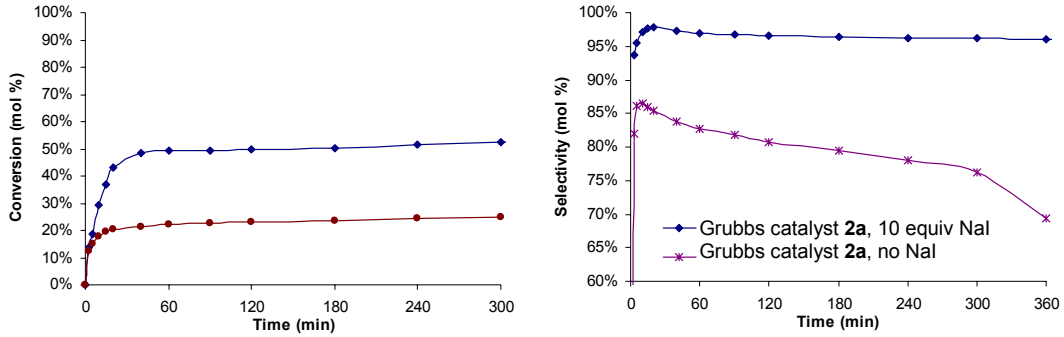

Figure 4.20: *Effect of the presence of 10 equivalents of NaI on the self metathesis of 1-octene using Grubbs catalyst* ***2a*** *(100 ppm Ru,[Ru] = 7.05 x 10^{-4} M, 50 °C, 20 mL 1-octene)*

4.7.3 Self-metathesis of 1-Octene in the Presence of Dissolved Salts

To make the halide more available, catalyst testing was repeated using Et_4NCl dissolved in chloroform (***Figure 4.21***). It was previously shown that presence of chloroform greatly increases both conversion and selectivity compared to the experiment with no chloroform added (***Figure 4.18***).

In comparison to the experiment containing only chloroform, decreased reaction rate and conversion was observed in the experiments with the added salt. Therefore, it appears that the addition of extra halide leads to inhibition of the catalyst in the presence of chloroform. This is the opposite trend to that observed when solid salt was added, but the same trend observed (although a much smaller effect) as when excess phosphine is added. Possibly the extra halide reduces the concentration of the propagating species in solution. Selectivity, however, remains high.

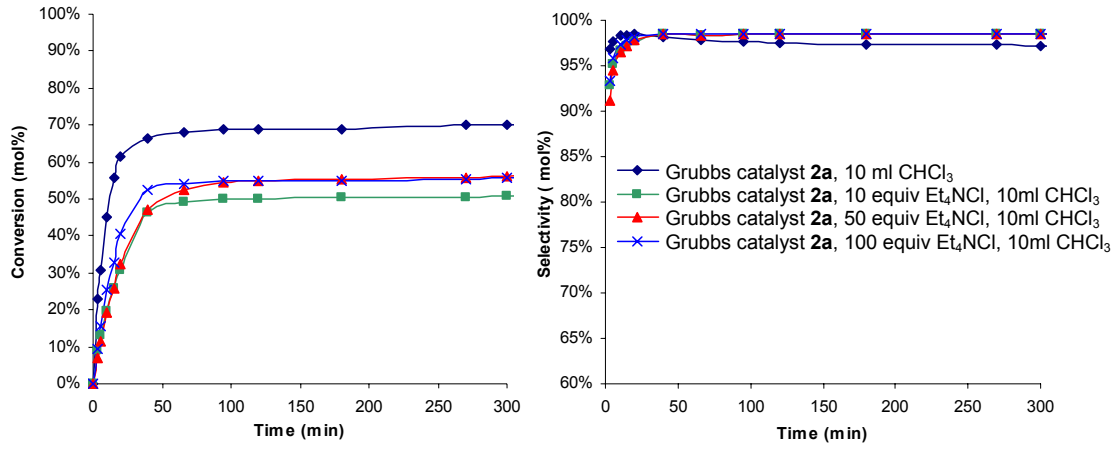

Figure 4.21: *Effect of the presence of Et_4NCl and/or chloroform on the self metathesis of 1-octene, using Grubbs catalyst* ***2a*** *(100 ppm Ru,[Ru] = 7.05 x 10^{-4} M (excluding $CDCl_3$) 50 °C, 20 mL 1-octene).*

4.8 Inhibition of Bimolecular Decomposition Using Additives

A bimolecular decomposition pathway will be inhibited by inhibiting the formation of the proposed dimeric intermediate **45**. Anything that reacts reversibly with the 14 electron intermediate **7a** will also slow down the formation of the dimeric intermediate and thus slow down bimolecular decomposition. These include excess ligand, ligand oxide, any other source of halide, whether organic or in salt form or the solvent itself. Note, however, that the 14 electron intermediate **7a** is also the propagating species in the metathesis reaction. Thus decreasing the concentration of this species in solution will also slow the metathesis reaction, as evidenced by the addition of excess phosphine[61] and excess halide (***Figure 4.21***).

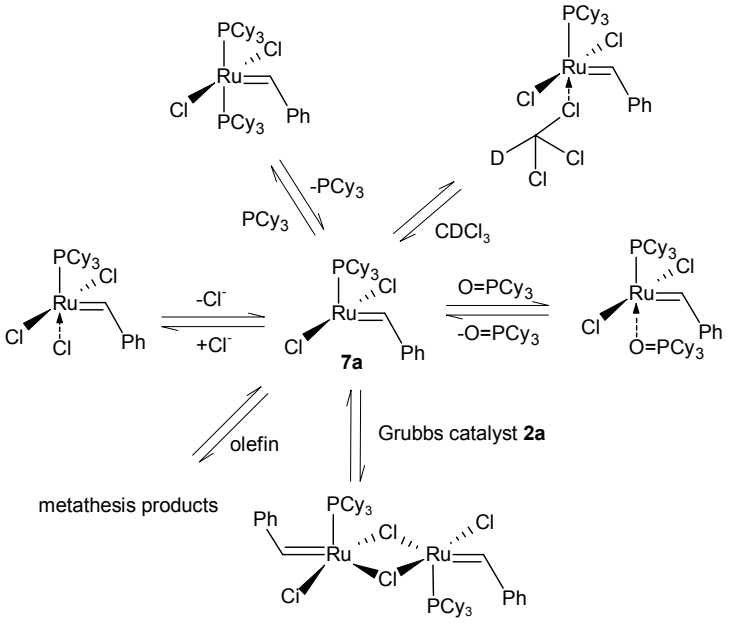

Figure 4.22**: Possible reactions from the 14 electron intermediate **7a

It has been reported that the decomposition of Grubbs catalyst **2a** in $CDCl_3$ results in the formation of paramagnetic decomposition products,[112] while in the absence of $CDCl_3$, no paramagnetic products have been noted. The reported formation of the paramagnetic decomposition products in $CDCl_3$ could be explained by the formation of the paramagnetic mixed valence ruthenium dimer **42** (see ***Scheme 4.8***). This mixed valence dimer is possibly formed by reaction of the dimeric intermediate with $CDCl_3$ (see ***Scheme 4.12***).

It has been shown previously that the addition of phenol greatly enhances the lifetime of the catalyst.[111] The addition of phenol does not inhibit halide exchange (see ***Figure 4.8***), thus the dimeric intermediate **45** is still formed. It is therefore proposed that the addition of phenol, a free radical scavenger, inhibits the formation of the mixed valent dimer **42** and thus that the reaction of the dimeric intermediate **45** with $CDCl_3$ to form the mixed valent dimer **42** is a free radical reaction (see ***Scheme 4.12***).

In Meyer and co-worker's experiment,[112] $SnCl_2$ is added to a solution containing a paramagnetic ruthenium species (see Section 2.12 on page 49),

resulting in the formation of a highly active Ru-Sn dimer-like complex **43**, for which a crystal structure was obtained. The Ru-Sn complex **43** is possibly formed by the reaction of the mixed valent dimer **42** (see Section 4.5.6 on page 80) with $SnCl_2$.

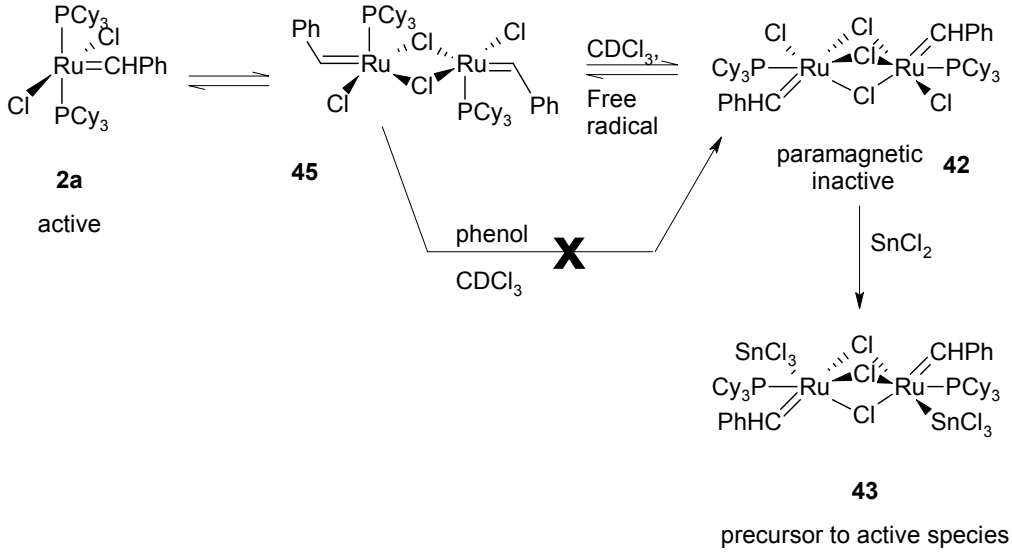

Scheme 4.12: *Possible role of phenol and $SnCl_2$ in the inhibition of decomposition of Grubbs catalyst **2a** in $CDCl_3$*

Both phenol and $SnCl_2$ are also beneficial in non-chlorinated homogeneous metathesis systems, where **42** presumably cannot form, thus they have other roles as well. Possibly in a non-chlorinated system a doubly halide bridged Ru-Sn dimer **47** may form which is in equilibrium with a highly active Ru-Sn monomer **48** (**Scheme 4.13**).

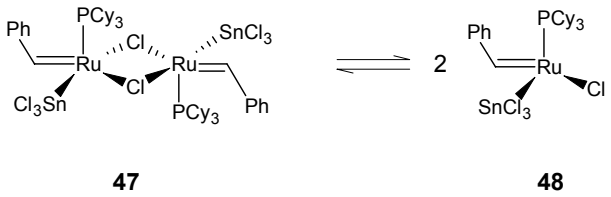

Scheme 4.13: *Possible catalytic species formed using Grubbs catalyst **2a** in the presence of $SnCl_2$*

4.9 Selectivity

Isomerisation of the feed and product reduces selectivity to the desired products when using Grubbs catalyst **2a** for cross metathesis. The results in Sections 4.7.1, 4.7.2 and 4.7.3 show that selectivity is much improved in the presence of $CDCl_3$ or tetra-alkyl ammonium salts, either solid or dissolved in $CDCl_3$, thereby indicating that the decomposition pathway that leads to isomerisation active species has been inhibited. In Chapter 5, it is shown that the β-hydride decomposition mechanism is also inhibited in the presence of $CDCl_3$. The β-hydride decomposition pathway includes the formation of a ruthenium hydride which is highly likely to be isomerisation active.[125] Thus it is thought that the improvement in selectivity in the experiments containing $CDCl_3$ is not due to the inhibition of bimolecular decomposition, but rather the inhibition of the β-hydride transfer decomposition pathway.

In the batch experiments where a solid salt is added and there is no $CDCl_3$ present, the improvement in selectivity and conversion may be due to the inhibition of the formation of a dimeric intermediate **45**, by the addition of excess halide, as proposed in Section 4.6.1 on page 83. Another possibility is that the presence of a solid salt may also inhibit the beta hydride decomposition pathway resulting in increased conversion and selectivity, however this has not been tested.

4.10 Conclusions on Bimolecular Decomposition

- The halides in Grubbs catalyst complexes are surprisingly labile. Halide exchange of Grubbs catalyst di-bromide **2b** is proposed to take place with chlorinated solvents *via* a metathesis-like mechanism. This reaction is not inhibited by excess phenol (100 equivalents), hence it unlikely to proceed *via* a free radical mechanism.

- Halide exchange between identical complexes occurs continuously in any solution of these complexes. Unfortunately, it is not possible to monitor this dynamic process with NMR because the product and the

starting material are identical. However, such exchange can be monitored between two complexes containing different halides (for example, Grubbs catalyst **2a** and the di-bromide **2b**).

- It is proposed that intermolecular halide exchange reactions between two Grubbs catalyst species containing different halides (for example, Grubbs catalyst **2a** and the di-bromide **2b** involve a dimeric intermediate **44a** or **44b** which can either form the halide exchange products or undergo bimolecular decomposition. Phenol does not retard this reaction hence it is unlikely to proceed *via* a free radical mechanism.

- It is proposed that intermolecular halide exchange between identical Grubbs catalysts (for example, Grubbs catalyst **2a**) involves a dimeric intermediate **45** which can either be converted back to the starting materials or undergo bimolecular decomposition.

- Further decomposition in $CDCl_3$ from the dimeric intermediate **45** is possibly *via* the formation of a paramagnetic, mixed valence triple chloride bridged monoalkylidene ruthenium dimer as suggested by Fogg *et al*.[107]

- It is possible to inhibit bimolecular decomposition in $CDCl_3$ in three ways:
    - It is proposed that the formation of the paramagnetic ruthenium dimer is a free radical reaction as this reaction is inhibited by the presence of phenol, a free radical scavenger.
    - It is proposed that $SnCl_2$ reacts with the mixed valent, triple chloride bridged paramagnetic species **42** to form the dimer-like Ru-Sn species **43**, which is a precursor to an active metathesis species.
    - Halide salts added in excess (10 or 20 equivalents) to the reaction may react with the 14 electron intermediate **7a**,

inhibiting the formation of a dimeric intermediate **44a**. Catalyst testing in the presence of salts shows increased conversion.

- Decomposition of the dimeric intermediate in non-chlorinated solvents may include formation of a triple chloride bridged species with loss of a carbene radical. This carbene radical then induces loss of a carbene radical from a neighbouring dimeric complex **45**, resulting in the formation of stilbene (see Section 4.5.6).[107]

- The life-time of the Grubbs catalyst **2a** is significantly improved in the presence of phenol or $SnCl_2$.[112] The mechanism for the improvement in the presence of $SnCl_2$ may involve formation of a dimeric species **47** that is in equilibrium with an active Ru-Sn monomer **48**.

- It is possible that in a reaction where the product does not undergo metathesis,[126] the reaction of the starting olefin with the 14 electron intermediate **7a** is favoured. Only once the starting olefin is substantially depleted do the complexes start to react with each other resulting in increased rate of formation of bimolecular decomposition species. Therefore, to avoid bimolecular decomposition, fresh olefin should be added continually in a commercial process.

- The low temperature behaviour of the mixed complex **2c** shows that there are two forms of **2c** which interchange at a rate that is much faster than phosphine dissociation. Therefore this process is proposed to be an intramolecular process without prior phosphine dissociation. The exact process is still unclear. This process probably occurs continuously for all Grubbs catalysts.

- The improved selectivity shown in all batch experiments containing $CDCl_3$ is probably due to the inhibition of the β-hydride transfer decomposition pathway (see Chapter 5).

- The improved selectivity and conversion shown in all batch experiments where Grubbs catalyst **2a** is reacted with a solid salt may be due to inhibition of the formation of the doubly bridged dimeric intermediate **45**.

Chapter 5: Decomposition of the Ruthenium Based Methylidene Species

5.1 Introduction

There are a few possible commercial processes under study at present which require an ethenolysis step. For some of these processes the available heterogeneous catalysts are not suitable, either due to poor selectivities or incompatibility with the substrate.

Dow Chemical Company[16] have researched the ethenolysis of methyl oleate for the production of 1-decene and methyl-9-dodecanoate for use in epoxy thermoplastics and thermosets, polyurethane foams, thermoplastic polyurethanes, polyolefin co-monomers and surfactants. The use of methyl oleate is significant because it involves making chemicals from renewable sources instead of fossil fuel derived feedstocks.

Another possible commercial process is the ethenolysis of a 2-alkene to produce α-olefins, which can be used as co-monomers in plastics, converted into poly α-olefins for the lubricants industry, or hydroformylated to alcohols for use in the surfactant and plasticiser industries.

The catalytic species produced in the ethenolysis of a 2-alkene using Grubbs catalyst **2a** are depicted in ***Scheme 5.1***.

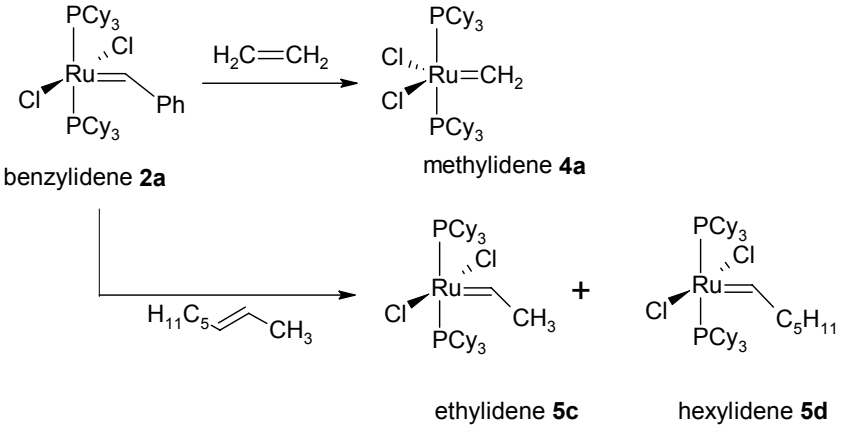

Scheme 5.1**: Ruthenium based alkylidene catalytic species formed during homogeneous ethenolysis of 2-octene using Grubbs catalyst **2a

The methylidene **4a** is present in large concentration because of the large excess of ethylene used in the reaction. Extensive thermal decomposition studies have shown that the Grubbs methylidene complex **4a** decomposes *via* a first order decomposition process which is independent of phosphine concentration, rather than *via* bimolecular decomposition. [11]

Deuterium labelling studies in C_6D_6 have shown that the CH_2 from the methylidene ends up in the ligand region (at about δ 0, broad peak) and thus all results point to deactivation of the catalyst *via* CH activation of the ligand.[11]

To the best of our knowledge, no studies have been carried out under catalytic conditions.

In this part of the study we investigate the halide exchange reaction with the methylidene **4a**, and also report the ethylene induced decomposition of the Grubbs catalyst methylidene **4a** and the second generation Grubbs catalyst methylidene **6** in benzene and chloroform, under ethenolysis conditions.

5.2 General Experimental

5.2.1 NMR

All ^{1}H NMR spectra (30° pulse angle, 2 second relaxation delay) and ^{31}P NMR spectra (30° pulse angle, 2 second relaxation delay) were recorded on a 500 MHz Bruker Avance NMR fitted with a QNP probe, or a 600 MHz Varian Unity Inova NMR fitted with a switchable 4 nucleus pulse field gradient 5 mm probe. The ^{31}P and ^{1}H spectra over time were recorded using the pulse program kinetik (Bruker[127]) or using the pre-acquisition delay (Varian).

All ^{2}H NMR spectra (45° pulse angle, 2 second relaxation delay) were recorded on a Varian 600 MHz NMR fitted with a switchable pulsed field gradient 5 mm probe. The lock was turned off, the lock gain and lock power set to zero, the lock barrel filter and quarter wave cable were placed in line with the X channel and the probe was tuned to ^{2}H.

All ^{1}H-^{31}P HMQC and HMBC spectra (128 increments, 4 scans) were recorded on a Varian 600 MHz Unity Inova. All ^{1}H-^{13}C HMBC and HMQC were recorded on a Bruker 500 MHz NMR (128 increments, 4 scans).

5.2.2 High Pressure NMR

A 10 mm high pressure ROE cell[128] was used to record ^{31}P NMR (45° pulse angle, 2 second relaxation delay) and ^{1}H NMR (45° pulse angle, 2 second relaxation delay) spectra on a Varian 600 MHz Unity Inova NMR fitted with a 10 mm broad banded probe tuned to ^{31}P and ^{1}H. ^{31}P NMR spectra were recorded over time using the pre-acquisition delay.

5.2.3 Gas Chromatography

GC/MS (PONA column)

Samples were injected on an Agilent GC/MS (helium carrier gas, split/splitless inlet, split 1:100, inlet temperature 250 °C, injection volume 0.5µl, PONA (50

m x 0.2 mm ID x 0.5 µm), 50 °C (1 min) to 320 °C (0 min) at a rate of 4 °C/min, ion source temperature 170 °C).

GC-FID (PLOT column)

Samples were injected on an Agilent GC-FID 6890 (hydrogen carrier gas, split/splitless inlet, split 1:100, inlet temperature 220 °C, 0.5 µL injection volume, PLOT Al_2O_3/KCl (50 m x 0.32 mm x 5 µm) column, 60 °C (2 min) to 200 °C at a rate of 5 °C/min, detector temperature 220 °C).

5.2.4 Possible Reaction of $CDCl_3$ with Bu_4NBr

Bu_4NBr (68 mg, 0.20 mmol) was dissolved in 0.6 mL $CDCl_3$ in a 5 mm NMR tube and heated at 40 °C overnight after which the sample was analysed with GC/MS (PONA column) and ^1H NMR. The $CDCl_3$ used in the experiment was analysed under the same conditions.

5.2.5 Possible Reaction of $CDCl_3$ with C_6D_6

$CDCl_3$ (0.3 mL) and C_6H_6 (0.3 mL) were heated overnight at 40 °C in a 5 mm NMR tube, after which the reaction mixture was analysed with GC/MS (PONA column) as described in Section 5.2.3.

5.2.6 Thermal Decomposition of Grubbs Methylidene 4a

Grubbs methylidene **4a** (19.5 mg, 0.026 mmol) was dissolved in 0.6 mL $CDCl_3$ in a 5 mm NMR tube and ^{31}P and ^1H NMR spectra were recorded at 30 °C. The sample was heated to 50 °C and ^1H and ^{31}P NMR spectra were recorded over time.

5.2.7 Bromide Substitution at Grubbs Catalyst Methylidene 4a using Bu_4NBr in $CDCl_3$

Grubbs catalyst methylidene **4a** (11 mg, 0.014 mmol) was reacted with Bu_4NBr (65 mg, 14 equiv) in 0.6 mL $CDCl_3$ and ^{31}P NMR spectra were

recorded over time. After 15 minutes at 30 °C the temperature was increased to 40 °C and spectra were recorded every 30 minutes overnight.

5.2.8 Ethylene Induced Decomposition of the Isolated Ruthenium Based Methylidenes

The required methylidene (0.0318 mmol) and 0.6 mL C_6D_6 or $CDCl_3$ was transferred to an NMR tube in a glove box after which the NMR tube was sealed with parafilm. ^{1}H and ^{31}P NMR spectra were recorded at 30 °C after which ethylene was slowly bubbled through the solution in the NMR tube for 60 seconds before sealing the NMR tube again. ^{1}H and ^{31}P NMR were recorded at 30 °C and 40 °C. ^{31}P NMR or ^{1}H NMR spectra were recorded every 30 minutes for 16 hours. At the end of the experiment final ^{1}H and ^{31}P NMR spectra, ^{1}H-^{31}P HMBC and HMQC and/or ^{1}H-^{13}C HMBC and HMQC spectra were recorded at 40 °C. In the case of the decomposition in $CDCl_3$, the solvent was removed and C_6H_6 was added, after which a deuterium spectrum was recorded.

5.2.9 Possible Interaction of Methyltricyclohexylphosphonium Salt with $O=PCy_3$

PCy_3 (22.3 mg, 70% pure, major impurity is $O=PCy_3$) was dissolved in C_6D_6 (0.6 mL) and a ^{31}P NMR spectrum was recorded. MeI (0.21 g, 2500 equivalents) was added to the NMR tube and a ^{31}P NMR spectrum was recorded again. $O=PCy_3$ (39 mg) was added to the NMR tube and a ^{31}P NMR spectrum was recorded. A ^{31}P NMR spectrum of $O=PCy_3$ dissolved in 0.6 mL C_6D_6 was also recorded.

5.2.10 Ethylene Induced Decomposition of the di-bromide Methylidene 4b formed *in situ*, in $CDCl_3$

The di-bromide **2b** (23 mg, 0.0252 mmol) and C_6H_6 (2 mL) was added to a high pressure NMR cell and ethylene was bubbled through the solution for 60 seconds. A ^{31}P NMR spectrum was recorded using the Varian 600 MHz NMR fitted with a 10 mm broad band probe. $CDCl_3$ (0.5 mL) was added and the

cell was pressurised to 10 bar with ethylene. ^{31}P NMR spectra were recorded every 30 minutes. Starting and ending ^{1}H NMR spectra were recorded. The reaction mixture was analysed with GC/MS (PONA column) at the end of the experiment.

5.3 Halide exchange of the Grubbs Catalyst Methylidene 4a with Dissolved Salts as Halide Source

Bimolecular decomposition is not the major decomposition pathway of the methylidene as no ethylene is formed on decomposition,[11] therefore it is expected that there will be little or no halide exchange with the Grubbs methylidene catalyst. It is uncertain whether this lack of bimolecular decomposition products is due to the lower susceptibility of the methylidene to bimolecular decomposition or because of the presence of another faster decomposition route.

The first step in the halide exchange reaction is the dissociation of phosphine to form the 14 electron intermediate **7a** $[Ru(Cl)_2(PCy_3)CHPh]$. Grubbs and co-workers were unable to measure the rate of dissociation of the phosphine from the methylidene **4a** $[Ru(Cl)_2(PCy_3)_2CH_2]$, but found the rate of initiation to be three orders of magnitude slower than for Grubbs catalyst **2a** $[Ru(Cl)_2(PCy_3)_2CHPh]$. Thus, phosphine dissociation is much slower for the methylidene **4a** than for the benzylidene **2a**. Halide exchange is therefore not expected to occur easily for the methylidene **4a**.

5.3.1 Possible reaction of Bu_4NBr and chloroform

Bu_4NBr and $CDCl_3$ were heated in a 5 mm NMR tube at 40 °C overnight to determine if there is any bromodichloromethane formed in the absence of a ruthenium alkylidene complex. The reaction mixture was analysed using NMR and GC/MS (PONA column) at the end of the experiment. The $CDCl_3$ used in the experiment was analysed using the same conditions to ensure that no bromodichloromethane was present.

The chromatogram obtained after the reaction of Bu_4NBr with $CDCl_3$ at 40 °C for 16 hours is shown in ***Figure 5.1***. The CCl_4 detected was found in the analysis of the $CDCl_3$ used in the experiment and is therefore not formed in the reaction. The syringe needle used for the GC injection was washed with xylene and this is probably the origin of the xylenes observed. The chromatogram shows the formation of tri-n-butylamine and 1-bromobutane as well as a small amount of chlorobutane and bromodichloromethane. Quantification of the brominated products formed was not carried out because Bu_4NBr is a non-volatile salt and remains in the inlet liner of the GC and thus the chromatogram obtained is not representative of the whole sample.

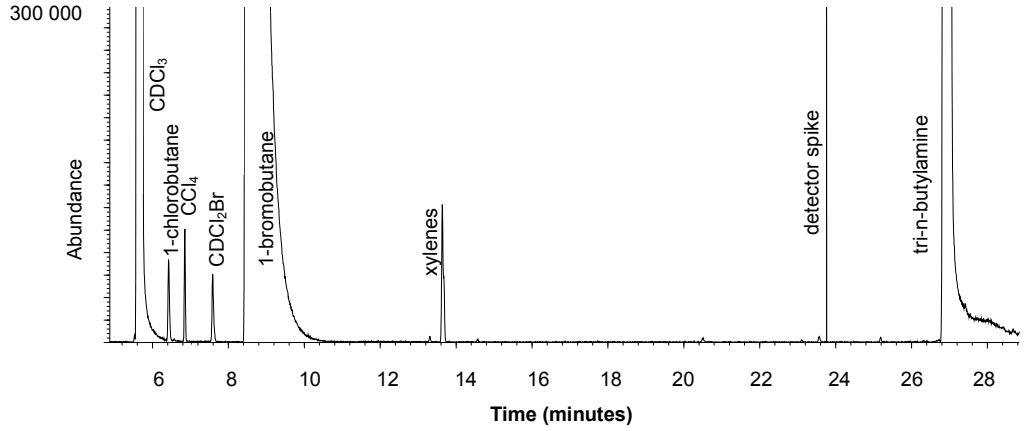

***Figure 5.1**: GC trace obtained after heating Bu_4NBr in $CDCl_3$, showing compounds formed inside the hot inlet of the GC ($[Bu_4NBr] = 3.52 \times 10^{-1}$ M, 40 °C for 16 hours, $CDCl_3$)*

However, in the ^1H NMR spectrum recorded after the experiment only the original N-butyl amine salt was detected (see ***Figure 5.2***). This indicates that the compounds observed in the in the GC/MS chromatogram are either formed in very small concentration and thus are not detected by NMR or are formed inside the hot inlet of the gas chromatograph.

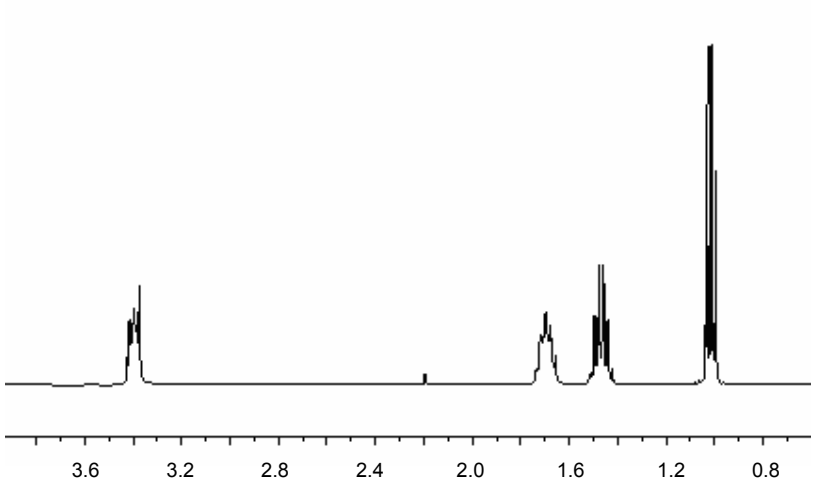

Figure 5.2: *^{1}H NMR spectrum obtained after heating Bu_4NBr in $CDCl_3$ for 16 hours, showing only the presence of Bu_4NBr (40 °C, [Bu_4NBr] = 3.52 x 10^{-1} M, $CDCl_3$)*

Thus, it is concluded that there is no appreciable reaction between the Bu_4NBr and chloroform in the absence of a ruthenium complex, thereby indicating that brominated products formed in the presence of a ruthenium alkylidene complex are formed in a ruthenium mediated process.

5.3.2 Thermal decomposition of Grubbs catalyst methylidene 4a in $CDCl_3$

Grubbs catalyst methylidene **4a** was thermally decomposed in chloroform at 50 °C as described in Section 5.2.6. The results of the experiment are summarised in ***Figure 5.3***. The carbene disappears in about 50 minutes at 50 °C. There is a steady decrease in the relative intensity of the ^{31}P NMR signal, indicating the probable formation of paramagnetic species, as previously seen by Fogg *et al.*[107] for other ruthenium carbene complexes.

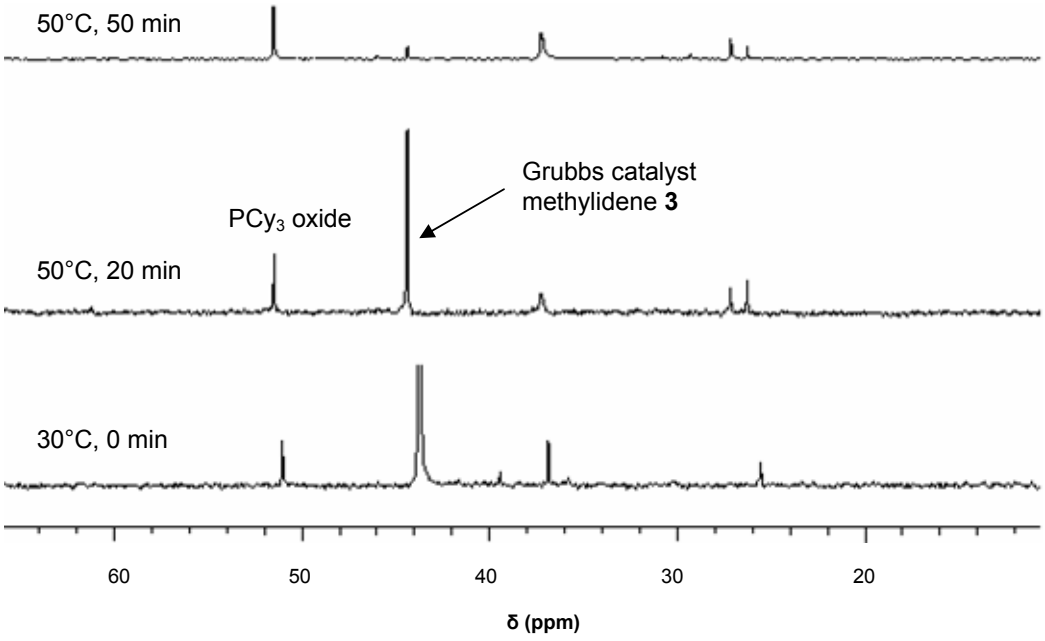

Figure 5.3: *^{31}P NMR stacked plot of the thermal decomposition of Grubbs methylidene **4a** ([Ru] = 4.35 x 10^{-2} M, 50 °C, $CDCl_3$)*

5.3.3 Bromide substitution at Grubbs catalyst methylidene 4a using Bu_4NBr in $CDCl_3$

^{31}P NMR over time

The reaction between Grubbs catalyst **2a** and Bu_4NBr reaches equilibrium in 15 minutes (see Chapter 4). The Grubbs catalyst methylidene **4a** showed no reaction with Bu_4NBr at all in 15 minutes at 30 °C. After the temperature was increased to 40 °C some bromide exchange was visible in the ^{31}P NMR. There was a steady decrease in signal until 240 minutes, where no signal was visible at all (***Figure 5.4***), probably because of the formation of paramagnetic decomposition products (see Section 5.3.2).

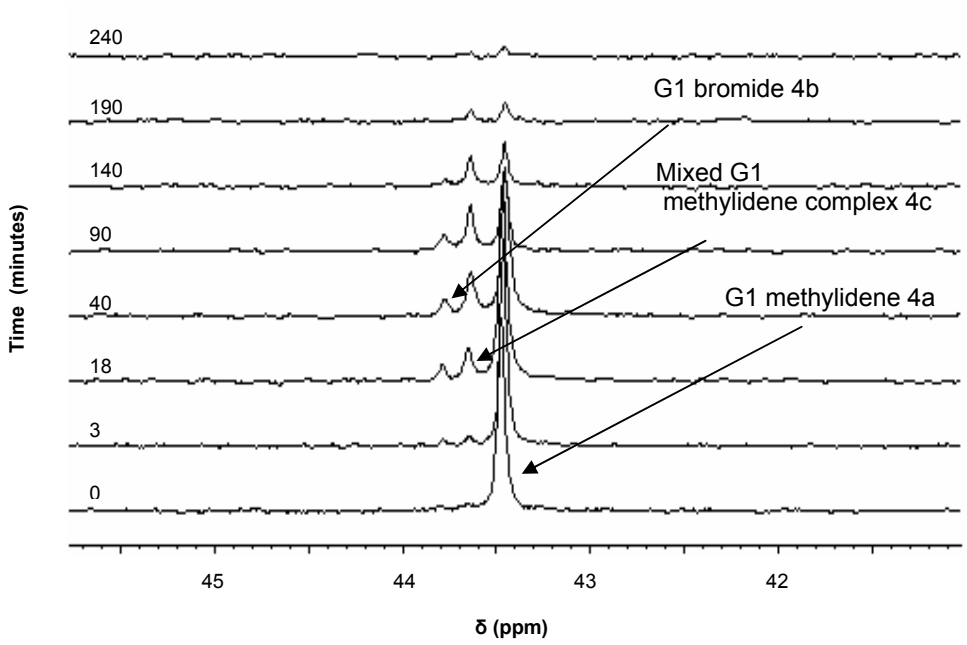

Figure 5.4: *^{31}P NMR stacked plot of the decomposition of Grubbs methylidene **4a** in the presence of 13 equiv Bu_4NBr ([Ru] = 2.45 x 10^{-2} M, [Br^-] = 3.36 x 10^{-1} M, 40 °C, $CDCl_3$)*

The methylidene decomposes before significant amounts of the mixed complex and the di-bromide **4c** form, thus, as expected, there is no significant halide exchange with the excess bromide. This is probably because of the slower dissociation of the phosphine from the methylidene complex and because of the much faster decomposition *via* activation of the ligand.

Thus, as expected, bimolecular decomposition does not play a major role in the decomposition of Grubbs methylidene **4a** $[Ru(Cl)_2(PCy_3)_2CH_2]$.

5.4 Ethylene-Induced Decomposition of the Ruthenium Methylidenes in C_6D_6

There has not been much study on the decomposition of the Grubbs type methylidenes under catalytic conditions. Molecular modelling indicated that there may be a possibility of decomposition from the metallacyclobutane,[106] thus the decomposition of Grubbs catalyst methylidene **4a** $[Ru(Cl)_2(PCy_3)_2CH_2]$ and the second generation Grubbs catalyst methylidene

6 $[Ru(Cl)_2(PCy_3)(NHC)CH_2]$ in the presence of ethylene was investigated as per ***Scheme 5.2***. Experimental proof (such as the formation of propene) to confirm the proposed route was therefore desired.

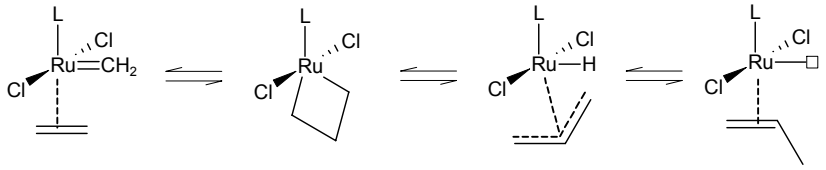

L=PCy_3 or NHC

Scheme 5.2: *The modelled and evaluated decomposition pathway for Grubbs catalyst methylidene **4a** and the second generation Grubbs catalyst methylidene **6***

5.4.1 Ethylene-Induced Decomposition of Grubbs Catalyst Methylidene 4a in C_6D_6

Grubbs catalyst methylidene **4a** $[Ru(Cl)_2(PCy_3)_2CH_2]$ was decomposed at 40 °C in C_6D_6 exactly as described in Section 5.2.8. ^{31}P NMR spectra were recorded over time, as well as starting and final ^1H NMR spectra. The reaction mixture was analysed with GC/MS using a PONA column as described in Section 5.2.3. The ethylene used in the decomposition reactions and the pentane used in the synthesis of the complexes were analysed using the GC-FID fitted with a PLOT column as described in Section 5.2.3.

5.4.1.1 Results and Discussion

^1H and ^{31}P NMR spectra over time

The starting complex contains a small amount of styrene. In the synthesis of the methylidene, the benzylidene was reacted with ethylene with the formation of styrene. The bulk of this styrene is removed by washing with pentane, however a small amount remains. The amount of residual styrene stays constant and does not interfere with the reaction.

Decomposition of the Grubbs methylidene **4a** $[Ru(Cl)_2(PCy_3)_2CH_2]$ at 40 °C in C_6D_6 results in complete disappearance of the Grubbs methylidene **4a** in 9

hours, (^{31}P NMR) with the formation of decomposition peaks at δ 34.0, δ 40.0 and δ 40.3 (***Figure 5.5***).

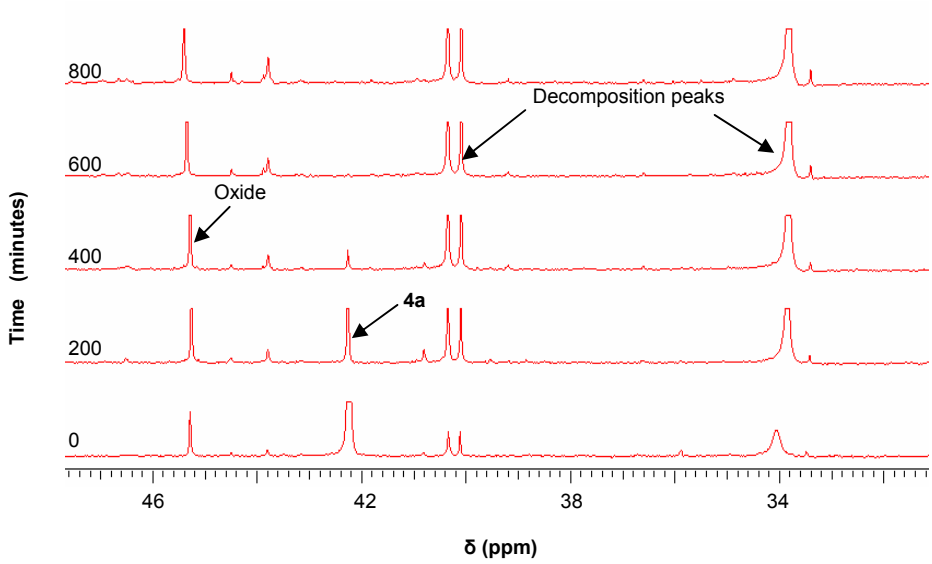

Figure 5.5: *^{31}P NMR stacked plot of spectra recorded over time for the ethylene-induced decomposition of methylidene **4a** ([**4a**] = 5.29 x 10^{-2} M, 40 °C, C_6D_6, ethylene bubbled through solution for 60 seconds*

The final ^{1}H spectrum at 40 °C (***Figure 5.6***) shows the formation of new resonances in the olefinic region and at δ 4.75 and δ 4.2. α-Olefins, as well as a small amount of *cis* and *trans* internal olefins, are visible.

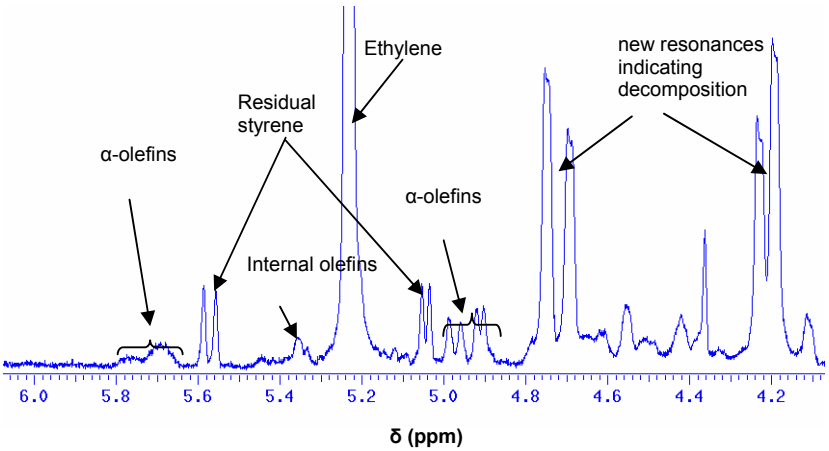

Figure 5.6: *Final ^{1}H spectrum at 40 °C after decomposition of Grubbs catalyst methylidene* ***4a*** *([Ru] = 5.29 x 10^{-2} M, 40 °C for 16 hours, C_6D_6, ethylene bubbled through solution for 60 seconds)*

GC-FID analysis after ethylene induced decomposition of Grubbs catalyst methylidene **4a** in C_6D_6

After ethylene-induced decomposition of the methylidene **4a,** the reaction mixture was analysed using a GC-FID fitted with a PLOT column as described in Section 5.2.3. In addition to the expected propene, a small amount of butenes, as well as some pentane, isopentane, butane, propane and cyclopropane were detected. The GC trace and relative area % of peaks are presented in ***Figure 5.7*** and ***Table 5.1***.

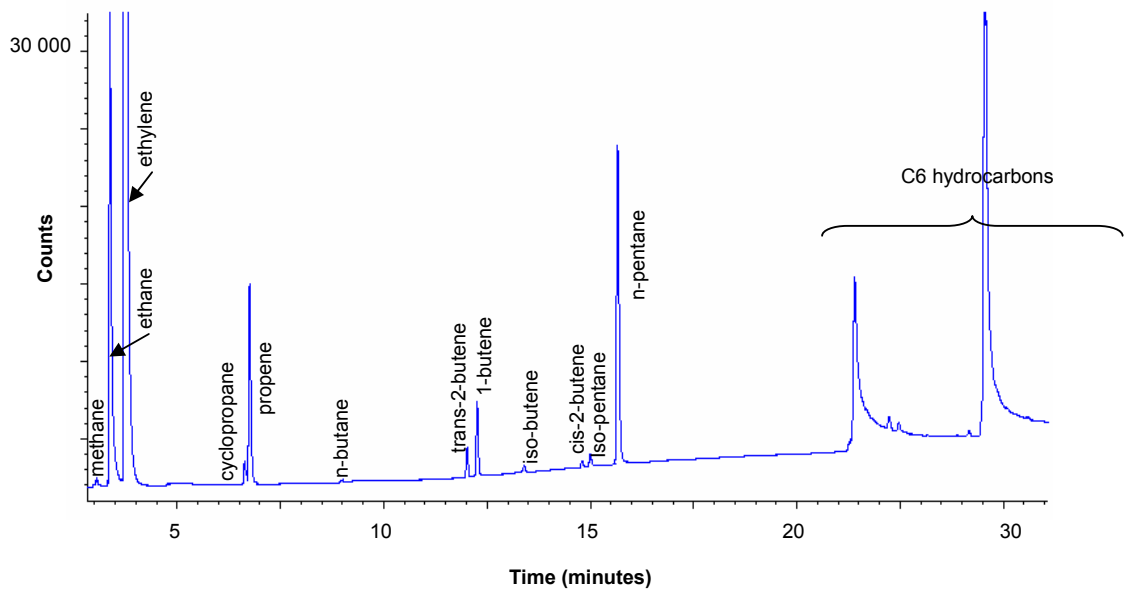

Figure 5.7: *Chromatogram of reaction mixture after decomposition of Grubbs catalyst methylidene **4a** ([Ru] = 5.29 x 10^{-2} M, 40 °C, C_6D_6, ethylene bubbled through solution for 60 seconds)*

Table 5.1: *GC analysis of the reaction mixture after decomposition of Grubbs catalyst methylidene **4a** ([Ru] = 5.29 x 10^{-2} M, 40 °C, C_6D_6, ethylene bubbled through solution for 60 seconds)*

Component	Area %	Component	Area %
Methane	0.26	*trans*-Butene-2	0.65
Ethane	13.23	1-Butene	1.67
Ethylene	69.05	Isobutene	0.14
Propane	0.05	*cis*-Butene-2	0.16
Cyclopropane	0.53	Isopentane	0.31
Propene	4.83	n-Pentane	9.05
n-Butane	0.08	Total	100.00

Analysis of ethylene using GC-FID (PLOT column)

The ethylene used for the decomposition of the methylidenes **4a** and **6** was found to be 99.5% pure with the major impurity being ethane.

Table 5.2**: Analysis of the ethylene used in the ethylene induced decomposition of Grubbs catalyst methylidene **4a** and the second generation Grubbs catalyst methylidene **6

Component	***Area %***
Methane	0.0006
Ethane	0.4950
Ethylene	99.5032
n-Butane	0.0005
1-Butene	0.0003
Isobutene	0.0004
Total	100.0000

Analysis of pentane using GC-FID (PLOT column)

The pentane used to wash the methylidenes **4a** and **6** during the synthesis was analyzed by GC-FID using a PLOT column and the results are shown in ***Table 5.3***.

Table 5.3**: Analysis of pentane used in the synthesis of methylidenes **4a** and **6

Component	***Area %***
n-Butane	0.0002
Isobutene	0.001
cis-2-Butene	0.01
Isopentane	6.59
n-Pentane	93.27
C6 Hydrocarbons	0.09
n-Hexane	0.04
Total	100.00

It is therefore clear that the pentane and isopentane found in the analysis of the reaction mixture are most likely explained by washing of the methylidene with pentane during the synthesis procedure.

5.4.1.2 Calculation of α-olefin (propene and 1-butene) yield

NMR was used for the *in situ* detection of any olefins formed over time to ensure that the olefins present at the end of the reaction were indeed formed in the reaction and were not due to contamination of equipment. Also, the olefins formed are volatile and once the sealed NMR tube is opened there may be loss of the volatile components.

The yield of α-olefins was determined (semi-quantitative) from the first and last ^{1}H NMR spectra recorded at 40 °C. As the aromatic region was not expected to change during the experiment, this region was used as an internal standard. Complete integration of resonances in the first spectrum (at 40 °C) was performed and the integral value for the aromatic (δ 6.9 – 7.3) and the carbene region (δ 19.3 – 19.4) noted. The carbene protons integrated for 1.13. The final spectrum was integrated and the integral for the aromatic region was set to the same value as obtained for the first spectrum at 40 °C. No carbene resonances were detected in this spectrum. The integral for the α-olefins (δ 4.8 – 5.0) was 0.23.

The % α-olefin formed is therefore:

$$\frac{0.23\ (\text{alpha olefins})}{1.13\ (\text{carbene protons})} \times 100 = 20.4\%$$

***Equation 1**: Quantification of α-olefins formed in the substrate induced decomposition reaction*

Only the propene in the liquid was detected. It is possible that the headspace also contained a small amount of propene that is not considered in this experiment. However, as the experiment was conducted in an NMR tube, the headspace is small.

This experiment was repeated twice with the results being 12.3 and 25.3% olefin formation. Note that the peaks are small and difficult to integrate accurately.

5.4.2 Ethylene Induced Decomposition of the Grubbs Catalyst Methylidene 4a in the Presence of Phenol

Decomposition of Grubbs catalyst methylidene **4a** [$Ru(Cl)_2(PCy_3)_2CH_2$] was carried out in deuterated benzene as described in Section 5.2.8, however 20 equivalents of phenol was added to determine the effect of the phenol on the

lifetime of the methylidene and the propene formed. ^{31}P NMR spectra were recorded overnight. From the ^{31}P NMR data, compound **4a** was present for 12 hours compared to 10 hours without phenol present. Unfortunately the OH of the phenol resonates in the olefinic region, making quantification of the propene formed unreliable. However, GC-FID confirmed the formation of propene.

5.4.3 Ethylene Induced Decomposition of the Second Generation Grubbs Catalyst Methylidene 6 in C_6D_6

The decomposition of the second generation Grubbs catalyst methylidene **6** $[Ru(Cl)_2(PCy_3)(NHC)CH_2]$ was investigated under ethenolysis conditions. The experiment was carried out exactly as described in Section 5.2.8 and ^{1}H spectra were recorded every 30 minutes for 16 hours. The experiment was repeated and ^{31}P NMR spectra were recorded.

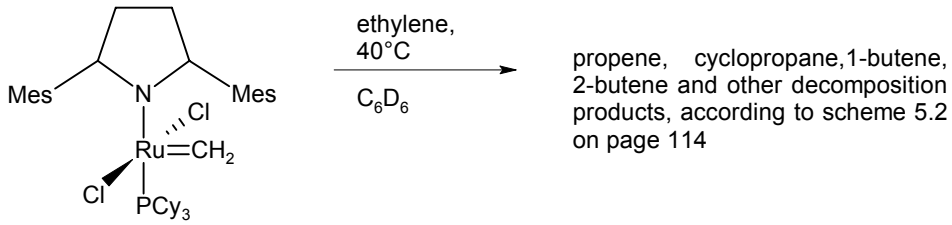

6

***Scheme 5.3**: Decomposition of the second generation Grubbs catalyst methylidene **6** in C_6D_6 in the presence of ethylene*

5.4.3.1 Results and Discussion

^{31}P NMR

There was 44% loss of the second generation Grubbs catalyst methylidene **6** after 16 hours.

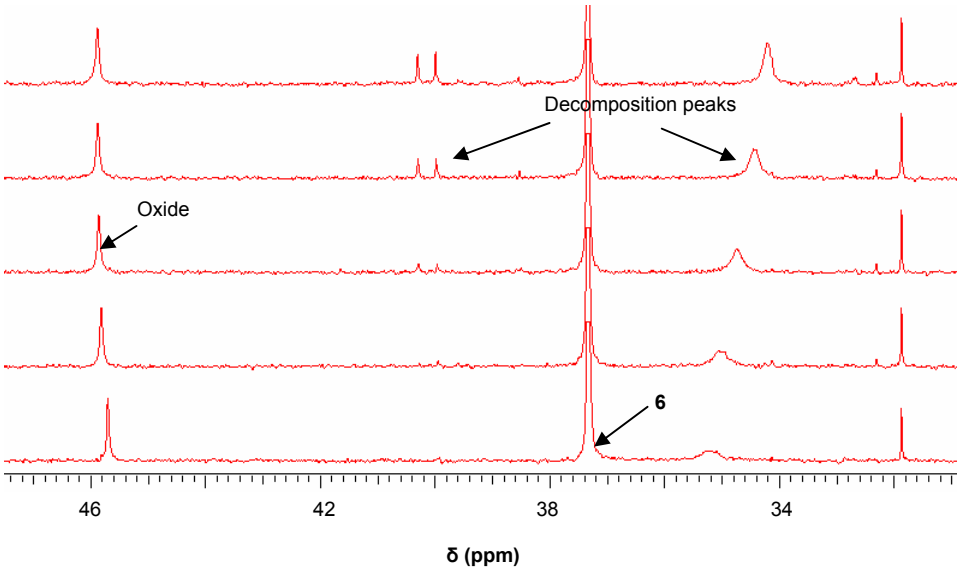

Figure 5.8: *^{31}P NMR stacked plot of spectra recorded over time for the ethylene-induced decomposition of the second generation Grubbs catalyst methylidene **6** ([**6**] = 4.48 x 10^{-2} M, 40 °C, C_6D_6, ethylene bubbled through solution for 60 seconds*

^{1}H NMR

A stacked plot of the ^{1}H NMR spectra (***Figure 5.9***) clearly shows the formation of α-olefins over time.

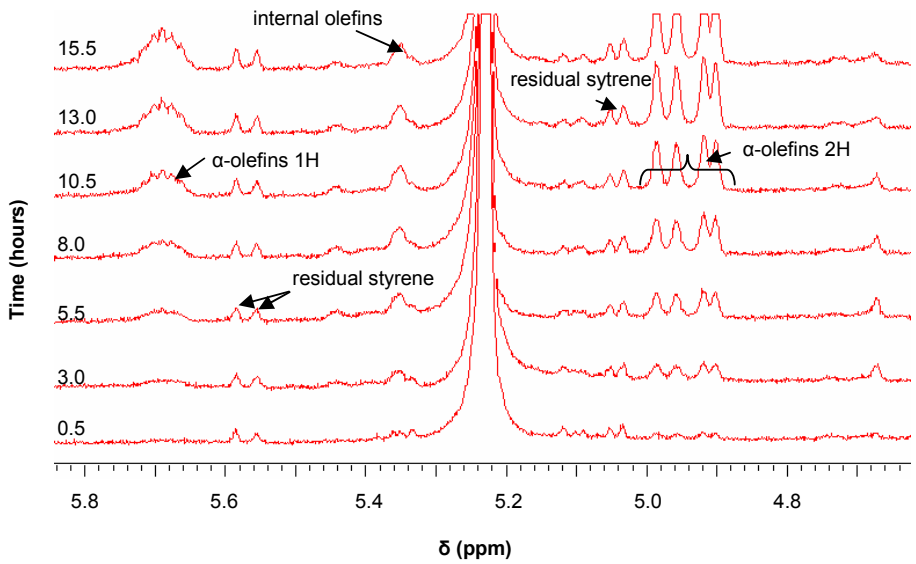

Figure 5.9: *Stacked plot of the olefinic region of the ^{1}H NMR over time for the decomposition of the second generation Grubbs catalyst methylidene* ***6*** *([Ru] = 4.48 x 10^{-2} M, 40 °C for 16 hours, C_6D_6, ethylene bubbled through solution for 60 seconds).*

GC-FID (PLOT column)

The reaction mixture was analyzed by GC-FID (PLOT column) after the reaction (***Table 5.4*** below, ***Figure 5.10***). The expected propene was found along with other hydrocarbons.

Table 5.4: *Light components detected after decomposition of the second generation Grubbs catalyst methylidene* ***6*** *in C_6D_6 ([Ru] = 4.48 x 10^{-2} M, 40 °C, C_6D_6)*

Component	***Area %***	***Component***	***Area %***	***Component***	***Area %***
Methane	1.11	n-Butane	0.10	Isopentane	1.72
Ethane	3.74	*trans*-2-Butene	2.33	n-Pentane	9.71
Ethylene	45.06	1-Butene	1.41	1,3 Butadiene	0.17
Propane	0.20	Isobutene	0.07		
Propene	33.31	*cis*-2-Butene	1.09	Total	100.00

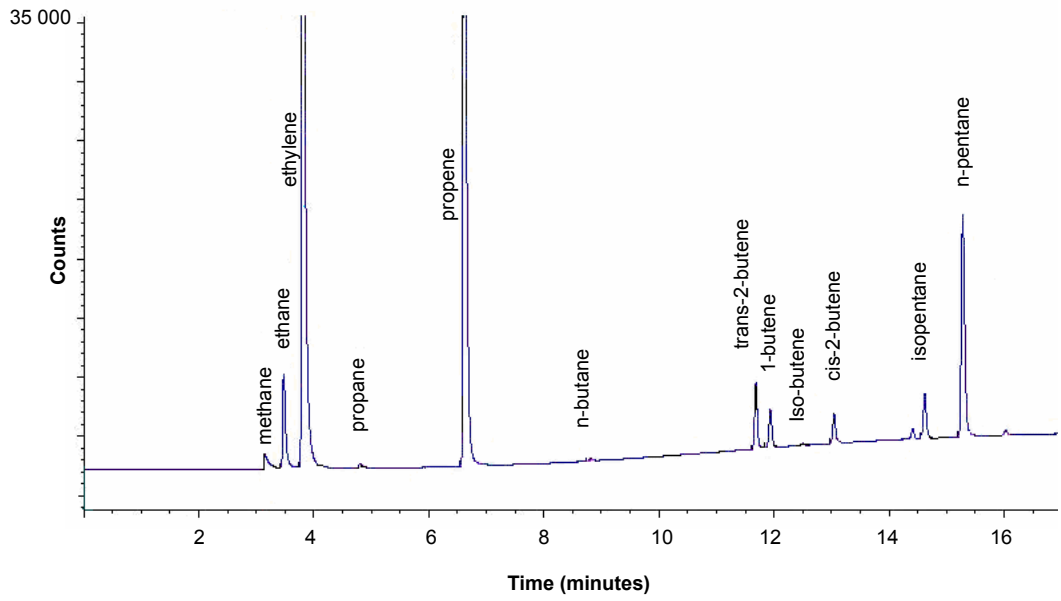

Figure 5.10: *Chromatogram of the reaction mixture after the decomposition of the second generation Grubbs catalyst methylidene **6** ([Ru] = 4.48 x 10^{-2} M,40 °C for 16 hours, C_6D_6, ethylene bubbled through solution for 60 seconds)*

5.4.3.2 Calculation of α-olefin (propene and 1-butene) yield

The calculations were carried out exactly as in Section 5.4.1.2 above. However in the case of the second generation Grubbs methylidene **6** $[Ru(Cl)_2(PCy_3)(NHC)CH_2]$, it was determined that the yield of propene was 1.5 times the loss of methylidene. This indicates that there is either another route for the formation of propene in the case of complex **6** or that the methylidene may be reformed after the β-hydride transfer step.

5.4.4 Characterisation of the Decomposition Products with NMR

Comparison of the ^{31}P NMR stacked plots for the decomposition of Grubbs catalyst methylidene **4a** $[Ru(Cl)_2(PCy_3)_2CH_2]$ and the second generation Grubbs methylidene **6** $[Ru(Cl)_2(PCy_3)(NHC)CH_2]$ (***Figure 5.11***) show that in addition to $O{=}PCy_3$ the same decomposition products are found, but that Grubbs catalyst methylidene **4a** decomposes significantly faster than the second generation Grubbs catalyst methylidene **6**. The decomposition of both

methylidenes **4a** and **6** result in resonances at δ 40.3 and δ 40.1 in the ^{31}P NMR spectrum.

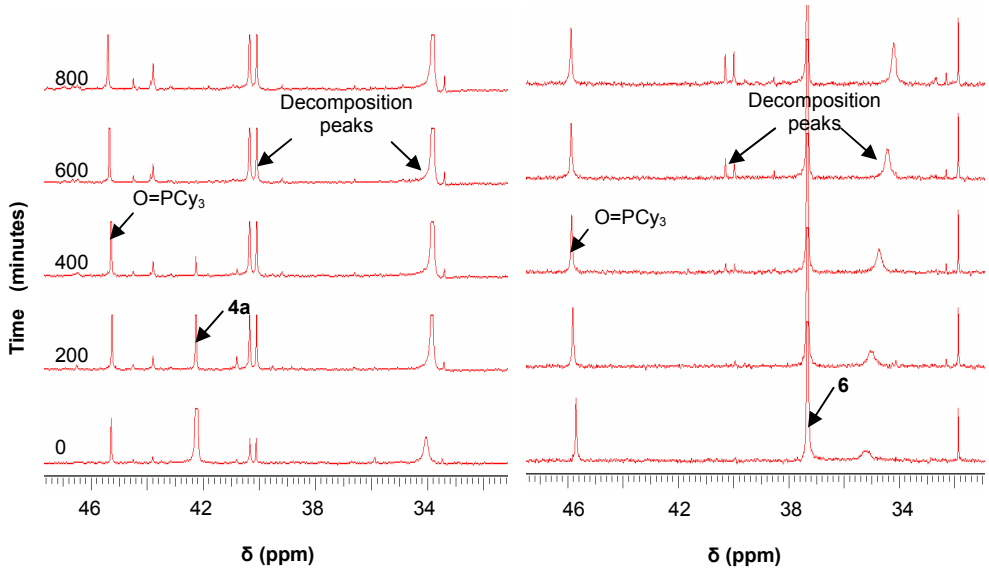

Grubbs catalyst methylidene **4a**

Second generation Grubbs catalyst methylidene **6**

***Figure 5.11**: Comparison of the ^{31}P NMR stacked plots of spectra recorded over time for the ethylene induced decomposition of methylidenes **4a** and **6** ([**4a**] = 5.29 x 10^{-2} M, 40 °C, C_6D_6 , ethylene bubbled though solution for 60 seconds; [**6**] = 4.48 x 10^{-2} M, 40 °C, C_6D_6, ethylene bubbled through solution for 60 seconds)*

The ^{1}H gCOSY[129] (***Figure 5.12***) shows that the resonances at δ 4.19 and δ 4.75, and δ 4.24 and δ 4.69 respectively, are coupled. The removal of the ethylene by the introduction of excess argon resulted in a decrease of the intensities of the resonances at δ 40.0 and δ 40.3 (^{31}P NMR) and those at δ 4.75, δ 4.69, δ 4.24 and δ 4.19 (^{1}H NMR). It is thus possible that the peaks at δ 40.0 and δ 40.3 (^{31}P NMR) represent ethylene-complexed ruthenium species containing a PCy_3 group.

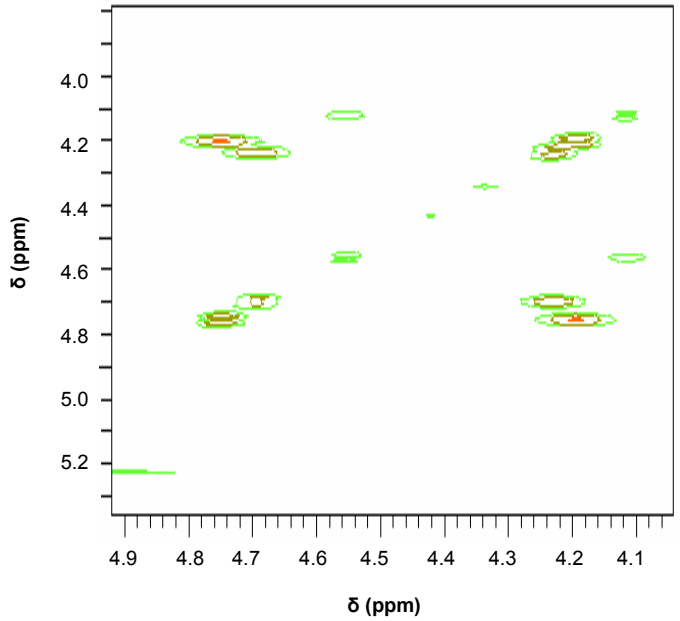

Figure 5.12: *^{1}H-^{1}H gCOSY after ethylene induced decomposition of Grubbs catalyst methylidene **4a** ([Ru] = 5.29 x 10^{-2} M, 40 °C for 16 hours, C_6D_6)*

The ^{1}H-^{31}P HMBC (***Figure 5.13***) shows that the resonance at δ 40.0 (^{31}P NMR) correlates to peaks in the ^{1}H NMR spectrum at δ 4.69 and δ 4.24 and the resonance at δ 40.3 (^{31}P NMR) correlates to resonances in the ^{1}H NMR spectrum at δ 4.75 and δ 4.19. As discussed for the gCOSY above, it is thought that these peaks represent some sort of coordinated ethylene complex.

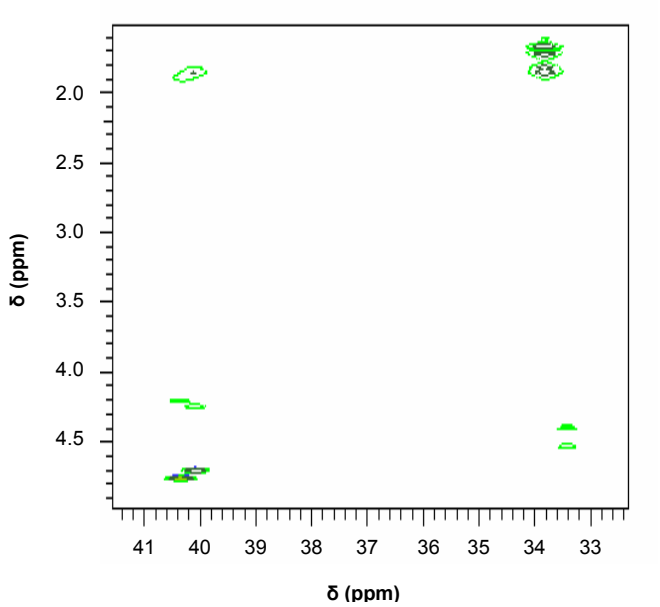

Figure 5.13: *^{1}H-^{31}P HMBC after ethylene induced decomposition of Grubbs catalyst methylidene* ***4a*** *([Ru] = 5.29 x 10^{-2} M, 40 °C, C_6D_6)*

An additional decomposition resonance is observed at δ 33.8 (^{31}P NMR) after the decomposition of methylidenes **4a** and **6**. The ^{31}P NMR spectra over time show that this peak is initially broad at *ca.* δ 36 and as the reaction progresses it becomes sharper and moves to *ca*. δ 33.8 (***Figure 5.11***). This resonance correlates to the ligand region (δ 0 – δ 2.5) in the ^{1}H NMR (^{1}H-^{31}P HMBC, ***Figure 5.13***).

It appears that the width and chemical shift of the resonance at δ 33.8 - 36 vary depending on the amount of PCy_3 and $O{=}PCy_3$ present. In the initial spectrum (***Figure 5.14***), there is a broad resonance present at δ 36. It is suggested that this might represent the complex interacting with $O{=}PCy_3$. As the reaction progresses, PCy_3 is released and the resonance shifts up field to *ca*. δ 33.8 (***Figure 5.14***). No free PCy_3 is seen however, any free PCy_3 would be expected to be extremely broad due to the proposed interaction with the decomposition product. If air is bubbled through the mixture, this resonance shifts closer to δ 36, as more $O{=}PCy_3$ is produced. If more air is bubbled through and the sample is heated at 40 °C, the residual methylidene

resonance decreases and the $O=PCy_3$ increases and no more of the complex at δ 33 - 36 is formed, indicating that ethylene is needed to form this complex. For further evidence, ethylene was again added and the resonance at δ 33 - 36 increased again. Thus it is proposed that the resonance at δ 33 - 36 forms in the presence of ethylene and represents an average NMR signal due to a decomposition product that interacts with the free PCy_3 and the $O=PCy_3$.

Although phenol has other roles in the system, it has been shown that phenol interacts with $O=PCy_3$ and that this new compound resonates at δ 56.[111] If phenol is added to the reaction mixture after the ethylene induced decomposition of the Grubbs catalyst methylidene **4a**, the decomposition resonance at δ 33 - 36 narrows significantly and shifts closer to δ 36, but the integration values are unchanged. The resonance representing the $O=PCy_3$ moves from δ 46 to δ 56, and sharpens. The change in the peak width of the decomposition peak shows that there is either an interaction between the 'free' $O=PCy_3$ and the peak at δ 33 - 36 or between the phenol and the decomposition complex. This suggests that there is a fast exchange process involving $O=PCy_3$ and the decomposition product at δ 33 - 36.

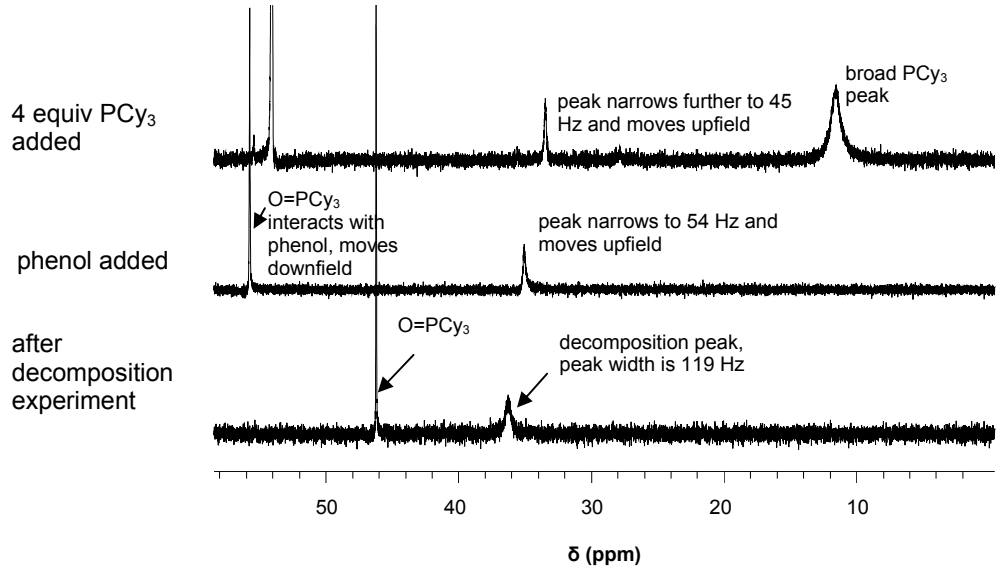

***Figure 5.14**:* *^{31}P NMR spectra recorded after ethylene induced decomposition of Grubbs catalyst methylidene **4a**, after addition of phenol and ligand ([Ru] = 5.29 x 10^{-2} M, 40 °C, C_6D_6, ethylene bubbled through solution for 60 seconds).*

If PCy_3 is added (4 equivalents) at this point, the peak moves to δ 33.4 and narrows 45 Hz, and the peak at δ 11 representing the free ligand (PCy_3) is extremely broad, showing that there is an interaction between the peak at δ 33.4 and the free ligand.

It is suggested that the resonance at δ 33 - 36 is an average signal and represents a ruthenium metal center that can complex either $O{=}PCy_3$ or PCy_3 and its chemical shift and width are determined by the concentration of free PCy_3 and $O{=}PCy_3$ present in the solution. This complex does not form in the absence of ethylene.

The work in Section 5.4 was published together with the Sasol homogeneous metathesis team[106] and has since been confirmed by others.[130]

5.4.5 Possible Interaction of Methyltricyclohexylphosphonium Salt with $O=PCy_3$

Grubbs and coworkers[13] reported a resonance at δ 34.5 (C_6D_6), identified as the methyltricyclohexylphosphonium salt, that was formed during the thermal decomposition of the second generation methylidene **6** in toluene. Although the Grubbs experiment studied thermal decomposition while our experiment focussed on ethylene induced decomposition, it was decided to determine whether the decomposition product at δ 33 - 36 (^{31}P NMR, ethylene induced decomposition, see Section 5.4.4) is, in fact, this salt, although it is not expected that the salt would interact with $O=PCy_3$.

The methyltricyclohexylphosphonium salt was formed *in situ* by the addition of methyl iodide to the ligand dissolved in C_6D_6 as described in Section 5.2.9. ^{31}P NMR showed a resonance at δ 34.2. The resonance at δ 34.2 remained sharp and the chemical shift did not change upon addition of $O=PCy_3$ indicating that there is no interaction between the methyltricyclohexylphosphonium salt and $O=PCy_3$. The decomposition product at δ 33 - 36 (ethylene induced decomposition, see Section 5.4.4) interacts with the PCy_3 and the $O=PCy_3$ and therefore the compound found after decomposition of methylidenes **4a** $[Ru(Cl)_2(PCy_3)_2CH_2]$ or **6** $[Ru(Cl)_2(PCy_3)(NHC)CH_2]$ in C_6D_6 under ethenolysis conditions is not the methyltricyclohexylphosphonium salt, although the chemical shifts are similar.

5.4.6 Conclusions – Ethylene Induced Decomposition in C_6D_6

The decomposition of the Grubbs catalyst methylidene **4a** $[Ru(Cl)_2(PCy_3)_2CH_2]$ is much faster than that of the second generation Grubbs catalyst **6** $[Ru(Cl)_2(PCy_3)(NHC)CH_2]$. The expected propene was found in the product after ethylene induced decomposition occurred. 1-butene is formed *via* the mechanism shown in ***Scheme 5.2*** on page 114 when propene is used as the starting material instead of ethylene.

The formation of α-olefins over time is clearly demonstrated by the stacked plot of ^{1}H NMR spectra over time (***Figure 5.9*** on page 122). The ethylene used in the reactions was 99.5% pure, showing no detected propene and only trace amounts of butene. It is thus concluded that the propene, 1-butene, 2-butene and cyclopropane are formed during the decomposition reaction.

The 2-butenes are products formed due to self-metathesis of propene or isomerisation of 1-butene. The pentane and isopentane are due to the use of pentane in the synthesis of **4a** and **6.** The ethane, propane and butane are probably the result of hydrogenation[131] inside the inlet of the gas chromatograph, as hydrogen was used as the carrier and the sample contained some decomposed catalyst species. The cyclopropane is possibly formed *via* reductive elimination from the ruthenacyclobutane (***Scheme 5.4***), again indicating that the ruthenacyclobutane is a precursor to decomposition.[106]

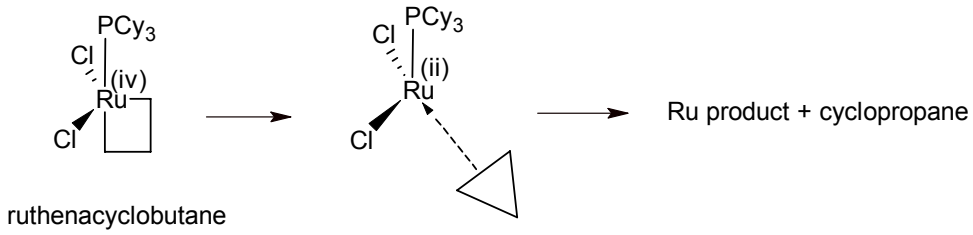

Scheme 5.4: *Elimination of cyclopropane from the ruthenacyclobutane intermediate*

The source of the isopentane found after the decomposition of the methylidenes is clearly the pentane used in the synthesis of the Grubbs methyldiene **4a** and the second generation Grubbs methylidene **6**, as confirmed by the analysis of the pentane (see ***Table 5.3*** on page 118).

It is clear that the decomposition products obtained from the ethylene induced decomposition of both Grubbs catalyst methylidene **4a** and the second generation Grubbs catalyst methylidene **6** (***Figure 5.11*** on page 124) have a similar chemical shift, indicating that they are the same or very similar

products. Therefore it appears that this decomposition product does not contain the NHC ligand either. This decomposition product interacts with both the PCy_3 and the $O=PCy_3$ and is not the methyltricyclohexylphosphonium salt reported by Grubbs after thermal decomposition of the second generation Grubbs catalyst methylidene **6**.

The addition of 20 equivalents of phenol to the reaction does not inhibit the formation of propene.

5.5 Ethylene Induced Decomposition of Ruthenium Methylidenes in Chlorinated Solvents

A few studies have shown that better results are obtained if homogeneous metathesis reactions are carried out in chlorinated solvents.[124] It was thought that the solvent may have an influence on ethylene induced decomposition and thus the decomposition of Grubbs catalyst methylidene was repeated in $CDCl_3$.

5.5.1 Ethylene Induced Decomposition of Grubbs Catalyst Methylidene 4a in $CDCl_3$

Grubbs catalyst methylidene **4a** $[Ru(Cl)_2(PCy_3)_2CH_2]$ was decomposed at 40 °C in $CDCl_3$ overnight, in the presence of ethylene, as described in Section 5.2.8.

5.5.1.1 Results and Discussion

NMR

The ^{31}P NMR spectra recorded over time show that the Grubbs catalyst methylidene **4a** decomposed in 5 hours (***Figure 5.15***).

Starting and ending ^{1}H NMR spectra (***Figure 5.16***) revealed the formation of a new species [δ 2.6 (t) and δ 3.7 (t)] and shows that no propene was formed. The new peaks are not formed in the absence of ethylene.

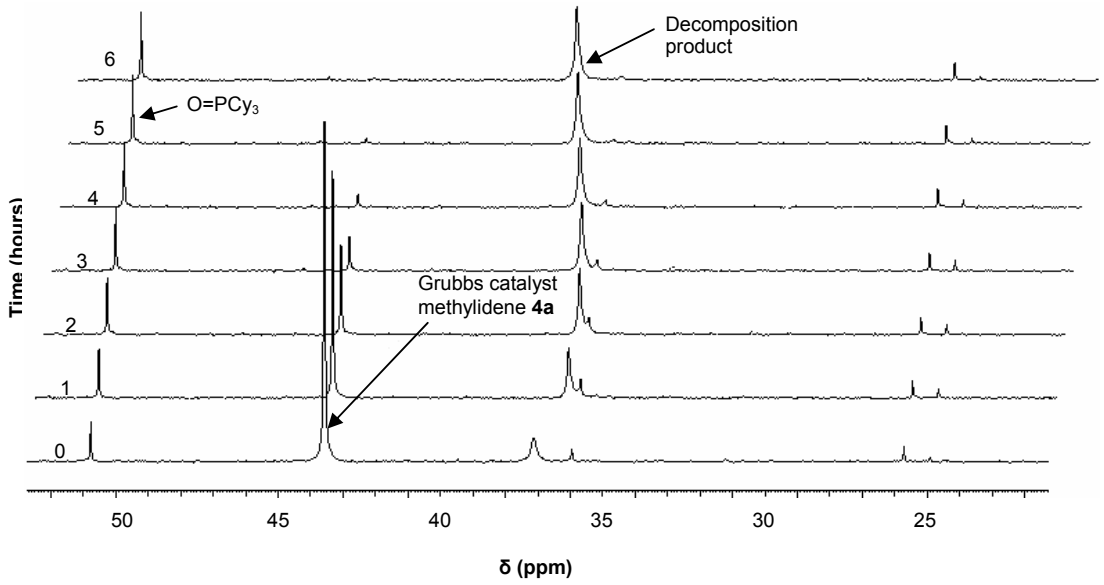

Figure 5.15: *^{31}P NMR spectra recorded over time for the ethylene induced decomposition of Grubbs catalyst methylidene **4a** ([Ru] = 4.35 x 10^{-2} M, 40 °C for 16 hours, $CDCl_3$, ethylene bubbled through solution for 60 seconds)*

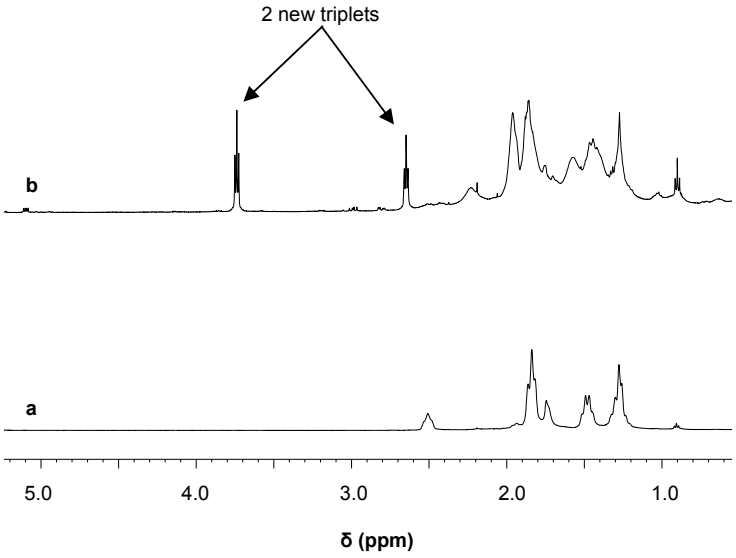

Figure 5.16: *Initial (a) and final (b) ^{1}H NMR spectra for the decomposition of Grubbs catalyst methylidene **4a** ([Ru] = 4.35 x 10^{-2} M, 40 °C for 16 hours, $CDCl_3$, ethylene bubbled through solution for 60 seconds)*

The ^{1}H gCOSY[129] (***Figure 5.17***) indicates that the new triplets are coupled. This indicates that the new compound has two CH_2's next to each other that do not couple to anything else.

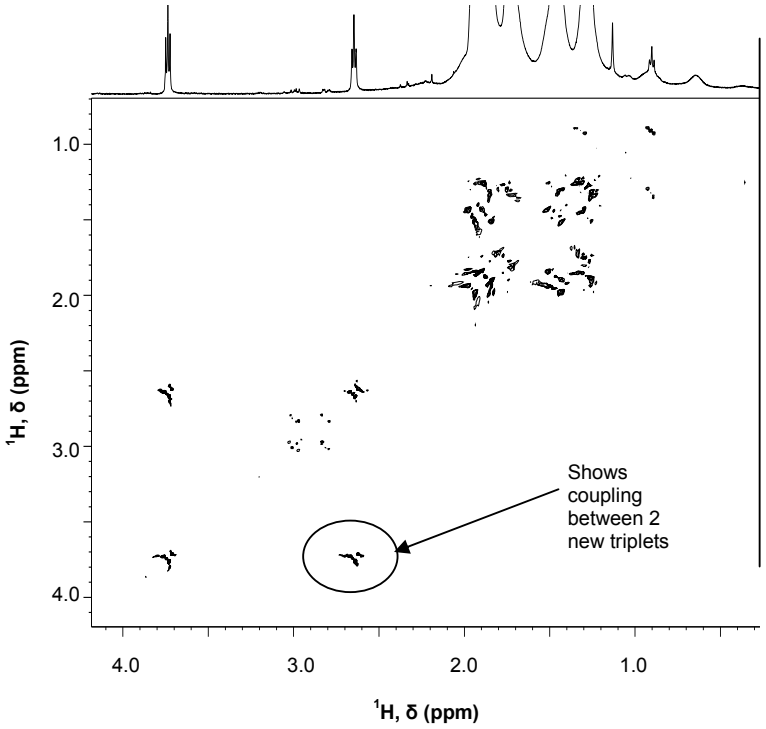

Figure 5.17: *^{1}H gCOSY after the decomposition of Grubbs catalyst methylidene **4a** ([Ru] 4.35 x 10^{-2} M, 40 °C for 16 hours, $CDCl_3$, ethylene bubbled through solution for 60s)*

The ^{1}H-^{13}C HSQC spectrum (***Figure 5.18***) provided the ^{13}C chemical shifts of the triplets while an HMBC (***Figure 5.19***) showed that the triplets had long range coupling to a singlet at δ 70.

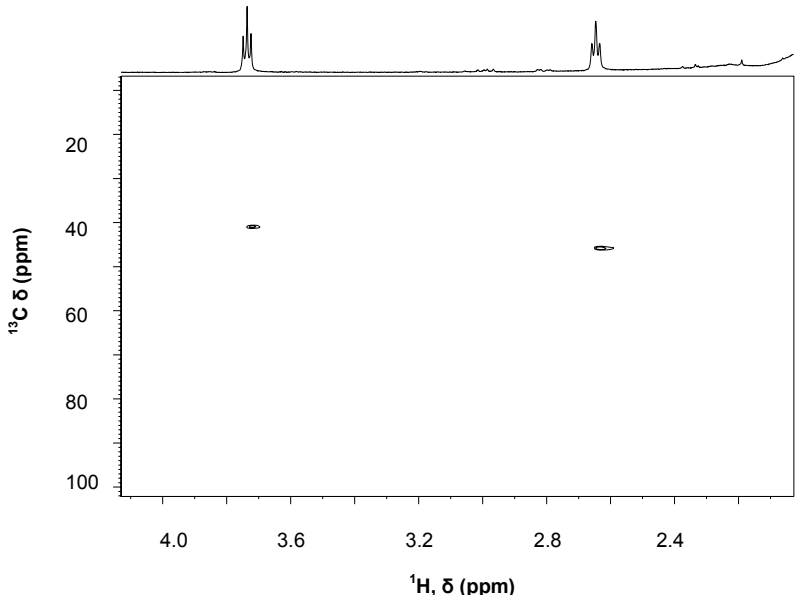

Figure 5.18: *^{1}H-^{13}C HMQC of reaction mixture after the ethylene induced decomposition of Grubbs catalyst methylidene **4a** ([Ru] = 4.35 x 10^{-2} M, 40 °C for 16 hours, $CDCl_3$, ethylene bubbled through solution for 60 seconds)*

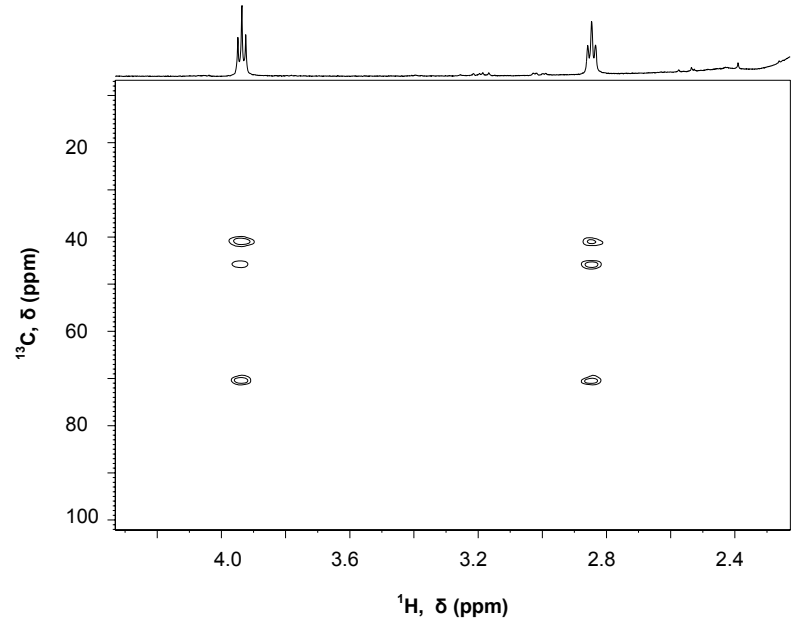

Figure 5.19: *^{1}H-^{13}C HMBC of reaction mixture after the ethylene induced decomposition of Grubbs catalyst methylidene **4a** ([Ru] = 4.35 x 10^{-2} M, 40 °C for 16 hours, $CDCl_3$, ethylene bubbled through solution for 60 seconds)*

The ^{2}H spectrum showed a peak at δ 6.25 (***Figure 5.20*** below). This spectrum was referenced to the natural abundance ^{2}H in the benzene used as solvent.

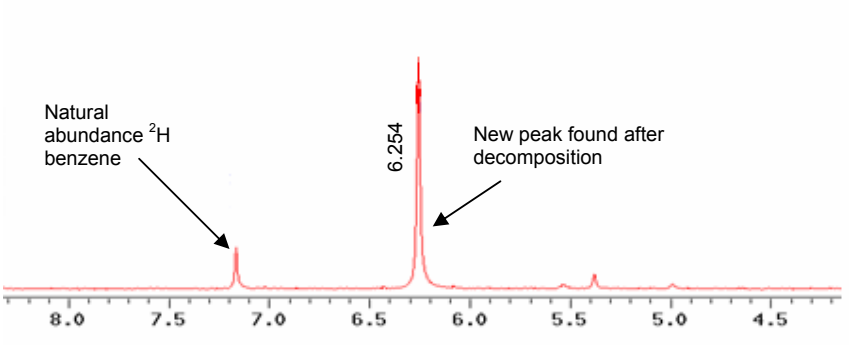

Figure 5.20: *^{2}H Spectrum of reaction mixture for the ethylene induced decomposition of Grubbs catalyst methylidene **4a** after removal of $CDCl_3$ and addition of C_6H_6 ([Ru] = 4.35 x 10^{-2} M, 40 °C for 16 hours, ethylene bubbled through solution for 60 seconds)*

GCMS

Analysis of the reaction mixture (***Figure 5.22***) using GC/MS fitted with a PONA column after the NMR experiment, detected a short chained chlorinated deuterated compound eluting at 13.5 minutes (***Figure 5.21***) which was not present in the Wiley database. The mass spectrum of the chlorinated deuterated compound is shown in ***Figure 5.22***.

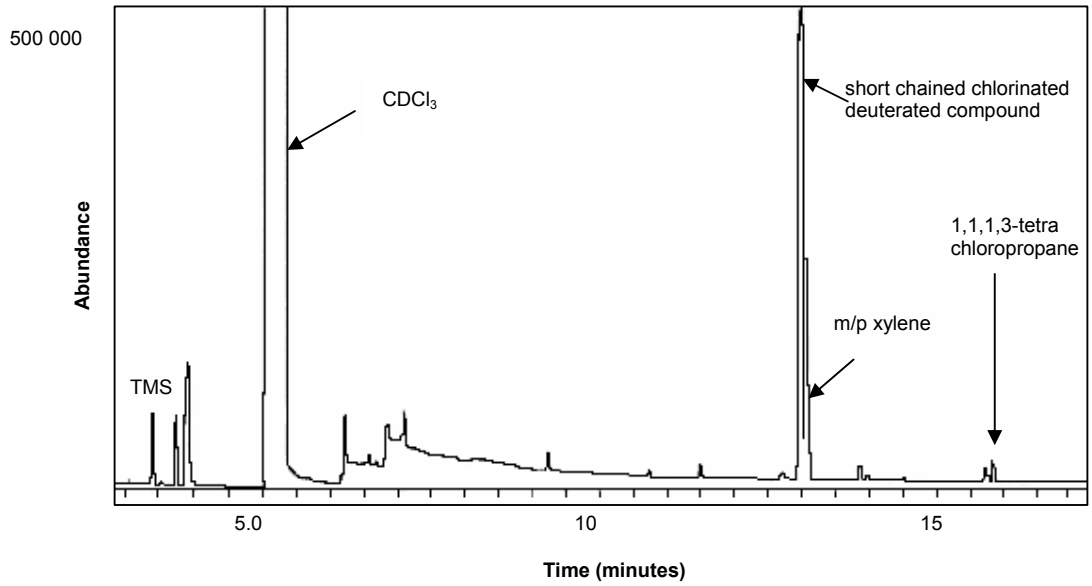

Figure 5.21: *Total ion chromatogram obtained after the ethylene induced decomposition of Grubbs catalyst methylidene* ***4a*** *([Ru] = 4.35 x 10^{-2} M, 40 °C for 16 hours, $CDCl_3$, ethylene bubbled through solution for 60 seconds)*

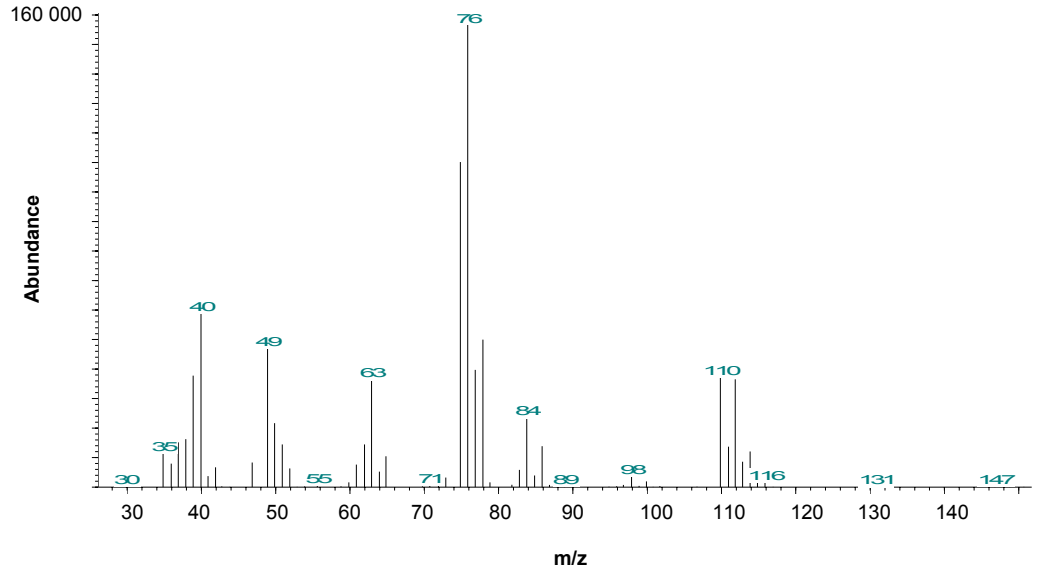

Figure 5.22: *MS scan of the peak at 13.5 min, sample of ethylene induced decomposition of Grubbs catalyst methylidene* ***4a****, ([Ru] = 4.35 x 10^{-2} M, 40 °C for 16 hours, $CDCl_3$, ethylene bubbled through solution for 60 seconds)*

Mass spectrometry (MS) is an excellent technique for the identification of chlorinated or brominated compounds because diagnostic patterns are formed due to the natural abundance of more than one isotope of chlorine (^{35}Cl, ^{37}Cl) and bromine (^{79}Br, ^{81}Br). From the isotope ratios it is possible to determine the number of chlorine and bromine atoms that are present in the molecule as shown in ***Figure 5.23*** below .[132]

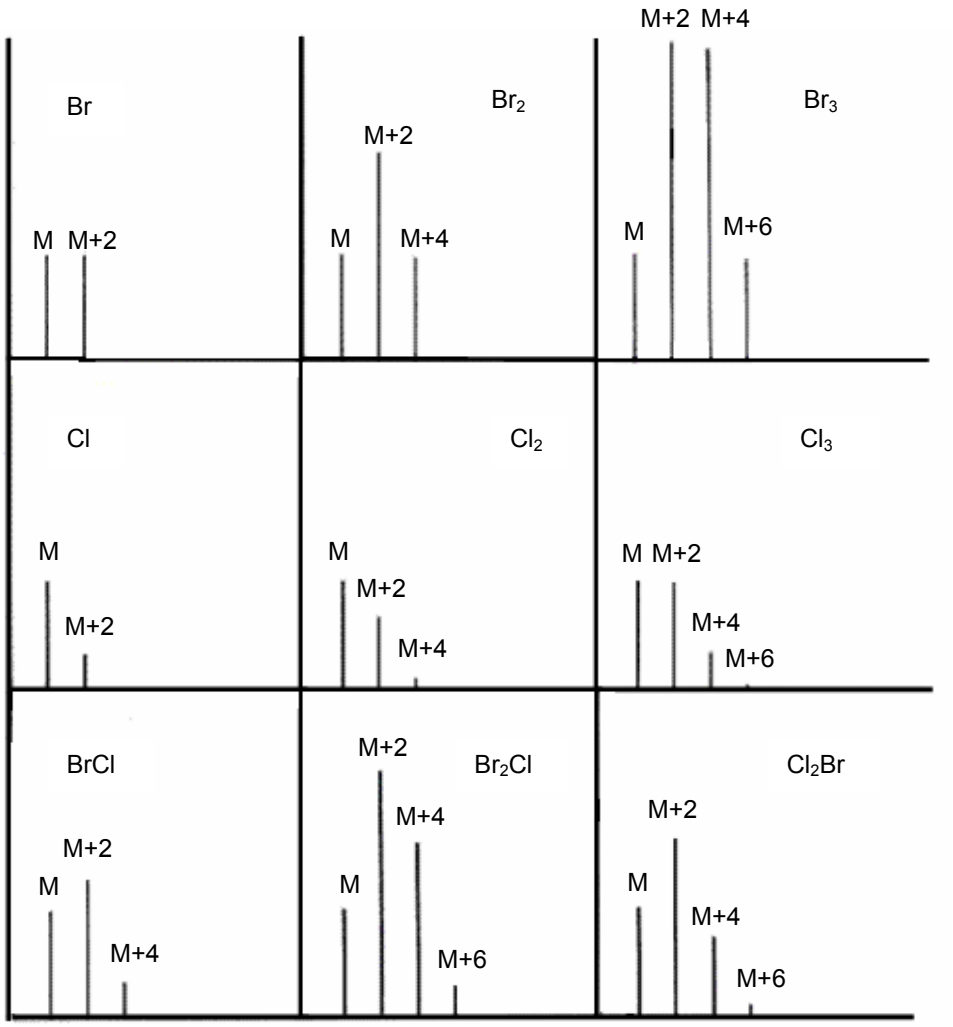

Figure 5.23: *MS isotope patterns[132] for compounds containing Cl and Br*

The molecular ion of the peak eluting at 13.5 minutes is not immediately visible, thus it is not possible to determine the number of chlorine atoms

present from the isomer distribution pattern of this ion. However, the fragments 110 and 111 contain either 2 or 3 chlorine atoms and the fragments 75 and 76 clearly contain one chlorine atom. It is not possible for the fragment at 110 to contain 3 chlorine atoms as the mass of the ion is too small.[133] Thus it is concluded that this fragment contains 2 chlorine atoms. The expected molecular ion for 1,1,3-trichloro-1-deuteropropane is 147. A small peak is indeed seen at 147. The difference between the 110 fragment and the expected molecular ion is 36 which is exactly the mass of HCl. It is therefore concluded that the unknown indeed contains three chlorine atoms.

The presence of ^{2}H complicates the identification of the unknown because the nitrogen rule[134] no longer holds, thus it is difficult to determine which ions are as a result of loss of a molecule and which are as a result of loss of a radical. It is made even more complex because of the presence of the deuterated and non-deuterated species, which co-elute on the GC column.

5.5.1.2 Identification of the unknown

As discussed above, the NMR spectra obtained after the reaction indicate that the product molecule contains two CH_2's that are adjacent to each other that do not couple to any other nucleus. One of these CH_2s is next to a quaternary carbon. The GC/MS spectrum of the peak at 13.5 minutes (***Figure 5.22***) showed that the compound of interest contains three chlorine atoms and a deuterium atom. It is therefore proposed and concluded that the unknown is 1,1,3-trichloro-1-deuteropropane.

The ACDlabs simulated ^{13}C spectrum[135] for 1,1,3-trichloro-1-deutero-propane shows peaks at δ 70, δ 45 and δ 41 which agrees well with the carbon chemical shifts obtained from the HSQC and HMBC shown above. The ACDlabs simulated ^{1}H spectrum shows coupling between the D and CH_2 at δ 2.6, which is not seen in the experimental ^{1}H spectrum recorded. It is possible that this coupling is too small to be seen in reality. However, the predicted shifts for the CH_2 protons (δ 2.6 and δ 3.8) agree well with those

obtained in the NMR spectrum recorded after the experiment (δ 2.6 and δ 3.7, see ***Figure 5.16***).

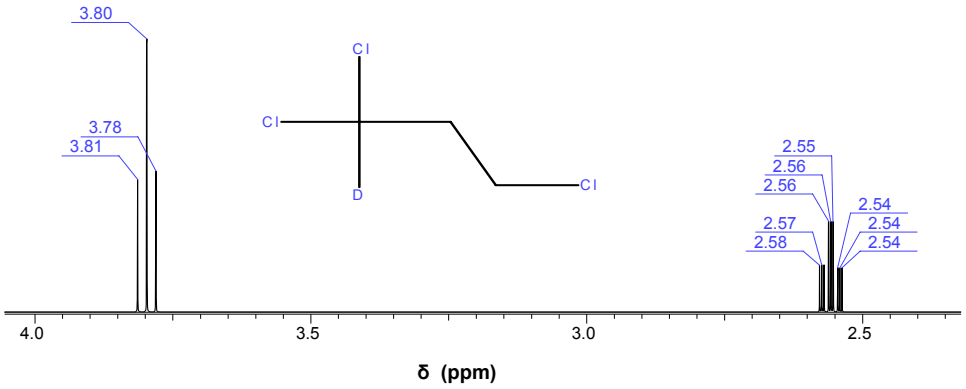

Figure 5.24: *ACDlabs simulated ^{1}H spectrum for 1,1,3-trichloro-1-deutero-propane*

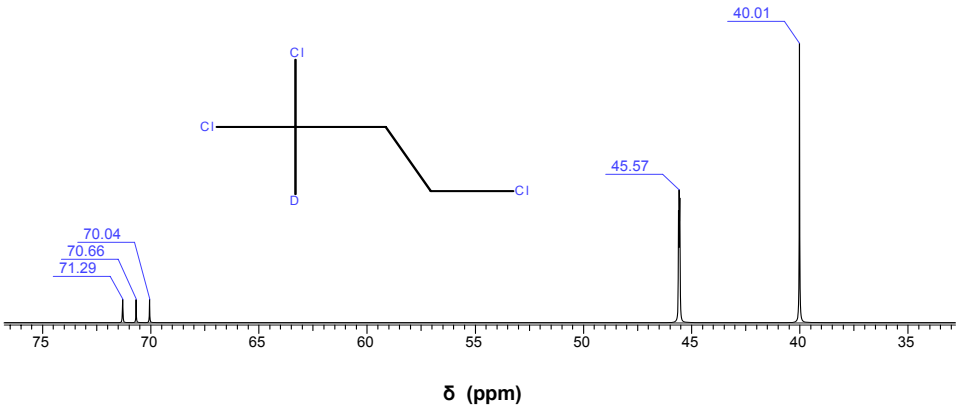

Figure 5.25: *ACDlabs simulated ^{13}C spectrum for 1,1,3-trichloro-1-deutero-propane*

The shift for the peak obtained in the ^{2}H NMR spectrum (see ***Figure 5.20***) corresponds well with that expected from the non-deuterated compound 1,1,3-trichloropropane.

5.5.1.3 Proposed schemes for the fragmentation of 1-1-3-trichloro-1-deuteropropane

Hydride migration[136] is an accepted fragmentation mechanism for primary alkyl halides. The mechanism is illustrated for chloropentane (***Scheme 5.5***), where m/z 70 is the base peak.[137]

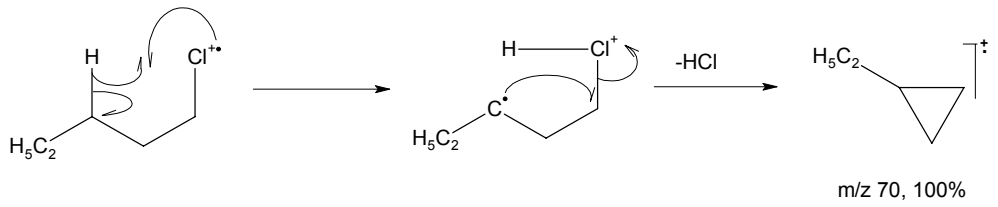

***Scheme 5.5**: Hydride migration fragmentation scheme for primary alkyl halides[136]*

Based on ***Scheme 5.5*** above, the following mechanisms (***Scheme 5.6*** to ***Scheme 5.12*** below) are proposed for the formation of the ions visible from the fragmentation of 1,1,3-trichloro-1-deuteropropane.

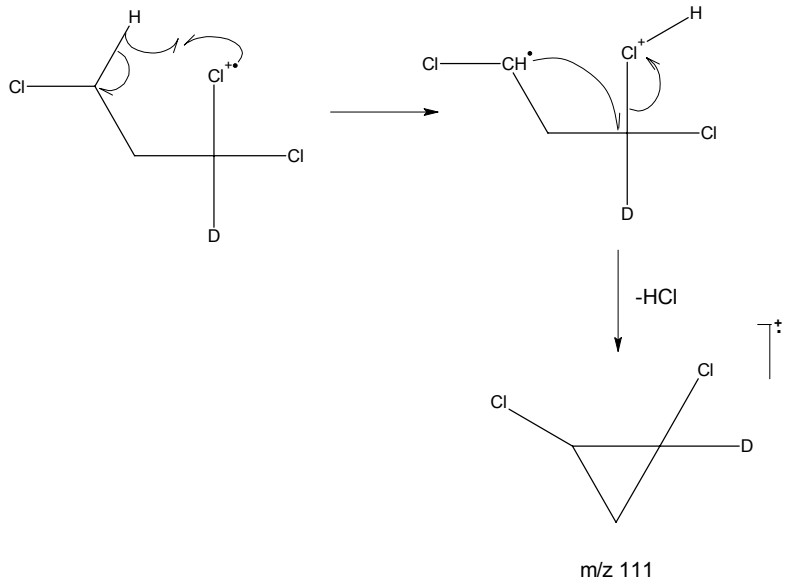

***Scheme 5.6**: Possible formation of the fragment at m/z 111 from 1,1,3-trichloro-1-deutero-propane*

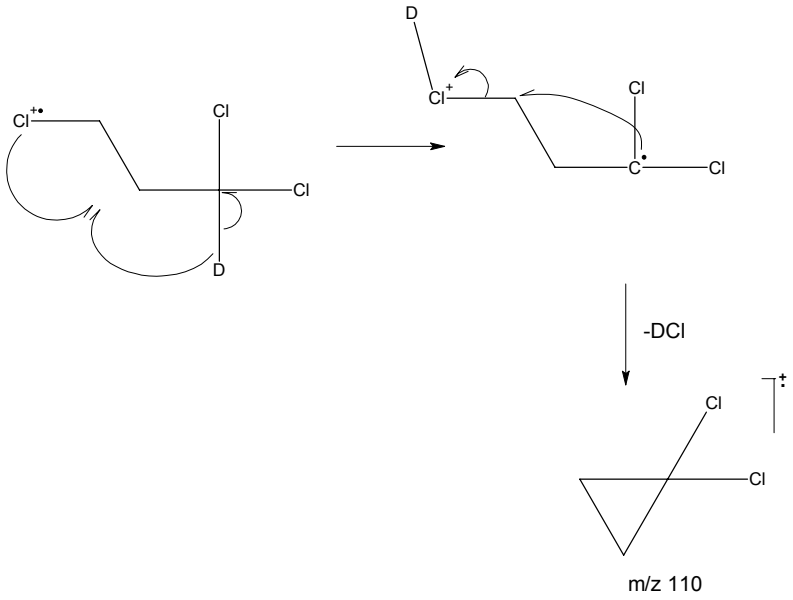

***Scheme 5.7**: Possible formation of the fragment at m/z 110 from 1,1,3-trichloro-1-deutero-propane*

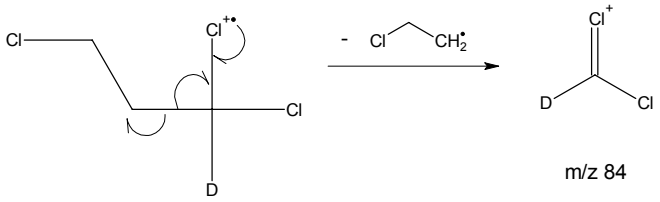

***Scheme 5.8**: Possible formation of the fragment at m/z 84 from 1,1,3-trichloro-1-deutero-propane*

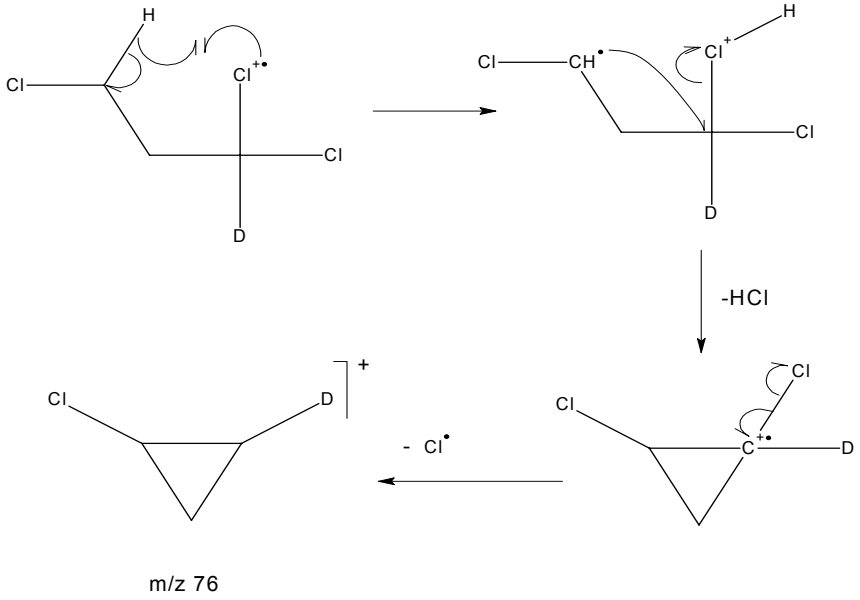

***Scheme 5.9**: Possible formation of the fragment at m/z 76 from 1,1,3-trichloro-1-deutero-propane*

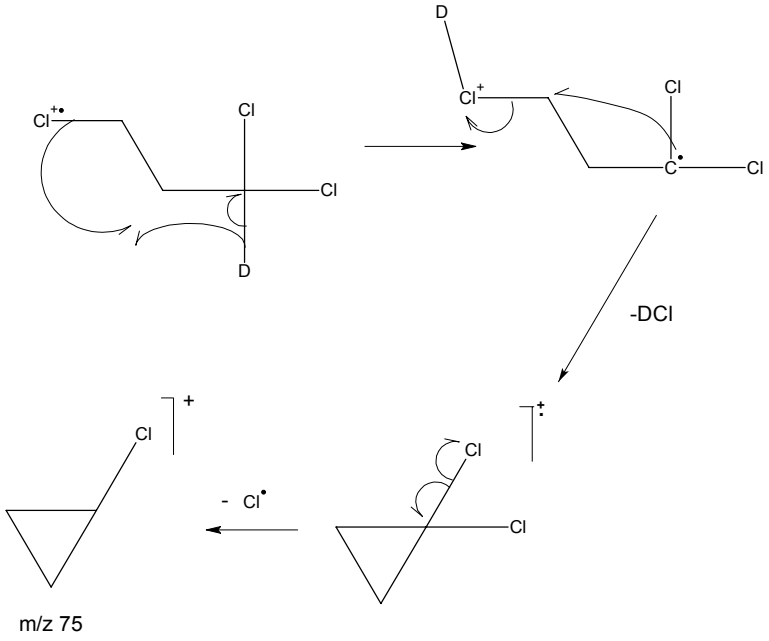

***Scheme 5.10**: Possible formation of the fragment at m/z 75 from 1,1,3-trichloro-1-deutero-propane*

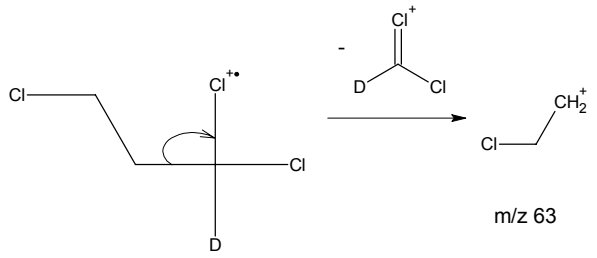

***Scheme 5.11**: Possible formation of the fragment at m/z 63 from 1,1,3-trichloro-1-deutero-propane*

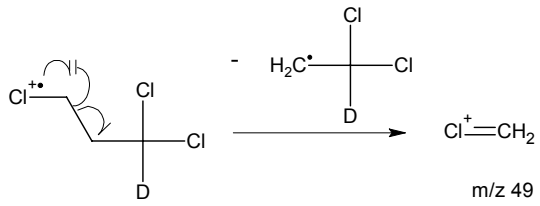

***Scheme 5.12**: Possible formation of the fragment at m/z 49 from 1,1,3-trichloro-1-deutero-propane*

Therefore all the major ions in the spectrum of the unknown can be explained as shown in Schemes 5.6 to 5.12. It is clear that GC/MS analyses and NMR analyses suggest the formation of 1,1,3-trichloro-1-deutero-propane during the ethylene induced decomposition of Grubbs methylidene **4a** in $CDCl_3$.

5.5.1.4 Conclusions on the decomposition of Grubbs methylidene 4a in $CDCl_3$

As previously described, the Kharasch reaction,[104] which involves the addition of $CDCl_3$ to a double bond, is known for mono and disubstituted olefins (see ***Scheme 2.27*** on page 43).

The formation of 1,1,3-trichloropropane on heating Grubbs catalyst methylidene **4a** in $CDCl_3$ in the presence of ethylene is therefore presumably due to addition of chloroform over the ethylene double bond *via* the Kharasch reaction as shown in ***Scheme 5.13*** on page 144. The 1,1,3-trichloro-1-deutero-propane formed is not necessarily a decomposition product as it is

not known whether the catalyst is destroyed in the formation of this product or by another process.

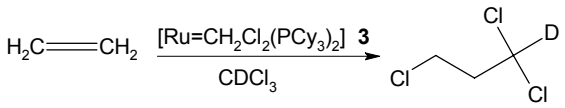

***Scheme 5.13**: Reaction of ethylene with $CDCl_3$ and Grubbs catalyst methylidene **4a** via the Kharasch reaction*

This is in contrast to the β-hydride transfer mechanism which results in the formation of propene over time and occurs in non-chlorinated solvents under catalytic conditions (see Section 5.4).

It is therefore concluded that there is a completely different decomposition pathway that occurs under catalytic conditions in the presence of a chlorinated solvent compared to that which occurs in non-chlorinated media. The decomposition products of Grubbs catalyst **2a** in non-chlorinated solvents are isomerisation active which leads to loss of selectivity. The decomposition products that result from decomposition in chlorinated solvents are possibly not isomerisation active and this may be why there is better selectivity in the batch reactions with $CHCl_3$ added. The decomposition in chlorinated solvents also appears to be slower than the decomposition that occurs in non-chlorinated solvents, leading to better conversions.

5.5.2 Ethylene Induced Decomposition of Grubbs Catalyst Methylidene 4a in $CDCl_3$ in the Presence of Excess Phenol

The decomposition of Grubbs methylidene **4a** in $CDCl_3$ was repeated in the presence of an excess of phenol, a free radical scavenger. No short chained chlorinated hydrocarbon products were found by GC/MS, however small peaks were visible at δ 2.6 and δ 3.7 in the ^{1}H NMR (***Figure 5.26***). It must be noted that phenol can have other roles in this system.[111] The GC/MS analysis was complicated by the presence of a large amount of phenol.

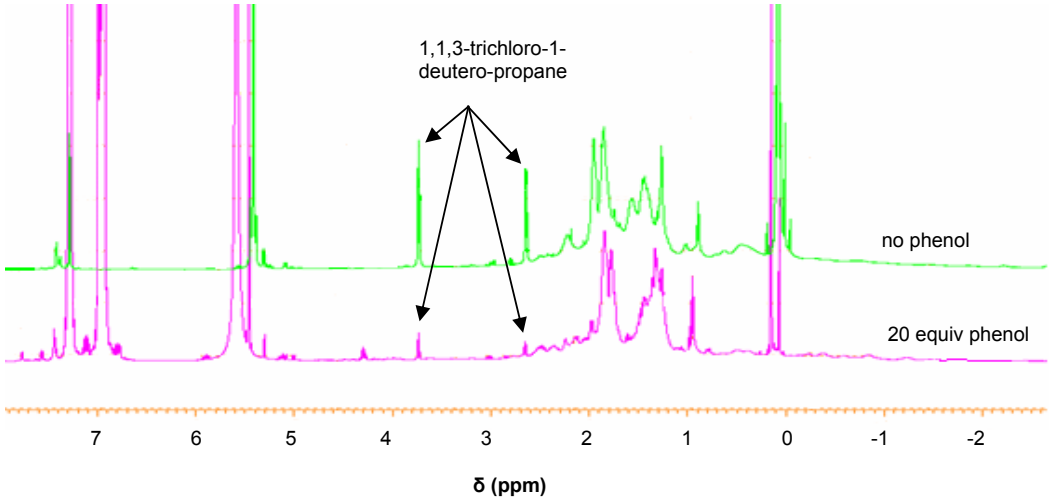

Figure 5.26: *^{1}H NMRs after the ethylene induced decomposition of Grubbs catalyst methylidene **4a** with and without 20 equivalents of phenol present ([Ru] = 4.35 x 10^{-2} M, 40 °C for 16 hours, $CDCl_3$,ethylene bubbled through solution for 60 seconds)*

The peaks at formed at δ 2.6 and δ 3.7 in the ^{1}H NMR spectra recorded after the reaction are much smaller in the presence of 20 equivalents of phenol. Therefore it is concluded that the formation of the peaks at δ 2.6 and δ 3.7 in the ^{1}H NMR is inhibited in the presence of phenol.

5.5.3 Ethylene Induced Decomposition of the Dibromo Methylidene 4b with Ethylene and $CDCl_3$

Attempts to were made repeat the ethylene induced decomposition in $CDCl_3$ using the dibromo methylidene **4b** [$Ru(Br)_2(PCy_3)_2CH_2$], to determine whether the halogens present in the Kharasch products originate from the ruthenium alkylidene complex or from the $CHCl_3$.

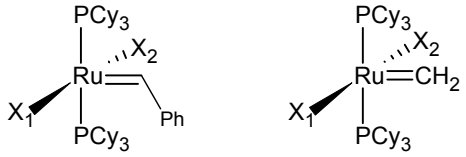

2b $X_1=X_2=Br$ **4b** $X_1=X_2=Br$

2c $X_1=Cl$ $X_2=Br$ **4c** $X_1=Cl$ $X_2=Br$

***Figure 5.27**: Selected ruthenium alkylidene complexes*

The dibromo methylidene **4b** was synthesised *in situ* by dissolving the dibromide **2b** in C_6H_6, and bubbling ethylene through the solution for 60 seconds. ^{31}P NMR confirmed that the dibromo methylidene **4b** was present. This was followed by addition of $CDCl_3$ and pressurising with 10 bar ethylene as described in Section 5.2.10. $PhCDCl_2$ was detected after the experiment.

In a separate experiment, $CDCl_3$ and C_6H_6 were mixed in an NMR tube and heated to 40 °C overnight to determine whether or not $PhCDCl_2$ can be formed in the absence of a ruthenium alkylidene complex. After the experiment the reaction mixture was analysed with GC/MS using a PONA column as described in Section 5.2.3 on page 106.

5.5.3.1 Possible reaction of $CDCl_3$ and C_6H_6 (Blank reaction)

$PhCDCl_2$ is formed on reaction of with Grubbs catalyst dibromide **2b** in a mixture of chloroform and C_6H_6 (see below), presumably due to a reaction of $CDCl_3$ with C_6H_6, however it was uncertain whether or not this reaction occurs in the absence of a ruthenium alkylidene species. Thus $CDCl_3$ and C_6H_6 were reacted overnight in the absence of any ruthenium species and the reaction mixture was analysed using GC/MS. The impurities found probably originate from the benzene used in the reaction. No $PhCDCl_2$ was found. Thus it was concluded that there was no reaction between the $CDCl_3$ and the C_6D_6 at 40 °C in the absence of a Ru species.

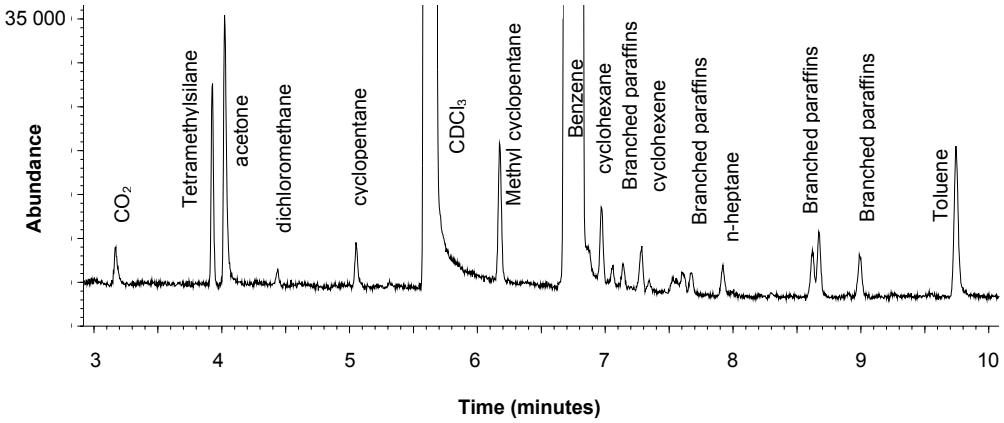

Figure 5.28: *GC/MS analysis after heating $CDCl_3$ and C_6H_6 at 40 °C overnight.*

5.5.3.2 Decomposition of the methylidene di-bromide 4b in $CDCl_3$

NMR

A stacked plot of the ^{31}P NMR spectra recorded over time (***Figure 5.29***) showed the concentration of the carbene halved in 90 minutes and disappeared completely in three and a half hours. As expected, there was very little evidence of formation of the mixed chloride bromide methylidene **4c** from the ^{31}P NMR spectrum. Again, a steady decrease in the ^{31}P NMR signal was observed over time indicating the formation of paramagnetic decomposition products.

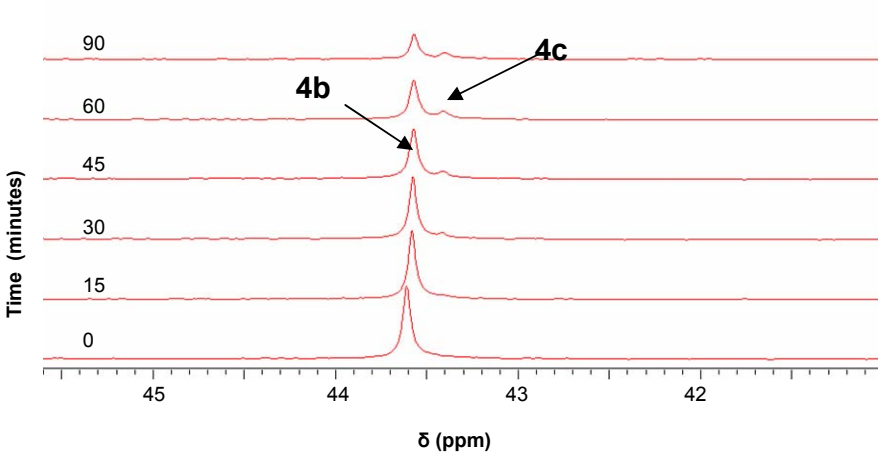

Figure 5.29: *^{31}P NMR spectra recorded over time for the decomposition of **4b** in $CDCl_3$ and C_6H_6 ([Ru] = 1.01 x 10^{-1} M, 40 °C, 10 bar ethylene)*

GC/MS

The GC/MS chromatogram obtained after analysis of the reaction mixture after the decomposition of the di-bromomethylidene **4b** in $CDCl_3$ and C_6H_6 in the presence of ethylene is shown in ***Figure 5.30***. The toluene, ethyl benzene and xylenes found in the reaction mixture are probably impurities in the C_6H_6 used or from the washing of the GC syringes with xylene. Methyl cyclohexane is a result of the hydrogenation of toluene. Hydrogenation takes place because the carrier gas is hydrogen and the catalyst is still dissolved in the sample when it is injected into the hot inlet of the gas chromatograph.

The $PhCDCl_2$ detected at 25 minutes is possibly the product of a radical reaction between the $CDCl_3$ and the benzene. This compound was not found in the reaction of C_6H_6 and $CDCl_3$ above therefore it suggests that this is a ruthenium mediated reaction.

The reaction of Grubbs di-bromide benzylidene **2b** with ethylene results in the formation of styrene. Because the di-bromide methylidene **4b** was not isolated, the reaction mixture contained styrene and ethylene. Both the ethylene and the styrene in the reaction mixture underwent the Kharasch reaction with $CDCl_3$ and the products formed show incorporation of bromide in the Kharasch products.

Although there was very little formation of the mixed halide methylidene **4c** *via* halide transfer as visible from the ^{31}P NMR spectrum over time (***Figure 5.29***), a surprisingly large amount of $CDCl_2Br$ (75%) relative to the total amount of brominated compounds detected (by GC/MS) was formed (***Figure 5.30***).

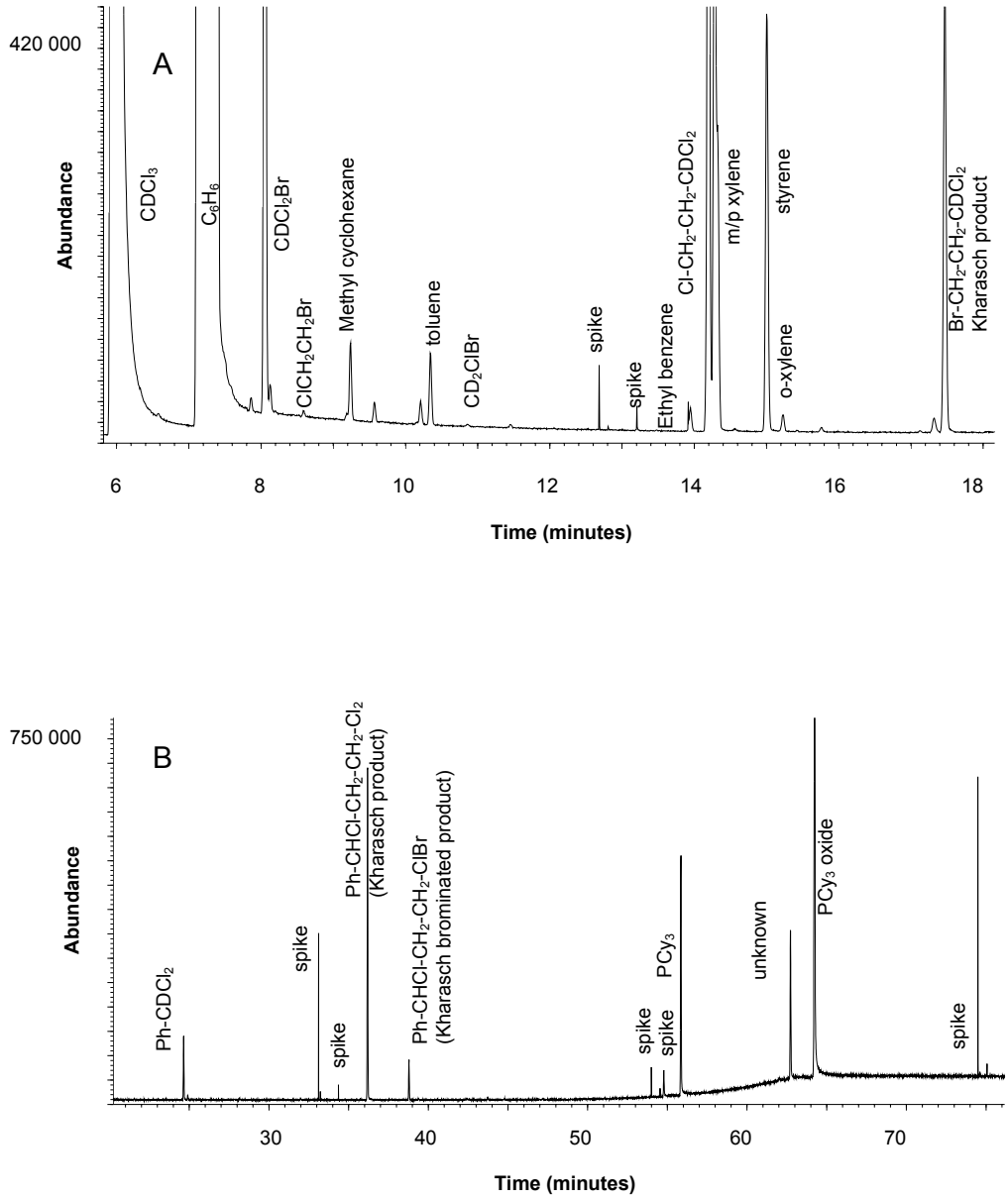

Figure 5.30: *GC/MS trace (A = 6 to 18 minutes, B = 20 to 75 minutes) obtained after decomposition of the dibromo methylidene **4b** in a mixture of $CDCl_3$ and C_6H_6 ([Ru] = 1.01 x 10^{-2} M, 40 °C for 16 hours, 10 bar ethylene)*

The unexpected formation of the $CDCl_2Br$ made interpretation difficult as it was uncertain whether the bromine in the products originated from the $CDCl_2Br$ or from the catalyst itself.

Integration of the total ion chromatogram (TIC) is not recommended in analytical chemistry because rates of ionisation are different for different compounds and the MS detector only detects positive ions and not the neutral species generated (unionised molecules and radicals). However, it can give an idea of the relative amounts of similar types of compounds present. For halogenated compounds, this is probably more accurate than the FID because the FID is not sensitive to halogenated compounds. Thus the TIC was integrated. The areas in the TIC for all brominated compounds were corrected to represent only the bromine in the compound of interest.

Considering that there is predominantly brominated methylidene **4b** present (from the first ^{31}P NMR spectrum), the detection of the major compounds being compounds containing only chlorides (75% of Kharasch products, TIC) indicates that the halogens come only from the solvent and the small amount of brominated products (25% of Kharasch products, TIC) present occurs because of the $CDCl_2Br$ formed in the reaction.

5.6 Conclusions on the Decomposition of the Methylidene Species 4a, 4b and 6

- As expected, the Grubbs catalyst methylidene **4a** rather undergoes decomposition than halide exchange with the solvent, although a large amount of brominated solvent was found after the experiment. This could be formed *via* a radical reaction of the solvent with the decomposed catalyst.

- Ethylene induced decomposition of the methylidenes **6** and **4a** in benzene occurs to a significant extent *via* the β-hydride pathway, with the formation of propene, as predicted by molecular modelling.

- The β-hydride decomposition pathway is inhibited in chloroform. Therefore the decomposition of the methylidene **4a** follows a *completely different pathway in the presence of chlorinated solvents*.

- The decomposition of Grubbs catalyst methylidene **4a** in chloroform, in the presence of ethylene, results in the formation of 1,1,3-trichloro-1-deuteropropane *via* the Kharasch addition of chloroform over the double bond, however the mechanism of this reaction is unclear.

- The halides in the Kharasch products originate from the solvent and not the catalyst itself. The mechanism of the Kharasch reaction is unclear and thus it is not certain whether or not this reaction leads to decomposition of the methylidene **4a**.

Chapter 6: Evaluation of the study

6.1 Scientific Relevance

The relevance and results of this study are briefly discussed according to the goals set out in Chapter 1.

It was conclusively shown that chlorinated solvents interact with Grubbs catalyst di-bromide **2b** in a halide exchange reaction with the chlorinated solvent itself, and a metathesis-like mechanism was proposed.

The intermolecular halide exchange between Grubbs catalyst **2a** and Grubbs catalyst di-bromide **2b** was discovered early in the study and the mechanism of this reaction was elucidated. This reaction was only mentioned in passing in the literature, [117] with no detailed study. The study of this reaction led to new insights into a bimolecular decomposition pathway, resulting in the proposal of additives (for example, salts) to inhibit the formation of the dimeric intermediate. Catalytic testing in the presence of salts showed a remarkable increase in selectivity and conversion.

It is proposed that the addition of phenol to Grubbs catalyst **2a** $[Ru(Cl)_2PCy_3CHPh]$ in $CDCl_3$ inhibits the free radical reaction of the dimeric intermediate to form the paramagnetic mixed valent species **42,** thereby inhibiting the bimolecular decomposition pathway. It is proposed that $SnCl_2$ reacts with the mixed valent species **42** in $CDCl_3$ to form the highly metathesis active Ru-Sn dimeric complex **43**. Both $SnCl_2$ and phenol are also beneficial to the metathesis reaction in non-chlorinated solvents, thus they have other roles in the system as well.

Substrate induced decomposition had been suggested from a modelling study by van Rensburg *et al.*[106] During this study, the proposed β-hydride transfer pathway was tested and the expected propene was found. The experimental proof found was published together with the modelling study.[106]

The study was extended by repeating the reaction in chloroform, where it was found that instead of propene formation, the Kharasch reaction took place, with the formation of 1,1,3-trichloro-1-deuteropropane. The identification of this product was carried out from first principles using GC/MS and 1D and 2D NMR.

In general it is concluded that the study was successful.

6.2 Future Research

When the Nobel prize was awarded to R.H. Grubbs, R.R. Schrock and Y. Chauvin recently, it was stated that metathesis is thought to be a key technology in the future leading to a new era in the production of drugs and plastics that are more efficient and less harmful to nature. It is therefore expected that research in this area will increase. This is especially the case where chemicals from renewable sources are under study. However, if the technology is to be commercialised on a large scale, the problems resulting from catalyst deactivation and decomposition will need to be addressed.

The results of the current study show intermolecular halide exchange between Grubbs catalyst **2a** and Grubbs di-bromide **2b**. It is necessary to determine whether the alkylidenes (for example, the propylidene) undergo the intermolecular halide exchange reaction. This is expected because alkylidenes also undergo bimolecular decomposition.

A detailed study of the kinetics of the intermolecular halide exchange between Grubbs catalyst **2a** and Grubbs catalyst di-bromide **2b** should be carried out, as the rate determining step could then be determined as well as all the rate constants. With this information the proposed mechanism for halide exchange could be further confirmed.

Use of the inert MALDI-TOF technology pioneered by Fogg[138] at University of Ottawa could prove useful in proving the existence of the dimeric

intermediate. This technology will help to prove whether or not the addition of salt or any other additive retards the formation of the dimeric intermediate.
It was shown in this study that the presence of chloroform inhibits the β-hydride decomposition pathway, resulting in much improved selectivity. Selectivity is also much improved in the presence of any salt, even ionic liquids and metal halide salts. It needs to be determined whether the additives react with the dimeric intermediate or inhibit its formation, and whether these additives also inhibit the β-hydride transfer decomposition pathway.

In general, for large scale industrial application, additional research towards the identification of a more stable catalyzed system needs to be achieved to enable widespread application.

References

[1] *Handbook of Metathesis*, (Ed) Grubbs, R.H., Wiley VCH, Wenheim, 2003, vol 2 and vol 3.
[2] Schrock, R.R., *Journal of Molecular Catalysis: A*, **2004,** *213(1)*, 21-30.
[3] Nguyen, S.T., Trnka T.M., in *Handbook of Metathesis*, (Ed) R.H. Grubbs, Wiley VCH, Wenheim, 2003, vol 1, 61-67
[4] Herrisson, J.L., Chauvin, Y., *Die Makromolekulare Chemie*, **1970**, *141***,** 161-176.
[5] see www.zaman.com, 10 October 2005.
[6] van Leeuwen, P.W.N.M., *Homogeneous Catalysis, Understanding the art*, Kluwer Academic Publishers, Dordrecht, 2004., 176- 183.
[7] Mol, J.C., *Journal of Molecular Catalysis A, Chemical*, **2004**, 213 (1), 39-45.
[8] Recent reviews: (a) Trnka, T.M., Grubbs R.H., *Acc. Chem. Res*. **2001**, 34, 18. (b) Furstner, A, *Angew. Chem. Chem., Int Ed*., **2000** , 39, 3012 (c) See reference 96.
[9] For example, ethenolysis of methyl oleate, self-metathesis of shorter chained olefins to detergent range olefins. For more information see references 7 and 16.
[10] For example, the cross metathesis and self metathesis of methyl oleate, see reference 16.
[11] Sanford M.S., Love J.A., in *Handbook of Metathesis* vol 1, (Ed) Grubbs, R.H., Wiley VCH, Wenheim, 2003, vol 1, 118-120.
[12] http:\www.science.uottawa.ca/~dfogg/overheads.pdf
[13] Hong, S.H., Day, M.W., Grubbs, R.H., *J. Am. Chem. Soc.*, **2004**, *126*(24), 7414-7415
[14] Dinger, M.B., Mol, J.C., *Organometallics*, **2003**, *22*, 1089-1095.
[15] Dinger, M.B., Mol, J.C., *Eur. J. Inorg. Chem.* **2003,** 2827-2833.
[16] Burdett, K.A., Harris L.D., Margl, P, Maughon, B.R., Mokhtar-Zadeh T., Saucier, P.C., Wasserman E.P., *Organometallics*, **2004**, *23(9)*, 2027-2047.
[17] Bowker, M, *The Basis and Applications of Heterogenous Catalysis*, 1998, Oxford University Press, Oxford, 2,3.
[18] Berzelius, J. J., *Edinburgh New Philosophical Journal*, **1836**, *21*, 223.
[19] Margarine is produced by the heterogeneous hydrogenation of plant oils.
[20] Biphasic catalysis, when the catalyst is dissolved a liquid phase that is not miscible with the reagents, is also a form of heterogeneous catalysis.
[21] HTFT™ is the Sasol high temperature Fischer-Tropsch process that uses an Fe based catalyst to produce synthol light oil (SLO) for the production of gasoline and light olefins. The original process from the 1950s used the Sasol Synthol reactor, while the newer more advanced process (from 1989) uses the SAS (Sasol Advanced Synthol) reactor. For more information see www.sasol.com, choose news center, Oryx GTL (gas to liquids) site visit.
[22] LTFT™ is the Sasol low temperature Fischer-Tropsch process that produces wax using an Arge Tubular reactor. The newer more advanced Sasol Slurry Phase Process is a low temperature process for the production of wax and diesel and has been in operation since 1993. For more information see www.sasol.com, choose news center, Oryx GTL (gas to liquids) site visit.
[23] SSPD™ is the Sasol Slurry phase distillate process that is used in the conversion of syngas (derived from natural gas), *via* a Co catalyst to waxy syncrude which is further processed *via* hydroisomerisation into liquid fuel. This technology will be used in the Oryx GTL plant currently being constructed at Ras Laffan Industrial City in Qatar. For more information see www.sasol.com, choose news center, Oryx GTL (gas to liquids) site visit.
[24] CTL™ is Coal to Liquids. This is Sasol's Fischer-Tropsch technology that is under consideration for implementation in China at present.
[25] Green, M, Damoense, L, Datt M, Steenkamp C, *Coordination Chemistry Reviews*, **2004**, *248*, 2393-2407.
[26] Dwyer, C, Assumption, H, Coetzee, J, Crause, C, Damoense, L, Kirk, M, *Coordination Chemistry Reviews*, **2004**, *248*, 653-669.
[27] Ionic liquids are salts with large anions and cations that are liquid are room temperature and that have no vapour pressure. For more information see Ajam M, 'Metathesis and hydroformylation reactions in ionic liquids', MSc Thesis, University of Johannesburg, June 2005.
[28] Conrad, J.C., Fogg, D.E., "Ring-Closing Metathesis: Advances, Limitations, and Opportunities", *Current Organic Chemistry*, **2005**, accepted.

[29] In the case of the HP NMR studies the starting material used was [Co_2CO_8] because the Co(II)carboxylate is paramagnetic, resulting in the loss of the NMR signal.
[30] Crause, C., Bennie, L., Damoense, L., Dwyer, C.L., Grove, C., Grimmer, N., van Rensburg, W., Kirk, M.M, Mokheseng, K., Otto, S., Steynberg, P.J., *Dalton Trans*., **2003**, 2036.
[31] Bailey, G.C., *Catalysis Reviews*, **1969**, *3(1)*, 37-60.
[32] Banks, R.L., *Chemtech*, **1979**, *August*, 495-500.
[33] Plotkin, J,S., Vice President, PERP Program, Nexant Chem Systems. Presentation entitled "Propylene: Olefin of the Future", at the meeting of the American Chemical Society on the 13th January 2005, and again at Sasol Technology R&D in March 2005.
[34] In this process ethylene and 2-butene react with each other in the liquid phase in the presence of Re_2O_7/Al_2O_3 at 35°C and 60 bar, see reference 7.
[35] US patent number US 6,586,649 B1.
[36] Ni is often used as an isomerisation catalyst, thus it is unexpected that a Ni catalyst would have such low isomerisation activity.
[37] Banks, R.L., Banasiak, P.S., Hudson, P.S., Norell, J.R., *J. Mol. Catal*, *15*, **1982**, 21.
[38]Katz, T.J., in *Handbook of Metathesis*, (Ed) Grubbs, R.H., Wiley VCH, Wenheim, 2003, vol 1, 47-57.
[39] Grubbs, R.H., in *Handbook of olefin metathesis* (Ed) Grubbs, R.H., Wiley VCH, Wenheim, 2003, vol 1, 4-6.
[40] Schrock, R.R., in *Handbook of olefin metathesis* (Ed) Grubbs, R.H., Wiley VCH, Wenheim, 2003, vol 1, 9-10.
[41] Tebbe, F.N., Parshall, G.W, Reddy, G.S., *J. Am. Chem. Soc.*, **1978**, *100*, 3611-3613.
[42] The favoured mechanism of the day involved the exchange of carbon atoms from a pair of olefins in the coordination sphere of a metal. See reference 4.
[43] Fischer, E.O., Maasbol, A.A., *Angewant. Chem. Int. Ed.Engl*., **1964**, *3*, 580.
[44] a) Casey, C.P., Burkhardt, T.J., *J. Am. Chem. Soc*., **1973**, *95*, 5833. b) Casey, C.P., Burkhardt, T.J., Bunnell,C.A., Calabrese, J.C., *J. Am. Chem. Soc.*, **1977**, *99*, 2127.
[45] Katz, T.J., McGinnis, J., Altus, C., *J. Am. Chem. Soc,* **1976***, 98,* 606.
[46] Cardin, D.J., Cetinkaya, B, Lappert, M.F., Chem Rev., **1972**, *72*, 575.
[47] Schrock, R.R., *J. Am. Chem. Soc*., **1974**, *96*, 6796.
[48] Schrock, R.R., *J. Am. Chem. Soc,* **1976**, *98*, 5399.
[49] a)Rocklage, S.M., Fellman, J.D., Rupprecht, G.A., Messerle, L.W., Schrock, R.R., *J. Am. Chem. Soc,* **1981***, 103,* 1440.
[50] Schrock, R.R., Rocklage, S.M., Wengrovious, J.H., Rupprecht, G.A., Fellman, J., *J. Mol. Catal*.,**1980**, *8*, 103.
[51] Wengrovious, J.H., Schrock, R.R., Churchill, M.R., Missert, J.R., Youngs, W.J, *J. Am. Chem. Soc,* **1980***, 102,* 4515,
[52] Pedersen, S.F., Schrock, R.R., Churchill, M.R., Wasserman, H.J., *J. Am. Chem. Soc,* **1982**, *104*, 6808.
[53] Schaverien,C.J., Dewan, J.C.,Schrock, R.R., *J. Am. Chem. Soc,* **1986**, *108*, 832.
[54] Feldman, J, Schrock, R.R., *Chem. Rev*., **2001**, *101*, 145.
[55] Murdzek, J.S., Schrock, R.R., *Organometallics*, **1987**, *6*, 1373.
[56] Schrock,R.R., Murdzek, J.S., Bazan, G.C., Robbins, J, DiMare, M., O'Regan, M., *J. Am. Chem. Soc.,* **1990***, 112,* 3875.
[57] Schrock, R.R., *Chem. Rev*., **2001**,*101*, 145.
[58] Robbins, J., Bazan,G.C., Murdzek, J.S., O'Regan, M.B., Schrock, R.R., *Organometallics*, **1991**, *10*, 2902.
[59] Schrock, R.R., Sharp, P.R., *J. Am. Chem. Soc.,* **1978***, 100,* 2389.
[60] Coperet, C., Lefebvre, F., Basset, J., in *Handbook of Metathesis*, (Ed) R.H. Grubbs, Wiley VCH, Wenheim, 2003, vol 1, 190-201.
[61] Sanford, M.S., Love, J.A., Grubbs, R.H., *J. Am. Chem. Soc.*, **2001**, 123, 6543-6554.
[62] Piers, W.E., Romero, P.E., *J. Am. Chem. Soc.,* in press, **2005**.
[63] The 3,3-dicyclopropenes were originally made by Jeffrey Moore and Eric Ginsburg for another project. See reference 3.
[64] Nguyen, S.T., Johnson, L.K, Grubbs, R.H., Ziller, J.W., *J. Am. Chem. Soc*., **1992**, *114*, 3974-3975.
[65] Finkelstein, H., *Ber.,* **1910,** *43*, 1528. A recent example of the use of this reaction in organic chemistry is Richardson, T.I., Rychnovsky, S.D, *J. Am. Chem. Soc*., **1977**, *119*, 12360-12361.

[66] Zoebel, B., Lim, A.E.K., Dunn, K., Dakternieks, D., *Organometallics*, **1999**, *18*, 4990-4890.
[67] Kocheschov, K.A., Nesmeyanov, A.N., *Chem. Ber*. **1931**, *64*, 628.
[68] Pikina, E.I., Talalaeva, T.N., Kocheschov, K.A., *J. Gen. Chem. USSR,* **1938**, *8***,** 1844.
[69] Weskamp,T, Schattermann, W.C., Spiegler,M., Herrmann, W.A., *Angew. Chem. Int. Ed.* **1998,** *37*, 2490-2493.
[70] Nguyen, S.T., Trnka T.M., in *Handbook of Metathesis*, (Ed) Grubbs, R.H., Wiley VCH, Wenheim, 2003, vol 1, p 68-74.
[71] Lehman, S.E., Scwendeman, J.E., O'Donnell, P.M., Wagener, K.B., *Inorganica Chemica Acta* 345, **2003,** 190-198.
[72] Forman, G.S., McConnell A.E., Hanton, M.J., Slawin, A.M.Z., Tooze, R.P., van Rensberg, W., Meyer, W.H., Dwyer,C, Kirk, M.M., Serfontein, D.W., *Organometallics*, **2004,** *23(21)* 4824-4827.
[73] Forman, G.S., McConnell, A.E., Tooze, R.P., Dwyer, C., Serfontein, D.W., Sasol Technology UK, *World Patent,* 2003, ZA03/00087.
[74] Cobalt hydroformylation technology makes extensive use of the phobane ligands, see reference 30.
[75] Extensive low temperature NMR studies show that Phobcat **23** is resolved into a number of rotational isomers. Full details of these studies will be disclosed soon.
[76] Kingsbury, J.S, Harrity J.P.A., Bonitatebus, Jr, P.J., Hoveyda, A.H., *J. Am. Chem. Soc.*, **1999**, *121*, 791-799.
[77] Hoveyda, A.H., Gillingham, D.G., Van Veldhuizen, J.J., Kataoaka, O., Garber, S.B., Kingsbury, J.S., Harrity, J.P.A., *Org. Biomol. Chem*., **2004**, *2*, 8-23.
[78] US patent number US2003/0220512 A1, 27 Nov 2003.
[79] Hansen, S.M., Volland, M.A.O., Rominger, F., Eisentrager, F., Hoffman, P., *Angew. Chem, Int Ed*., **1999**, 38, No.9, 1273-1276.
[80] Volland, M.A.O., Hansen, S.M., Rominger, F., Hoffman, P., *Organometallics*, **2004**, *23*, 800-816.
[81] Nubel, P.O., Hunt C.L., *Journal of Molecular Catalysis A: Chemical* **1999**, *145*, 323-327.
[82] Vosloo, M, Van Schalkykwyk, C, Botha, J.M, *Journal of Molecular Catalysis A: Chemical*, **2002**, *3668*, 1-11.
[83] Nguyen, S.T., Trnka T.M., in *Handbook of Metathesis*, (Ed) R.H. Grubbs, Wiley VCH, Wenheim, 2003, vol 1, 74-80.
[84] Melis, K., De Vos, D., Jacobs, P., Verpoort, F., *J. Mol. Catal. A: Chem*, **2001**, 169, 47-56
[85] Nguyen, S.T., Grubbs, R.H., *J. Organomet. Chem.* **1995**, *497*, 195-200
[86] Ahmed M., Barrett, A.G.M., Braddock, D.C., Cramp S.M., Procpiou, P., *Tetrahedron Letters*, **1999**, *40(49)*, 8657-8662
[87] http://www.peakdale.co.uk/about/glaxo.htm
[88] Dowden, J., Savovic, J., J Chem. Commun., **2001**, 37-38
[89] Yao, Q., Angew. Chem. Int. Ed. **2000**, *39*, 3896-3898
[90] Connon, S.J., Blechert, S., *Bioorg. Med. Chem. Lett*., **2002**, 12, 1873-1876
[91] Kingsbury, J.S., Garber S.B., Giftos, J.M., Gray, B.L., Okamoto, M.M, Farrer, R.A., Foukras J.T., Hoveyda, A.H., *Angew. Chem. Int. Ed.* **2001**, 40, 4251-4256
[92] Nieczypor, P., Buchowicz, W., Meester, W.J.N., Rutjes F.J.P.T., Mol, J.C., *Tetrahedron Letters*, **2001**, *42(40)*, 7103-7105.
[93] Grela, C., Tryznowski M., Bieniek, M*., Tetrahedron Letters*, **2002**, 43(50), 9055-9059
[94] Cetinkaya B., Gurbuz, N., Seckin, T., Ozdemir, I., *Journal of Molecular Catalysis:A: Chemical*, **2002,** *184*, 31-38
[95] Black, G, Maher, D, Risser, W., in *Handbook of Metathesis*, (Ed) R.H. Grubbs, Wiley VCH, Wenheim, 2003, vol 3, 2-72.
[96] Blechert, S., Cannon, S.J., *Angew. Chem. Int. Ed*., **2003**, *42*, 1900-1923
[97] Lehman Jr, Wagener, K.B, in *Handbook of Metathesis*, (Ed) R.H. Grubbs, Wiley VCH, Wenheim, 2003, vol 3, 283-353.
[98] Han, S., Chang S., in *Handbook of Metathesis*, vol 2, (Ed) R.H. Grubbs, Wiley VCH, Wenheim, 2003, vol 1, 5-7.
[99] Sworen, A., Pawloa, J.H., Case, W., Lever, J., Wagener, K., *Journal of Molecular Catalysis A: Chemical,* **2003**, *194*, 69-78. See also reference 71.
[100] Grubbs, R.H., Lynn, D.M., *J. Am. Chem. Soc.*, **2001,** *123(14)*, 3187-3193.
[101] Fogg, D.E., Conrad, J.C., Amoroso, D., Czechura P., Yap, G.A.P, *Organometallics*, **2003**, *22(18)*, 3634-3636.

[102] Krause, J.O., Nuyken, O, Wurst, K, Buchmeister, M.R., *Chem. Eur. J.* **2004**, *10*, 777-784.
[103] Simal, F, Delfosse, S., Demonceau, A, Noels A.F., Denk, K., Kohl F.J., Weskamp T, Hermann, W.A., *Chem Eur. J.* **2002** , 8, No 13, 3047-3052.
[104] Snapper, M.L., Tallaricao, J.A., Malnick, L.M., *J. Org. Chem*. **1999**, 64, 344-345.
[105] Sworen, J.C., Pawlow, J.H., Case, W., Lever, J., Wagener, K.B., *Journal of Molecular Catalysis: A Chemical*, *194*, **2003,** 69-78.
[106] Janse van Rensburg, W, Steynberg, P.J., Meyer, W.H., Kirk, M.M., Forman, G.S., *J. Am. Chem. Soc.*, **2004**, *126(44)*, 14332-14333.
[107] Fogg, D.E., Yapp, G.P.A., Amoroso, D., *Organometallics,* **2002,** *21,* 3335-3343.
[108] Amoroso, D., Snelgrove, J. L., Conrad, J.C., Drouin, S.D., Yap, G.A.P, Fogg, D.E., *Adv. Syn. Cat*., **2002**, *344*(6+7), 757-763.
[109] Fraser, A.J.F., Gould, R.O., *Dalton Trans.*, **1974**, 1139.
[110] Mieock, K, Eum, M., Jin, M.J., Jun, K., Lee, C.W., Kucn, K.A., Kim, C.H., Chin, C.S., *Journal of Organometallic Chemistry*, **2004**, *689*, 3535-3540.
[111] Forman, G.S., Mc Connell, A.E., Tooze, R.P., Janse van Rensburg, W., Meyer, W.H, Kirk, M.M., Dwyer, C.L., Serfontein, D.W., *Organometallics*, **2005**, in press.
[112] Meyer, W.H., McConnell, A. E., Forman, G.S., Dwyer, C.L., Kirk, M.M., Ngidi, E.L., Blignaut, A., Saku, D., Slawin, A.M.Z., submitted to *Inorganica Chimica Acta*, **2005**.
[113] An HMBC is a ^{1}H-X long range correlation 2D NMR spectrum. In this case a ^{1}H-^{31}P HMBC spectrum was recorded.
[114] Macomber, R.S., A complete introduction to modern NMR sepctroscopy, 1998, John Wiley and Sons incorporated, Toronto, There are a few software programs to simulate spectra at varying stages of exchange. One of these is WinDNMR which can be downloaded at the following website: http://www.chem.wisc.edu/areas/reich/plt/windnmr.htm.
[115] Green, M.L.H., Wong, L, *Organometallics*, **1992**, *11*, 2660.
[116] Thermal decomposition is of importance particularly in substrates that require high temperatures or long contact times for the reaction to reach completion, and for catalyst recycle loops for industrial applications.
[117] Only 3 papers mentioning halide lability were found. One was halide lability in protic solvents and the other was halide exchange in an ATRP reaction employing a Ru alkylidene catalyst, a) Grubbs, R.H., Lynn, D.M., *J. Am. Chem. Soc.*, **2001,** *123(14)*, 3187-3193. b) Simal, F, Delfosse, S., Demonceau, A, Noels A.F., Denk, K., Kohl F.J., Weskamp T, Hermann, W.A., *Chem Eur. J.* **2002** , 8, No 13, 3047-3052 c) Lynn, D.N., Mohr, B., Grubbs, R.H., Henling L.M., Day, M.W., *J. Am. Chem. Soc.,* **2000,** *122*, 6601-6609.
[118] Modelling was carried out by W Meyer, using density functional theory, at Sasol Technology R&D.
[119] The rate of phosphine dissociation was measured using NMR magnetisation transfer techniques and reported per coordinated phosphine. Rates of initiation were measured using ^{1}H NMR, by monitoring the disappearance of the starting complex when various complexes were reacted with ethyl vinyl ether. This is an irreversible first order reaction and as such represents the rate of dissociation of the phosphine. The rates of initiation correlated well with the rates of phosphine dissociation. For more information see reference 61.
[120] This can be achieved by simple modification of a Varian flow probe designed for HPLC-NMR, such that the solutions can be injected directly into the cell, with mixing, with minium time before the first spectrum is recorded. This was discussed with D. Agriopoulus of Varian during a visit to Darmstadt applications laboratories in May 2005.
[121] Discussions were held with Fogg at Sasol technology R&D on the 18th October 2006.
[122] The Microsoft Excel spreadsheet used was obtained from Simon Duckett at York University. This spreadsheet was developed originally by Bill Jones for use in magnetisation transfer experiments. The spreadsheet was slightly modified for the current application. Jones, W.D., Rosini, G.P., Maguire, J.A., *Organometallics*, **1999**, *18*, 1754-1760.
[123] Modelling was carried out by Gideon Steyl at the University of the Free State using density functional theory.
[124] Buchiwicz W., Mol, J.C., *J. Mol Catalysis A: Chem*, **1999**, *148*, 97-103.
[125] Many unsaturated transition metal hydride complexes catalyse isomerisation, for example monohydrides of Rh(1), Pd(II), Ni(II), Pt(II), Ti(IV) and Zr(IV). For more information see van Leeuwen, P.W.N.M., *Homogeneous Catalysis, Understanding the Art*, Kluwer Academic Publishers, Dordrecht, 2004, 101-103.
[126] In the self-metathesis of 1-octene, the starting olefin is far more reactive than the product.

[127] The Bruker pulse program kinetik was modified for ^{31}P NMR detection with ^{1}H decoupling by Peter Dvortsak of Bruker Germany.
[128] The high pressure NMR cell is a ROE cell and was manufactured at Amsterdam University and can be pressurised to 100 bar. Strict safety precautions are taken when using the cell. For more information see reference 26.
[129] A gCOSY (gradient correlated spectroscopy) is a 2D NMR technique where the spectrum of the same nucleus (in this case ^{1}H) is found along both axes and the cross peaks show which peaks are coupled to each other.
[130] Nizotsev A. V., Bespalova N.B., "Substrate induced Olefin Metathesis decomposition', poster at ISOM 16, as well as reference 62.
[131] There is some debate on this issue. Nizotsev and Bespalova used helium as a carrier gas and report formation of ethane in the decomposition reaction. See reference 130.
[132] Pavia, D.L., Lampman, G.M., Kritz, G.S., in Introduction to Spectroscopy, third edition, Harcourt College Publishers, New York, 2001, 403.
[133] The mass of 3 chlorine atoms is 105, and the mass of the ion is 110. This means that the molecule does not contain any carbon atoms (mass=12), which is unlikely.
[134] The nitrogen rule states that a molecule having an even number of nitrogens or no nitrogens will have a molecular ion (an odd electron ion, charged fragment with an odd number of electrons) with an even mass number. Also if an even electron ion (charged fragment with an even number of electrons) contains no nitrogen atoms or an even number of nitrogen atoms, its mass will appear at an odd number. This applies to all ions, not just the molecular ion. Thus for a molecule containing no nitrogens, the molecular ion is even, fragments resulting from the loss of molecules are even and fragments resulting from the loss of radicals are odd. This information helps in the identification of the molecular ion and identification of possible mechanisms for formation of the fragments seen.
[135] This is software used to predict NMR spectra. See www.acdlabs.com for more information
[136] McLafferty F.W., Turecek F., in *Interpretation of Mass Spectra*, Fourth edition, University science books, Sausalito, California, 1993, 77.
[137] The base peak is the largest peak in the mass spectrum and is set to 100%.
[138] Unpublished results. Fogg gave a lecture at Sasol technology on the 18th October 2005, on the use of MALDI to monitor organometallic reactions.